

1. REPORT NUMBER CA02-0004	2. GOVERNMENT ASSOCIATION NUMBER	3. RECIPIENT'S CATALOG NUMBER
4. TITLE AND SUBTITLE Predicting the Ultimate Axial Resistance of Single Driven Piles	5. REPORT DATE 01/01/2001	
6. PERFORMING ORGANIZATION CODE		7. AUTHOR Rollins Patrick
8. PERFORMING ORGANIZATION REPORT NO.		9. PERFORMING ORGANIZATION NAME AND ADDRESS University of Texas at Austin
10. WORK UNIT NUMBER		11. CONTRACT OR GRANT NUMBER
12. SPONSORING AGENCY AND ADDRESS California Department of Transportation Division of Research and Innovation, MS-83 1227 O Street Sacramento CA 95814		13. TYPE OF REPORT AND PERIOD COVERED
14. SPONSORING AGENCY CODE		15. SUPPLEMENTARY NOTES

16. ABSTRACT

Caltrans' pile load-test data was collected, evaluated. And put into a database. Additional field work was performed at approximately 50 load-test locations to improve the site characterization information. Existing pile capacity estimation procedures were evaluated using the load-test database. Current methods predicted capacity reasonably well at clay dominated sites, but did relatively poorly at sand dominated sites. A simple SPT based predictive method was developed for sand sites.

17. KEY WORDS Caltrans, Axial Resistance, Single Driven Piles	18. DISTRIBUTION STATEMENT No restrictions. This document is available to the public through the National Technical Information Service, Springfield, VA 22161	
19. SECURITY CLASSIFICATION (of this report) unclassified	20. NUMBER OF PAGES 182	21. COST OF REPORT CHARGED

DISCLAIMER STATEMENT

This document is disseminated in the interest of information exchange. The contents of this report reflect the views of the authors who are responsible for the facts and accuracy of the data presented herein. The contents do not necessarily reflect the official views or policies of the State of California or the Federal Highway Administration. This publication does not constitute a standard, specification or regulation. This report does not constitute an endorsement by the Department of any product described herein.

For individuals with sensory disabilities, this document is available in Braille, large print, audiocassette, or compact disk. To obtain a copy of this document in one of these alternate formats, please contact: the Division of Research and Innovation, MS-83, California Department of Transportation, P.O. Box 942873, Sacramento, CA 94273-0001.

PREDICTING THE ULTIMATE AXIAL RESISTANCE OF SINGLE DRIVEN PILES

Publication No. _____

Rollins Patrick Brown, Ph.D.
The University of Texas at Austin, 2001

Supervisor: Roy E. Olson

Sixteen existing methods of predicting the ultimate side resistance of single driven piles were evaluated against the uplift test pile database compiled from Caltrans' archives. These methods included methods based on standard penetration tests (SPT), laboratory tests, electric cone penetration tests (CPT), and piezocone penetration tests (CPTU). From this evaluation, the overall variability in the predictions made by these methods was found to be due primarily to variability in the predictions of the methods in sand. For this particular dataset, of the methods for piles in sand, the method with the lowest variability was Decourt's (1982) SPT-based method. Decourt's method, which is applicable to piles in both sand and clay, was also found to perform reasonably well in clay.

Based on this evaluation, Decourt's method was selected as the basis for the development of an improved side resistance method for Caltrans' use. This improved side resistance method, modeled after Decourt's method, was developed using regression analyses to fit the model parameters to a dataset of 97 uplift tests. To develop a companion toe resistance method and to establish an empirical relationship between uplift side resistance and compressive side resistance, regression analyses were also performed to fit these additional model parameters to a dataset of 44 tests piles having both uplift and compressive tests.

Once the improved methods for the prediction of the axial resistance of single piles were developed, an analysis of the reliability of the method was conducted to provide recommendations for appropriate factors of safety. In this analysis, the reliability of Caltrans' current methods was used as a benchmark.

TABLE OF CONTENTS

1. INTRODUCTION	1
1.1 BACKGROUND	1
1.2 DATA	2
1.3 OBJECTIVES.....	2
2. AXIAL LOAD TEST DATA	4
2.1 INTRODUCTION.....	4
2.2 SELECTION CRITERIA.....	4
2.3 DEFINITIONS OF MEASURED ULTIMATE RESISTANCE	5
2.4 TEST PILES.....	8
<i>2.4.1 Locations</i>	<i>11</i>
<i>2.4.2 Pile Details</i>	<i>14</i>
<i>2.4.3 Pile Types</i>	<i>20</i>
<i>2.4.3.1 Open-Toed Steel Pipe Piles</i>	<i>20</i>
<i>2.4.3.2 Closed-Toed Steel Pipe Piles.....</i>	<i>20</i>
<i>2.4.3.3 Steel H-Piles</i>	<i>20</i>
<i>2.4.3.4 Solid Precast Concrete Piles.....</i>	<i>21</i>
<i>2.4.3.5 Hollow Precast Concrete Piles</i>	<i>21</i>
<i>2.4.4 Methods of Installation.....</i>	<i>22</i>
<i>2.4.4.1 Impact Driving</i>	<i>22</i>
<i>2.4.4.2 Vibratory Driving.....</i>	<i>22</i>
<i>2.4.4.3 Jetting.....</i>	<i>22</i>
<i>2.4.4.4 Casing</i>	<i>23</i>
<i>2.4.4.5 Predrilling</i>	<i>24</i>
<i>2.4.4.6 Relief Drilling</i>	<i>24</i>
<i>2.4.5 Soil Profiles</i>	<i>24</i>
<i>2.4.5.1 Profile Compositions</i>	<i>30</i>
<i>2.4.5.2 Geology.....</i>	<i>31</i>
<i>2.4.6 Setup Times.....</i>	<i>32</i>
<i>2.4.7 Load Test Procedures</i>	<i>33</i>
2.5 CONCLUSION	33
3. SITE CHARACTERIZATION DATA	35

3.1 INTRODUCTION.....	35
3.2 DRILLING AND SAMPLING.....	35
3.3 STANDARD PENETRATION TESTING.....	36
3.3.1 <i>Equipment and Procedures</i>	36
3.3.1.1 <i>Drive-Weight Assembly</i>	36
3.3.1.2 <i>Hammer Drop Systems</i>	37
3.3.1.3 <i>Sampling Rods</i>	37
3.3.1.4 <i>Sampler</i>	38
3.3.2 <i>SPT Energy Correction</i>	38
3.3.2.1 <i>Rod Energy Ratio</i>	39
3.3.2.2 <i>Effect of Rod Length</i>	40
3.3.2.3 <i>Effect of Borehole Diameter</i>	41
3.3.2.4 <i>Other Factors</i>	42
3.4 PIEZOCONE PENETRATION TESTING.....	42
3.4.1 <i>Equipment and Procedures</i>	43
3.4.2 <i>CPTU/SPT Correlations</i>	43
3.5 LABORATORY TESTING.....	45
3.6 CONCLUSION.....	46
4. OBSERVATIONS ON PILE BEHAVIOR.....	47
4.1 INTRODUCTION.....	47
4.2 CALTRANS' TESTS.....	47
4.2.1 <i>Bridge 34-0048 (Bayshore Freeway Viaduct)</i>	47
4.2.2 <i>I-880 IPTP</i>	49
4.2.2.1 <i>Effects of Method of Installation on Axial Resistance</i>	51
4.2.2.2 <i>Effects of Toe Condition on Axial Resistance</i>	52
4.2.2.3 <i>Effect of Prior Compression Test on Uplift Resistance</i>	52
4.3 OBSERVATIONS.....	53
4.3.1 <i>General</i>	53
4.3.2 <i>Effects of Method of Installation on Axial Resistance</i>	54
4.3.2.1 <i>Findings from Caltrans' Tests</i>	54
4.3.2.2 <i>O'Neill et al. 1990</i>	54
4.3.2.3 <i>Conclusions</i>	55
4.3.3 <i>Effects of Toe Condition on Axial Resistance</i>	56

4.3.3.1 Findings from Caltrans' Tests.....	56
4.3.3.2 O'Neill and Raines 1991.....	56
4.3.3.3 De Nicola and Randolph 1999	57
4.3.3.4 Conclusions.....	57
4.3.4 Effect of Prior Compression Test on Uplift Resistance	58
4.3.4.1 Findings from Caltrans' Tests.....	58
4.3.4.2 De Nicola and Randolph 1999	58
4.3.4.3 Conclusions.....	59
4.4 OTHER EFFECTS OF INTEREST.....	59
4.4.1 Effect of Direction of Loading on Side Resistance	59
4.4.2 Effect of Setup Time on Axial Resistance in Clay.....	60
4.5 CONCLUSION	62
5. DESCRIPTION OF SIDE RESISTANCE METHODS.....	63
5.1 INTRODUCTION.....	63
5.2 METHODS BASED ON SPT AND LABORATORY TESTS.....	63
5.2.1 Caltrans/FHWA Methods.....	63
5.2.1.1 Tomlinson 1971.....	64
5.2.1.2 Tomlinson 1979.....	66
5.2.1.3 Nordlund 1963.....	67
5.2.2 API Methods.....	71
5.2.2.1 API – Clay	71
5.2.2.2 Dennis and Olson 1983 – Clay.....	72
5.2.2.3 API – Sand.....	74
5.2.2.4 Olson 1990.....	75
5.2.2.5 Toolan et al. 1990.....	77
5.2.3 Methods Based on Recent Instrumented Tests	77
5.2.3.1 Jardine and Chow 1996 – Clay (Imperial College)	78
5.2.3.2 Karlsrud 1999 (NGI).....	81
5.2.4 Other Methods.....	82
5.2.4.1 Decourt 1982.....	82
5.2.4.2 Kraft et al. 1981 – Revised λ -Method.....	83
5.2.5 Application of Methods	83
5.3 METHODS BASED ON CPT AND CPTU.....	84

5.3.1 CPT-Methods from Caltrans' 1989 Study.....	84
5.3.1.1 Bustamante and Gianeselli 1982.....	85
5.3.1.2 Schmertmann 1978.....	87
5.3.2 Recent CPTU-Methods.....	90
5.3.2.1 Eslami and Fellenius 1997.....	90
5.3.2.2 Takesue et al. 1998.....	92
5.3.3 Application of CPT/CPTU-Methods.....	93
5.4 CONCLUSION	95
6. EVALUATION OF SIDE RESISTANCE METHODS	96
6.1 INTRODUCTION.....	96
6.2 STATISTICAL INTERPRETATION.....	96
6.3 METHODS BASED ON SPT AND LABORATORY TESTS	97
6.3.1 Against 26 Uplift Test Piles in Clay/Sand Profiles.....	97
6.3.2 Against 11 Piles in Predominantly Clay Profiles.....	99
6.4 METHODS BASED ON CPT AND CPTU.....	100
6.5 CONCLUSIONS.....	100
7. DEVELOPMENT OF SIDE RESISTANCE METHOD	102
7.1 INTRODUCTION.....	102
7.2 REGRESSION ANALYSES.....	102
7.2.1 Methodology.....	102
7.2.2 Uplift Test Piles	103
7.2.3 Stage 1.....	105
7.2.4 Stage 2.....	107
7.2.5 Stage 3.....	110
7.2.6 Stage 4.....	112
7.3 IMPROVED SPT-METHOD.....	114
7.3.1 Description.....	114
7.3.2 Potential Bias.....	115
7.3.3 Alternative Method in Clay	115
7.3.3.1 Re-Evaluation of UU-Based Clay Methods	115
7.3.3.2 Modified α -Method	117
7.3.4 Additional Recommendations.....	118
7.3.4.1 Oversized Toe Plates.....	118

7.4 CONCLUSION	118
8. DEVELOPMENT OF TOE RESISTANCE METHOD	119
8.1 INTRODUCTION.....	119
8.2 EXISTING METHODS.....	119
8.2.1 Description	119
8.2.1.1 Caltrans/FHWA Methods.....	119
8.2.1.2 Decourt's Method	123
8.2.2 Evaluation.....	123
8.3 REGRESSION ANALYSES	124
8.3.1 Methodology.....	124
8.3.2 Test Piles	126
8.3.3 Stage 1.....	127
8.3.4 Stage 2.....	128
8.3.5 Stage 3.....	130
8.4 IMPROVED SPT-METHOD.....	133
8.4.1 Description	133
8.4.2 Additional Recommendations.....	134
8.4.2.1 Large Diameter Piles.....	134
8.4.2.2 Jetted Piles.....	134
8.4.3 Evaluation.....	135
8.5 CONCLUSION	137
9. RELIABILITY.....	138
9.1 INTRODUCTION.....	138
9.2 METHODOLOGY.....	138
9.3 CALTRANS' CURRENT PRACTICE.....	143
9.3.1 Without an Axial Load Test.....	143
9.3.2 With an Axial Load Test.....	146
9.4 IMPROVED METHOD.....	146
9.5 CONCLUSION	149
10. CONCLUSION.....	151
10.1 SUMMARY.....	151
10.2 IMPROVED METHOD.....	152

10.2.1 Uplift Resistance	152
10.2.1.1 Ultimate Resistance	152
10.2.1.2 Unit Side Resistance	152
10.2.1.3 Modified α -Method	153
10.2.2 Compressive Resistance	154
10.2.3 Additional Recommendations	155
10.2.3.1 Pile Weight	155
10.2.3.2 Oversized Toe Plates	155
10.2.3.3 Large Diameter Piles	156
10.2.3.4 Jetted Piles	156
10.3 FACTORS OF SAFETY	157
10.4 RECOMMENDATIONS FOR FUTURE RESEARCH	158
10.4.1 Site Characterization for Piles in Gravel and Rock	159
10.4.2 Pile Acceptance Criteria	159
10.4.3 Group Behavior	160
11. REFERENCES	161
12. VITA	169

LIST OF TABLES

Table 2.1 Test Pile Composition.....	9
Table 2.2 Bridge Details.....	11
Table 2.3 Test Pile Details.....	15
Table 2.4 Soil Profiles of Test Piles.....	26
Table 3.1 Sampling Rod Specifications.....	38
Table 3.2 Rod Energy Ratio.....	40
Table 3.3 Correction Factors for Rod Length (Skempton 1986).....	40
Table 3.4 Correction Factors for Borehole Diameter (Skempton 1986).....	42
Table 3.5 Soil Behavior Type.....	45
Table 4.1 Bayshore Freeway Viaduct Sites.....	48
Table 4.2 Results of Bayshore Freeway Viaduct Tests.....	49
Table 4.3 I-880 IPTP Sites.....	50
Table 4.4 Results of I-880 IPTP Tests.....	50
Table 4.5 Effects of Method of Installation at I-880 IPTP.....	51
Table 4.6 Effects of Toe Condition at I-880 IPTP.....	52
Table 4.7 Effect of Prior Compressive Test on Uplift Test at I-880 IPTP.....	53
Table 4.8 Unit Side Resistance from Laboratory Model Tests (O'Neill et al. 1990)	55
Table 5.1 Design Parameters for Cohesionless Siliceous Soil (API 1993).....	74
Table 5.2 Soil Properties Assumed for RP 2A Analyses (Olson 1990).....	75
Table 5.3 Soil Properties (Olson 1990).....	76
Table 5.4 Values of Skin Friction in Revised Method (Toolan et al. 1990).....	77
Table 5.5 Correlation between Density Descriptions and N_{corr} (Peck et al. 1974).....	77
Table 5.6 Performance of CPT-Methods for 13 Driven Piles (Richman and Speer 1989).....	85
Table 5.7 Distribution of Pile Types (Bustamante and Ganeselli 1982).....	86
Table 5.8 Design Parameters for Side Resistance (Bustamante and Ganeselli 1982).....	87
Table 5.9 Coefficients for Side Resistance in Sand (Briaud and Miran 1992).....	90
Table 5.10 Adhesion Factors from Soil Type (Eslami and Fellenius 1997).....	92
Table 6.1 Evaluation of Existing Methods.....	98

Table 6.2 Evaluation of Clay Methods with Decourt's Sand Method	99
Table 6.3 Evaluation of CPT/CPTU-Methods	100
Table 7.1 Uplift Test Piles in Regression Analyses for SPT-Method.....	104
Table 7.2 Stage 1 Results	106
Table 7.3 Set 1 Trials	106
Table 7.4 Stage 2 Results	107
Table 7.5 Set 3 Performance by Subset.....	108
Table 7.6 Stage 3 Results	110
Table 7.7 Stage 4 Results	112
Table 7.8 Performance of Improved Side Resistance Method by Subset	113
Table 7.9 Evaluation of Clay Methods with Improved Sand Method	116
Table 7.10 Performance of Dennis and Olson's Clay Method by Subset.....	116
Table 8.1 Evaluation of Existing Toe Resistance Methods.....	124
Table 8.2 Test Piles in Regression Analyses for Toe Resistance Method	127
Table 8.3 Stage 1 Results	127
Table 8.4 Stage 2 Results	128
Table 8.5 Stage 3 Results	130
Table 8.6 Performance of Set 3 by Subset.....	132
Table 8.7 Plug Mobilization Factor F_p	134
Table 8.8 Performance of Improved Toe Resistance Method by Subset	135
Table 9.1 Evaluation of Caltrans' Methods against 45 Uplift Tests.....	145
Table 9.2 Evaluation of Caltrans' Methods against 46 Compressive Tests	145
Table 9.3 Reliability of Caltrans' Methods for $Q_d/Q_m = 1$	145
Table 9.4 Factors of Safety for Reference Values of P	146
Table 10.1 Plug Mobilization Factor F_p	155

LIST OF FIGURES

Figure 2.1 Fleming's Extrapolation: Graphical Construction	7
Figure 2.2 Fleming's Extrapolation: Hyperbolic Curve.....	7
Figure 2.3 Uplift Test Piles (118) by Pile Type and Method of Installation.....	10
Figure 2.4 Compressive Test Piles (88) by Pile Type and Method of Installation	10
Figure 2.5 Northern California Bridges.....	13
Figure 2.6 Southern California Bridges.....	13
Figure 2.7 Profile Compositions of Test Piles.....	31
Figure 2.8 Cumulative Probability Plot of Setup Times	32
Figure 4.1 Effect of Setup Time on Axial Resistance in Clay (Seed and Reese 1957, cited by Vesic 1977).....	61
Figure 5.1. Adhesion Factors for Piles in Clay: Case I (Tomlinson 1971)	65
Figure 5.2. Adhesion Factors for Piles in Clay: Case II (Tomlinson 1971).....	65
Figure 5.3 Adhesion Factors for Piles in Clay: Case III (Tomlinson 1971).....	66
Figure 5.4 Adhesion Values for Piles in Cohesive Soils (Hannigan et al. 1997) .	67
Figure 5.5. Relationship between A and δ/ϕ (Nordlund 1963).....	69
Figure 5.6. Relationship between N_{corr} and ϕ (Peck et al. 1974)	69
Figure 5.7. Design Curve for Evaluating K_s where $\delta = \phi$ (Nordlund 1963).....	70
Figure 5.8. Correction Factor for K_s when $\delta \neq \phi$ (Nordlund 1963)	70
Figure 5.9 Adhesion Factors for Piles in Clay (Dennis and Olson 1983a)	73
Figure 5.10 Correction Factor F_L for Pile Penetration (Dennis and Olson 1983a)	73
Figure 5.11 Trend for $\tan(\delta_{ultimate})$ Values from IC Ring Shear Tests on North Sea Clays (Jardine and Chow 1996)	79
Figure 5.12 Relationship between ψ and OCR	81
Figure 5.13 Relationship between β and OCR (Karlsrud 1999).....	82
Figure 5.14 Adhesion Factors for Piles in Clay (Briaud and Miran 1978)	89
Figure 5.15 Adhesion Factors for Piles in Sand (Briaud and Miran 1992).....	89
Figure 5.16 Soil Classification Chart (Eslami and Fellenius 1997).....	92
Figure 5.17 Adhesion Factors from Δu (Takesue et al. 1998).....	93
Figure 5.18 Soil Classification Chart (Douglas and Olsen 1981).....	95
Figure 7.1 Effect of Setup Time on Q_m/Q_c in Profiles Containing Clay (Final Model).....	105

Figure 7.2 Scatter Diagram for Set 3 in Stage 2	108
Figure 7.3 Cumulative Probability Plot of Set 3 in Stage 2	109
Figure 7.4 Scatter Diagram of Set 4 in Stage 3.....	111
Figure 7.5 Cumulative Probability Plot for Set 4 in Stage 3	111
Figure 7.6 Scatter Diagram of Set 5 in Stage 4.....	112
Figure 7.7 Cumulative Probability Plot for Set 5 in Stage 4	113
Figure 7.8 Effect of Embedment on Q_c/Q_m	115
Figure 7.9 Adhesion Factors for Piles in Clay (Dennis and Olson 1983a)	117
Figure 8.1. Bearing Capacity Factor N_q (Thurman 1964)	121
Figure 8.2. Depth Factor α (Thurman 1964)	121
Figure 8.3. Relationship between N_{corr} and ϕ (Peck et al. 1974)	122
Figure 8.4. Limiting Unit Toe Resistance (Meyerhof 1976).....	122
Figure 8.5 Scatter Diagram for Set 3 in Stage 2	129
Figure 8.6 Cumulative Probability Plot for Set 3 in Stage 2	130
Figure 8.7 Scatter Diagram for Set 3 in Stage 3	131
Figure 8.8 Cumulative Probability Plot for Set 3 in Stage 3	132
Figure 8.9 Scatter Diagram of Improved Method.....	136
Figure 8.10 Cumulative Probability Plot of Improved Method.....	136
Figure 9.1 Average Normalized Load-Displacement Curve in Uplift	139
Figure 9.2 Average Normalized Load-Displacement Curve in Compression	140
Figure 9.3 Plot of Q_c/Q_m for 97 Uplift Test Piles on Log-Normal Paper	141
Figure 9.4 Plot of Q_c/Q_m for 71 Compressive Test Piles on Log-Normal Paper	141
Figure 9.5 Correlation between N_{60} and s_u	144
Figure 9.6 Relationship between FS and P	147
Figure 9.7 Caltrans' Reduction in Piling with Improved Method	148
Figure 10.1 Adhesion Factors for Piles in Clay (Dennis and Olson 1983a)	154

1. INTRODUCTION

1.1 BACKGROUND

In 1989, the California Department of Transportation (Caltrans) conducted a study to evaluate six existing methods of predicting the compressive resistance of single piles using electric cone penetration test (CPT) data (Richman and Speer 1989). The database used for this previous study consisted of 32 compressive load tests on bored and driven piles at 27 sites.

Continuing this line of research, Caltrans' New Technology and Research Program funded a project at The University of Texas at Austin in 1998. As established in the project's first oversight panel meeting, Caltrans' primary objectives for the project were (1) to create an electronic database of Caltrans' axial static load test data, (2) to evaluate existing methods and develop improved methods of predicting the compressive and uplift resistances of single piles, and (3) to collect additional site characterization data needed for the evaluation and development of these predictive methods. Unlike the 1989 study, which only examined predictive methods using CPT data, this project was to examine predictive methods using any feasible site characterization technique, including both laboratory and in situ testing. Through the implementation of the improved predictive methods produced by the project, Caltrans hopes to be able to design more efficient pile foundations and reduce the overall cost of both new bridges and seismic retrofits of existing bridges.

1.2 DATA

Although Caltrans' archives contain axial load test data for driven and bored piles, the data are predominantly for driven piles, and the scope of current the project was ultimately limited to untapered driven piles. The database developed for this project contains data from 319 load tests on 227 untapered driven piles in 161 pile groups at 75 bridge locations throughout California. In all of these tests, only pile-head load and displacement were measured.

In terms of site characterization data, Caltrans' archives provided data from numerous borings, with the data consisting primarily of visual classifications and standard penetration test (SPT) results. However, since many modern predictive methods rely on data from other in situ or laboratory tests, it was necessary to collect additional data as part of the project. In the project's field exploration phase, 46 borings and 56 piezocone penetration test (CPTU) soundings were made to provide additional site characterization data needed for the evaluation and development of predictive methods. Both pushed samples and driven SPT samples were obtained from these borings. Laboratory tests were performed on these samples. The laboratory tests included unconsolidated-undrained triaxial compression (UU) tests, one-dimensional vertical consolidation tests, Atterberg liquid limit (LL) and plastic limit (PL) determinations, and sieve analyses.

1.3 OBJECTIVES

As a graduate research assistant (GRA) on the project, the author was charged with the completion of two of Caltrans' three project objectives: (1) the creation of an electronic database of Caltrans' axial load test data and (2) the evaluation of existing methods and development of improved methods of predicting the compressive and uplift resistances of single untapered driven piles. In addition, the author shared with another

GRA the responsibility of completing the project's third objective: the collection of additional site characterization data.

The primary objective of this dissertation is the evaluation of existing methods and the development of improved methods for the prediction of side resistance in both uplift and compression. To this end, sixteen existing methods of predicting side resistance are evaluated against the uplift tests from Caltrans' archives. The best performing methods in this evaluation are then modified and re-calibrated. Using the improved side resistance methods, the author then analyzes the compressive tests from Caltrans' archives to establish an empirical relationship between uplift side resistance and compressive side resistance and to develop a companion toe resistance method. Finally, the reliability of these improved methods is compared with the reliability of Caltrans' current methods, and recommendations regarding appropriate factors of safety for the improved methods are given.

2. AXIAL LOAD TEST DATA

2.1 INTRODUCTION

All of the axial load test data used in this dissertation were furnished by Caltrans. These load tests were performed to verify the axial resistance of piles to be used on Caltrans' projects. These projects were either new bridges or seismic retrofits of existing bridges. None of the test piles were instrumented. The only measurements were of pile-head load and displacement.

The axial load test data used in this dissertation are summarized in this chapter. For a more straightforward discussion, the data are organized by pile rather than by test. In this chapter, the selection criteria used to determine which test piles would be included in the analyses are discussed, the methods used to define measured ultimate resistance are described, and the data for the 155 test piles included in the analyses are presented. This presentation includes discussions of the test pile locations, pile details, pile types, methods of installation, soil profiles, setup times, and load test procedures.

2.2 SELECTION CRITERIA

The author's database contains load test data for 227 untapered driven piles. However, only 155 of these piles were included in the analyses presented in this dissertation. The included piles were those with adequate site characterization data and at least one load test, in either uplift or compression, run to sufficient displacement for the measured ultimate resistance to be defined by both Caltrans' offset-limit and Fleming's extrapolation (Fleming 1992). To be included, uplift test piles had to have a

representative boring or piezocone penetration test (CPTU) sounding extending to the pile toe, and compressive test piles had to have a boring or sounding extending to a depth of four pile diameters below the pile toe. The excluded test piles were primarily those which were loaded to such a small pile-head displacement that only the elastic compression/extension of the pile could be discerned.

2.3 DEFINITIONS OF MEASURED ULTIMATE RESISTANCE

To evaluate and develop predictive methods, the calculated ultimate resistance (Q_c) had to be compared to a measured ultimate resistance (Q_m). In this dissertation Q_m is defined by Fleming's extrapolation. However, the measured ultimate resistance defined by Caltrans' offset limit (Q_{CT}) is also used since this value has particular significance to Caltrans. Caltrans defines the measured ultimate resistance as the pile-head load at 12.7 mm of pile-head displacement and the allowable resistance as 50% of Q_{CT} .

(D.S.-m.v)

Fleming's extrapolation is a modification of the Chin-Konder extrapolation (Chin 1970, cited by Fellenius 1996; Konder 1963). The extrapolation, as presented in this dissertation, was adapted from Fleming's method for predicting load-displacement behavior. In the extrapolation, Q_m is graphically defined as illustrated in Figure 2.1. Computationally, Q_m is defined using Equations 2.1, 2.2 and 2.3. The straight line in Figure 2.1 corresponds to the dashed curve in Figure 2.2.

$$Q = \frac{S_p}{mS_p + b} \quad (2.1)$$

$$\frac{S_p}{Q} = mS_p + b \quad (2.2)$$

$$Q_m = \frac{1}{m} \quad (2.3)$$

where,

Q = pile-head load

S = pile-head displacement

S_e = elastic compression/extension of pile

$S_p = S - S_e$ = corrected displacement in Figure 2.1.

m = slope of straight line in Figure 2.1

$b = S_p/Q$ -intercept of straight line in Figure 2.1

In this dissertation, S_e was calculated as the elastic compression/extension of a free-standing column using Equation 2.4.

$$S_e = \frac{Q L}{A E} \quad (2.4)$$

where,

L = length of pile below point of measurement of S

A = cross-sectional area of pile

E = Young's modulus of pile material

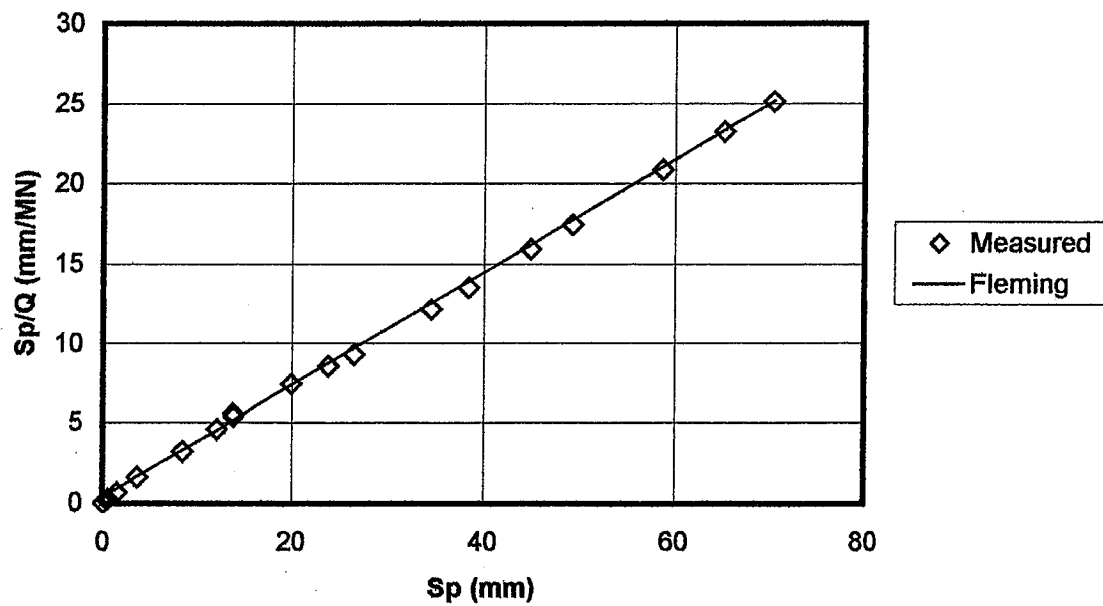


Figure 2.1 Fleming's Extrapolation: Graphical Construction

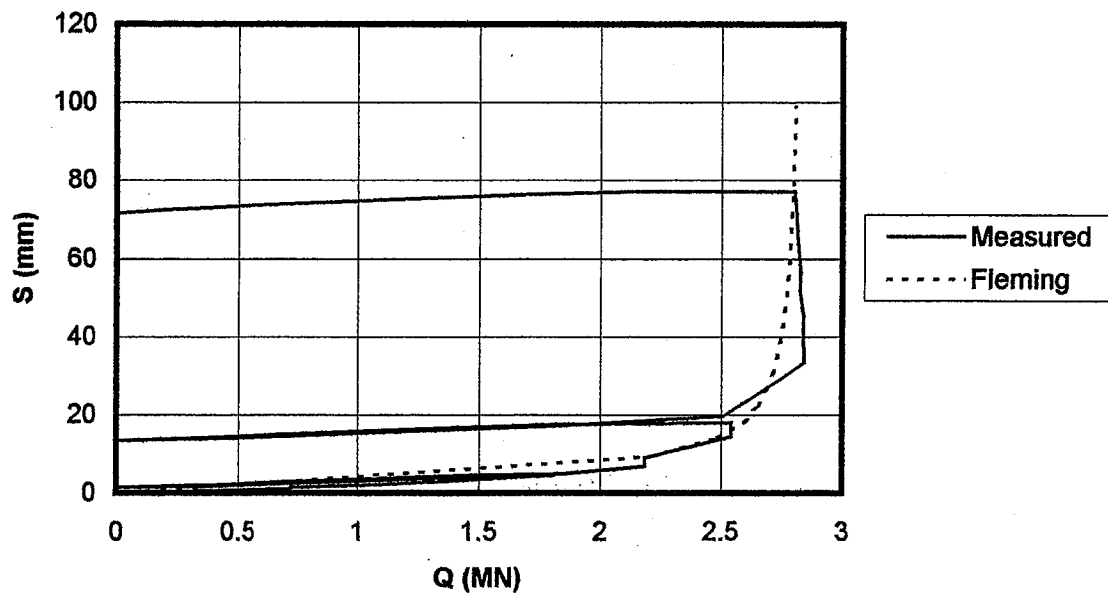


Figure 2.2 Fleming's Extrapolation: Hyperbolic Curve

An extrapolation, rather than an offset limit, was selected to define Q_m so that it would correspond as closely as possible to the load associated with a plunging or pullout failure and to allow for the inclusion of tests not run to clear plunging or pullout failure. Of the extrapolations evaluated, Fleming's performed the best in this role, primarily because of its consideration of elastic compression/extension of the pile. Although Davisson's offset-limit (Davisson 1972, cited by Fellenius 1996) is probably the definition of measured ultimate resistance most commonly used in the U.S., it was not used in this dissertation because it yields unreasonably low values of measured ultimate resistance in uplift tests.

2.4 TEST PILES

In Table 2.1, the composition of the database's test piles is presented in terms of pile type, method of installation, and direction of loading. The pile types are open-toed steel pipe piles, closed-toed steel pipe piles, steel H-piles, solid precast reinforced concrete piles and hollow precast reinforced concrete piles. The steel piles are further categorized by method of installation: impact-driven and vibro-driven. The number of piles in each of these eight categories is provided in the "Total" column. In each category, the numbers of piles with compressive tests and uplift tests are provided in the "Comp." and "Uplift" columns, respectively. The numbers of piles with both compressive and uplift tests are given in the "Both" column.

Table 2.1 Test Pile Composition

Pile Type	No. of Piles			
	Total	Comp.	Uplift	Both
Open-Toed Steel Pipe Piles (Impact)	56	33	49	26
Open-Toed Steel Pipe Piles (Vibratory)	13	8	13	8
Closed-Toed Steel Pipe Piles (Impact)	32	21	23	12
Closed-Toed Steel Pipe Piles (Vibratory)	2	2	1	1
Steel H-Piles (Impact)	17	4	15	2
Steel H-Piles (Vibratory)	7	0	7	0
Solid Precast Concrete Piles	26	18	10	2
Hollow Precast Concrete Piles	2	2	0	0
TOTALS	155	88	118	51

The distributions of the 118 piles with uplift tests and the 88 piles with compressive tests are illustrated in Figure 2.3 and Figure 2.4, respectively. Given these distributions, it is clear that impact-driven steel pipe piles are the most important category of piles for this dissertation. The pile types and methods of installation are described later in this chapter.

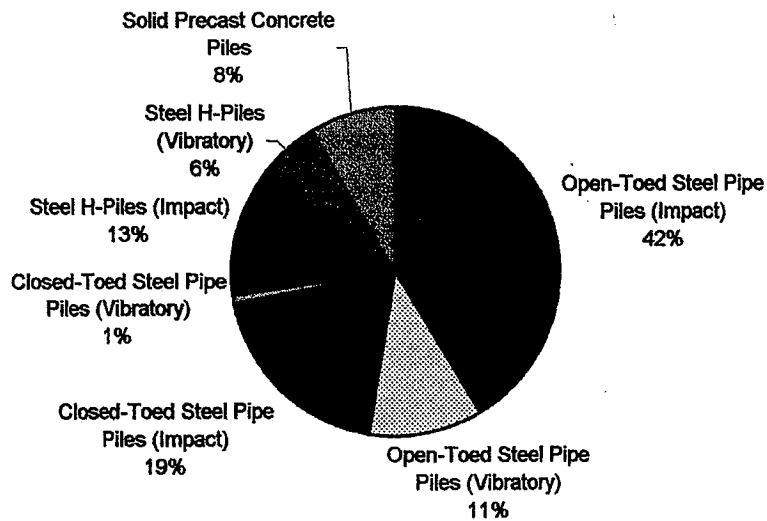


Figure 2.3 Uplift Test Piles (118) by Pile Type and Method of Installation

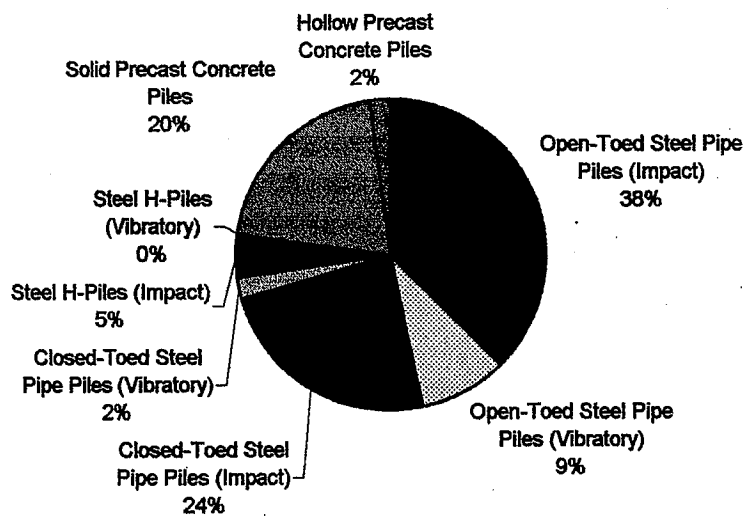


Figure 2.4 Compressive Test Piles (88) by Pile Type and Method of Installation

2.4.1 Locations

The 155 test piles are located in 115 pile groups at 55 bridges across California. Identifying information for these 55 bridges is given in Table 2.2. Figure 2.5 and Figure 2.6 show the locations of these 55 bridges. In these maps, an individual bridge is marked by a pushpin while a group of concentrated bridges is marked by a cluster of three squares. The only bridge not shown on these two maps is Bridge 04-0017, which is located approximately 160 km south of the Oregon border, just south of Eureka, near the coast.

Table 2.2 Bridge Details

Number	Name	County	City	Route
04-0017	Van Duzen River Bridge	Humboldt	Fortuna	101
20-0251	Central Cloverdale Undercrossing	Sonoma	Cloverdale	101
20-0254	Russian River Bridge	Sonoma	Guerneville	116
22-0032	Sacramento River Bypass	Yolo	Bryte	16
22-0062	Mullen Overhead	Yolo	Woodland	113
28-0249	West Connector Overcrossing	Contra Costa	Concord	4
29-0013	Stanislaus River Bridge	San Joaquin	Modesto	99
33-0025	San Francisco-Oakland Bay Bridge	Alameda	Oakland	80
33-0393	West Grand Ave. Viaduct	Alameda	Oakland	880
33-0611	East Bay Viaduct	Alameda	Oakland	880
33-0612	Port of Oakland Connector Viaduct	Alameda	Oakland	880
34-0046	Southern Freeway Viaduct	San Francisco	San Francisco	280
34-0070	280/101 Retrofit	San Francisco	San Francisco	101
34-0088	Bayshore Freeway Viaduct	San Francisco	San Francisco	80
34-0100	China Basin Viaduct	San Francisco	San Francisco	280
35-0038	Dumbarton Bridge	Alameda	Fremont/Newark	84
35-0284	Mariners Island Blvd. Overhead	San Mateo	San Mateo	97
37-0011	Bassett St. Overhead	Santa Clara	San Jose	87
37-0270	Three Connector Viaduct	Santa Clara	San Jose	87
37-0279	First St. Separation	Santa Clara	San Jose	101
37-0410	Guadalupe Connector Viaduct	Santa Clara	San Jose	87
44-0030	San Lorenzo Creek Bridge	Monterey	King City	198
44-0216	Salinas River Bridge	Monterey	Marina	1
46-0252	Linwood St. Bridge	Tulare	Visalia	198

Number	Name	County	City	Route
46-0254	Demaree St. Bridge	Tulare	Visalia	198
46-0255	County Center Bridge	Tulare	Visalia	198
49-0133	Tefft St. Overcrossing	San Luis Obispo	Nipomo	101
51-0273	Garden St. Seal Slab	Santa Barbara	Santa Barbara	101
51-0276	State St. Seal Slab	Santa Barbara	Santa Barbara	101
52-0118	Santa Clara River Bridge	Ventura	Fillmore	23
52-0178	Ventura Underpass	Ventura	Ventura	2
52-0217	Chestnut St. Off-Ramp Overhead	Ventura	Ventura	2
52-0271	Nyeland Acres Overcrossing	Ventura	Ventura	2
53-0527	Route 2/5 Separation	Los Angeles	Los Angeles	5
53-1181	Griffith Park Off-Ramp Overcrossing	Los Angeles	Los Angeles	5
53-1193	Los Coyotes Diagonal Undercrossing	Los Angeles	Long Beach	405
53-1424	Elysian Viaduct	Los Angeles	Los Angeles	5
53-1851	Route 90/405 Separation Retrofit	Los Angeles	Culver City	90
53-2733	HOV Viaduct No. 1	Los Angeles	Los Angeles	110
53-2791	LaCienega-Venice Separation	Los Angeles	Los Angeles	10.
54-0823	Colton Interchange	San Bernardino	Ontario	10
54-0967	Southeast Connector Separation	San Bernardino	Fontana	15
55-0438	Northeast Connector Overcrossing	Orange	Costa Mesa	55
55-0642	Southbound Off-Ramp Overcrossing	Orange	Tustin	5
55-0681	Route 57/5 Separation	Orange	Orange	5
55-0689	HOV Connector Viaduct	Orange	Tustin	5
55-0794	WS Connector Overcrossing	Orange	Yorba Linda	231
57-0488	San Diequito River Bridge	San Diego	San Diego	5
57-0720	Mission Valley Viaduct	San Diego	San Diego	8
57-0783	Northeast Connector Overcrossing	San Diego	San Diego	5
57-0982	Spring Canyon Rd. Undercrossing	San Diego		52
57-0989	Route 5/56 Separation	San Diego	San Diego	5
57-1017	Mission Ave. Viaduct	San Diego	Oceanside	76
I-5/I-8 IPTP	I-5/I-8 Interchange IPTP	San Diego	San Diego	5
I-880 IPTP	I-880 Replacement Project IPTP	Alameda	Oakland	880

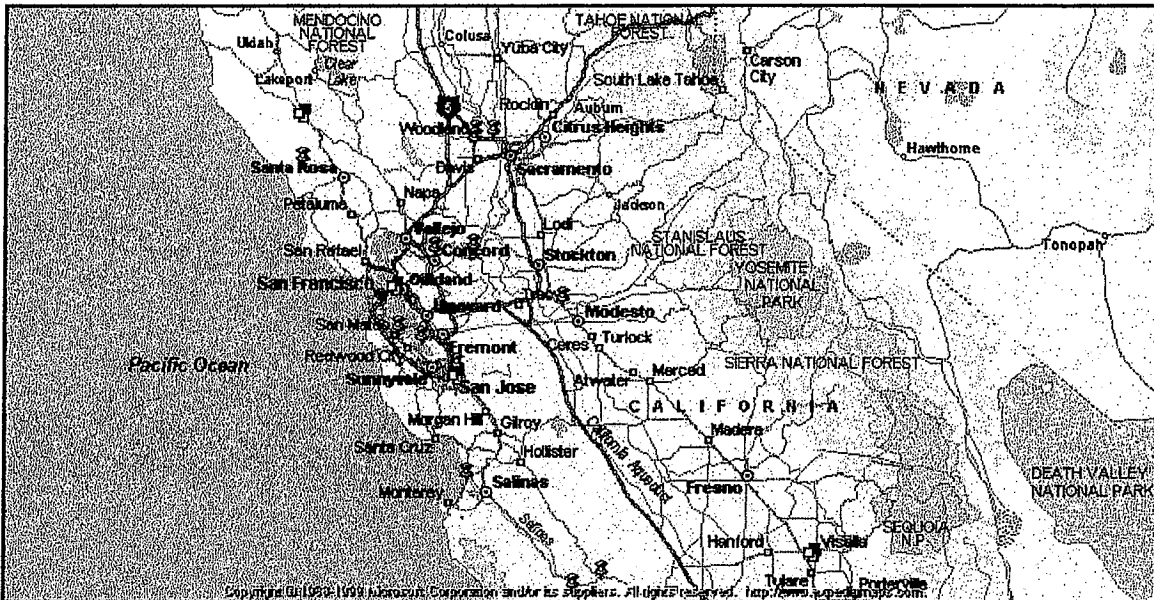


Figure 2.5 Northern California Bridges

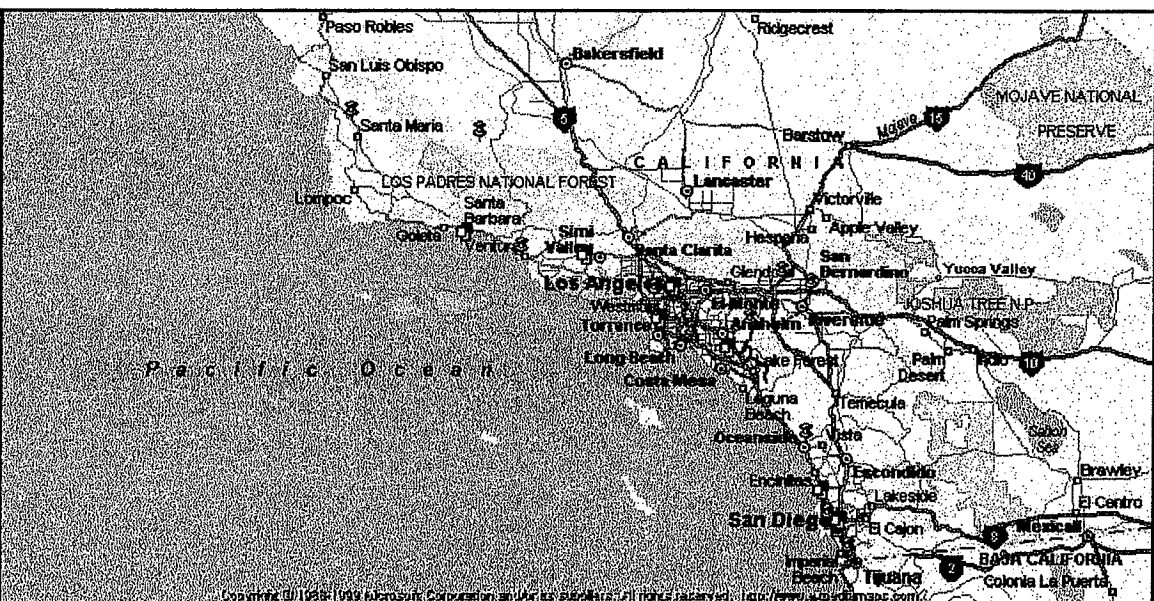


Figure 2.6 Southern California Bridges

2.4.2 Pile Details

The details of the uplift test piles are provided in Table 2.3. The "Embed." column contains the pile embedment or length of pile in contact with soil, from the pile mudline to the pile toe. The pile mudline is the upper boundary of the soil in contact with the side of the pile. The "Depth Range" columns provides the pile mudline depth on the left side and the pile toe depth on the right side. The depths are referenced to the ground surface at the time of the test.

If a vibratory hammer was used to install the pile, even in conjunction with an impact hammer, an "X" indicates this in the "Vibro-Driven" column. The "Jetted" column similarly indicates the use of jetting to install the pile. An "X" in the "Cased" column indicates that at the time of testing the pile was cased over a portion of its embedment, between the pile mudline and the pile toe. In the "Predrilled" and "Relief-Drilled" columns, an "X" indicates that predrilling or relief drilling was used in the installation of the pile. In relief drilling a portion of the soil plug inside the open-toed steel pipe pile is removed to reduce driving resistance to facilitate driving under difficult conditions.

The leftmost columns, " Q_{mu} " and " Q_{mc} ", are respectively the measured ultimate resistances in uplift and compression as defined by Fleming's extrapolation. A dash in one of these two columns indicates that the measured ultimate resistance for that particular direction of loading could not be determined, either because no test was performed in this direction or because the test was not run to sufficient displacement for Fleming's extrapolation to be applied.

Table 2.3 Test Pile Details

Bridge	Group	Pile	Type	Width (mm)	Embed. (m)	Depth Range (m)		Vibrated	Jetted	Cased	Predrilled	Relief Drilled	Q_{ms} (MN)	Q_{mc} (MN)
04-0017	Pier 2	72	HP	370	7.0	7.2	14.2						2.41	-
	Pier 3	108	HP	370	13.4	10.7	24.1						2.46	-
20-0251	Abutment 2R	28	SC	305	16.0	0.8	16.8						-	1.42
20-0254	Pier 3	14 (#1)	OP	610	17.4	7.6	25.0						0.53	3.02
22-0032	Pier 37	2	SC	305	23.8	0.8	24.6						-	1.25
22-0062	Bent 2R	21	SC	305	15.0	2.1	17.1						-	1.78
28-0249	Bent 8	20	OP	406	10.7	2.4	13.1						0.73	-
29-0013	Bent 6	1	CP	406	16.6	0.0	16.6	X					-	0.82
33-0025	Bent E28L	17	OP	610	12.8	1.6	14.4						1.06	2.07
	Bent E31R	1	OP	610	13.1	3.9	17.0						1.38	2.76
33-0393	Bent 3F	27	CP	610	21.2	3.3	24.4			X			1.89	2.64
33-0611	Bent 13L	8	CP	610	21.5	2.4	23.9			X			2.96	-
	Bent 17R (LT)	17	CP	610	16.2	3.4	19.5						0.99	3.42
	Bent 29R	23	CP	610	20.3	2.7	23.0			X			2.02	3.00
33-0612	Bent 10NC1	3	OP	1067	26.2	2.7	29.0			X			2.84	3.81
	Bent 17NC1 (LT)	6	OP	1067	27.7	1.8	29.6			X			4.11	4.59
	Bent 27NC (RT)	9	OP	1067	25.3	2.7	28.0						4.32	5.73
	Bent 31NC (LT)	9	OP	1067	22.3	3.7	26.0						4.34	5.54
34-0046	Bent 34R	17	OP	457	10.1	2.1	12.1						-	3.51
	Bent 43AL	13	OP	610	10.7	2.1	12.8						-	3.38
	Bent 45AR	13	OP	610	11.3	3.0	14.3						-	5.69
	Bent 52C	21 (#1)	CP	610	17.4	2.1	19.5				X		0.44	-
		21 (#2)	CP	508	17.8	2.1	19.9				X		0.71	-
	Bent 52R	15	CP	610	23.6	2.1	25.7						1.02	-
	Bent B-88	D	OP	406	2.9	3.4	6.2						0.42	-
	Bent SE-68	11	CP	406	15.5	0.0	15.5						2.04	-
	Bent SE-71	4	OP	406	25.0	0.0	25.0	X					1.33	-
	Tension Pile Test Site	48	OP	406	25.9	6.1	32.0							1.43
49		OP	406	26.1	6.1	32.2							1.30	1.17
34-0070	Bent WU-28	19	OP	406	9.0	21.8	30.8				X		1.68	-
34-0088	Site A	2	OP	610	13.0	3.0	16.0	X					2.94	4.89
		3	OP	610	9.8	3.0	12.8						2.67	4.47
	Site B	1	OP	610	15.7	3.7	19.4						3.60	-

Bridge	Group	Pile	Type	Width (mm)	Embed. (m)	Depth Range (m)		Vibrated	Jetted	Cased	Predrilled	Relief Drilled	Q_{mu} (MN)	Q_{mc} (MN)	
	Site C	2	OP	610	15.5	3.7	19.2	X					0.64	2.22	
		1	OP	406	16.0	2.1	18.1							1.78	4.24
		2	OP	406	15.8	2.1	18.0	X						1.53	2.78
	Site D	2	OP	610	16.2	3.0	19.2	X				X		2.56	3.56
	Site E	1	OP	610	24.1	4.3	28.3							0.90	0.95
		2	OP	610	23.8	4.3	28.0	X						0.86	0.81
	Site F	1	OP	610	14.9	5.5	20.4							2.00	4.02
		2	OP	610	14.8	5.5	20.3	X						0.89	2.58
	Site G	5	OP	610	24.7	0.0	24.7			X				1.36	1.39
34-0100	Bent 20	14	HP	362	18.1	2.1	20.2	X					1.88	-	
	Bent 22, Column 4	4	HP	362	23.8	2.0	25.8						2.54	-	
	Bent 23, Column 4	5	HP	362	25.3	2.3	27.6						2.20	-	
	Bent 29, Column 2	19	HP	362	20.3	1.7	21.9						1.96	-	
	Site 2	2	HP	362	20.7	4.3	25.0	X					3.39	-	
	Site 3	3	HP	362	28.2	3.8	32.0	X					2.43	-	
	Site 4	4	HP	370	35.1	3.7	38.7	X					3.91	-	
	Site 5	7	HP	370	53.6	3.7	57.3	X					4.43	-	
	Site 6	8	HP	370	46.3	3.7	50.0	X					4.43	-	
	Site 7	10	HP	370	33.5	3.7	37.2	X					2.84	-	
35-0038	Pier 04	33	CP	508	16.2	1.8	18.0						-	1.71	
	Pier 16	29	CP	508	20.7	2.4	23.2						-	1.25	
	Pier 18	3	HC	1372	13.4	0.0	13.4		X				-	3.20	
	Pier 23	9	HC	1372	12.0	0.0	12.0		X				-	3.51	
	Pier 31	24	CP	508	16.2	0.5	16.6							-	1.07
		36	CP	508	16.2	0.5	16.6							-	1.11
	Pier 36	24	CP	508	20.1	1.2	21.3							-	1.60
		34	CP	508	20.1	1.2	21.3							-	1.85
		35	CP	508	22.6	1.2	23.7							-	1.51
36		CP	508	20.1	1.2	21.3							-	1.47	
35-0284	Bent 8B	3	SC	305	30.0	2.7	32.7						-	1.25	
37-0011	Bent 4	8	SC	305	18.3	2.0	20.3						-	1.78	
37-0270	Line GC-4, Bent 14	25	CP	356	15.5	1.0	16.6						0.54	1.11	
	Line GD-2, Bent 06	22 (#1)	CP	356	14.0	1.1	15.0						0.29	0.80	
		22 (#2)	CP	356	15.8	1.1	16.9						0.49	0.76	

Bridge	Group	Pile	Type	Width (mm)	Embed. (m)	Depth Range (m)		Vibrated	Jetted	Cased	Predrilled	Relief Drilled	Q_{mc} (MN)	Q_{mc} (MN)
	Line GD-2, Bent 14	22	CP	356	20.7	1.0	21.7						0.91	-
	Line GD-4, Bent 03	22	CP	356	14.9	1.0	15.9						0.62	1.67
37-0279	Bent 3R-2	1	CP	356	17.4	2.4	19.8				X		0.67	-
	Bent 6L-2	11	CP	356	18.3	1.7	20.0						0.76	-
37-0410	Bent 3	34	SC	305	11.1	2.3	13.5						-	0.93
44-0030	Pier 2	13	OP	356	11.9	3.3	15.2						1.41	1.87
	Pier 3	13	OP	356	12.2	2.9	15.1						2.06	-
44-0216	Test Group	Test Pile	OP	1829	34.7	0.0	34.7						6.74	6.73
46-0252	Bent 2	Test Pile	SC	381	5.8	8.0	13.8						-	2.02
46-0254	Bent 2	Test Pile	SC	381	5.5	8.5	14.0						-	1.78
46-0255	Bent 2	Test Pile	SC	381	7.7	8.9	16.6						-	1.80
49-0133	Bent 2, Column 1	11	SC	356	6.1	0.0	6.1						0.86	-
51-0273	Station 20+04	Test Pile	SC	305	7.6	6.4	14.1						0.71	1.07
	Station 22+58	2	SC	305	7.3	6.2	13.6						0.89	-
51-0276	Bent 5	907	SC	305	7.0	8.4	15.4						0.89	-
52-0118	Pier 02	25	HP	309	10.4	8.1	18.4						1.27	2.45
	Pier 11	406	HP	309	10.8	7.6	18.4						1.07	2.89
52-0178	Abutment 3	113	OP	305	11.9	1.4	13.4						-	1.25
52-0217	Bent 6	101	OP	305	16.3	2.9	19.2						-	1.24
52-0271	Bent 3	24	CP	273	10.6	0.8	11.4						-	0.88
53-0527	Ramp 7, Bent 10	31	HP	257	15.5	1.2	16.8						0.36	-
		35	HP	257	13.7	1.2	14.9						0.18	-
	Ramp 8, Bent 04	27	HP	257	10.5	0.5	11.0						0.67	-
53-1181	Bent 5	25	HP	257	9.8	3.7	13.4						1.60	-
53-1193	Bent 6	5	OP	356	14.9	1.7	16.7						1.59	-
53-1424	Ramp 18, Bent 5	8	OP	340	14.6	0.0	14.6						0.55	-
53-1851	Bent 21, Footing A	2	OP	406	11.3	0.4	11.7						0.72	-
53-2733	Bent 02	36	SC	356	10.4	1.7	12.1						-	1.98
	Bent 20	Test Pile	SC	356	12.2	2.3	14.5				X		-	1.78
53-2791	Bent 5	71	HP	362	16.5	2.4	18.9						1.96	-
54-0823	Smooth Pile Group	#1-2	OP	406	10.8	9.5	20.3						-	2.32
		#1-4	OP	406	7.8	9.5	17.3						1.13	1.79
54-0967	Bent 09	Test Pile	HP	362	9.4	2.6	12.0						1.51	-
	Bent 13	Test Pile	HP	362	14.0	3.0	17.0						1.00	2.85

Bridge	Group	Pile	Type	Width (mm)	Embed. (m)	Depth Range (m)		Vibrated	Jetted	Cased	Predrilled	Relief Drilled	Q_{mu} (MN)	Q_{mc} (MN)
55-0438	Bent 9	22	OP	305	12.2	2.3	14.5						1.07	-
55-0642	Bent 6	18	SC	356	13.7	5.5	19.2				X		1.35	-
		21	SC	356	13.7	5.5	19.2				X		-	2.20
55-0681	Bent 5	1C	SC	356	11.9	2.4	14.3						1.60	-
		3C	SC	356	21.0	2.4	23.5						-	2.58
		4S	HP	362	22.9	2.4	25.3						-	2.58
55-0689	Bent 16	16	SC	356	16.3	3.0	19.4				X		-	2.14
		21	SC	356	16.3	3.0	19.4				X		1.42	-
55-0794	Bent 8	23	SC	356	13.0	4.1	17.1				X		0.93	2.49
		47	HP	362	13.9	4.1	18.0						1.73	2.98
		48	SC	356	13.0	4.1	17.1				X		0.80	-
57-0488	Test Group	Test Pile	OP	356	9.1	3.4	12.5			X			0.69	1.61
57-0720	Control Location 01	5	OP	610	6.4	19.2	25.6			X			2.31	-
	Control Location 02	5	OP	610	9.3	11.0	20.3			X			0.97	4.49
	Control Location 03	5	OP	610	12.2	13.1	25.3			X			2.89	-
	Control Location 06	5	OP	610	5.8	9.4	15.2			X			1.65	-
	Control Location 07	5	OP	610	9.3	12.8	22.1			X			0.80	4.89
	Control Location 08	5	OP	610	8.0	13.7	21.8			X			1.60	3.56
	Control Location 10	5	OP	610	11.1	18.1	29.2			X			7.45	12.46
	Ramp 3, Bent 11	7	OP	610	18.4	2.0	20.4					X	2.27	-
	Ramp 5, Bent 11	2	OP	610	13.5	2.6	16.1					X	1.13	-
	Ramp 7, Bent 19	7	OP	610	14.0	0.0	14.0					X	1.11	-
57-0783	Bent 5	18	OP	406	13.1	2.1	15.2						1.07	-
57-0982	Pier 2L	48	HP	370	12.2	2.9	15.1						0.98	-
57-0989	Bent 4L	8	CP	356	29.0	3.2	32.2						2.40	3.31
57-1017	Abutment 7R	5	SC	356	7.3	-1.2	6.1						-	1.05
	Bent 2L	5	SC	356	10.4	2.1	12.5						0.61	1.16
	Retaining Wall 179	5	SC	356	5.2	-2.4	2.7				X		-	1.29
I-5/I-8 IPTP	Site 1	1C	OP	406	13.2	14.6	27.7			X			1.08	1.68
		1D	OP	406	27.8	0.0	27.8						2.12	-
		1E	OP	356	25.9	0.0	25.9	X					1.52	-
	Site 2	1F	OP	356	11.3	14.6	25.9			X			0.79	1.46
		2C	OP	406	14.8	14.3	29.1			X			1.77	3.20
		2D	OP	406	29.1	0.0	29.1						2.36	-

Bridge	Group	Pile	Type	Width (mm)	Embed. (m)	Depth Range (m)		Vibrated	Jetted	Cased	Predrilled	Relief Drilled	Q_{ms} (MN)	Q_{mc} (MN)
I-880 IPTP		2E	OP	356	27.3	0.0	27.3	X					1.78	-
		2F	OP	356	13.1	14.2	27.3			X			0.98	2.00
	Site 1	1B	CP	610	8.6	2.3	10.9				X		3.36	-
		1C	OP	610	8.5	2.3	10.8				X		1.65	-
		1J	OP	610	8.5	2.3	10.8				X		4.60	7.81
		1U	OP	610	8.5	2.3	10.8	X					1.19	3.34
		2-H	OP	610	12.2	2.3	14.5	X			X		1.25	1.61
	Site 2	2-L	CP	610	13.1	2.3	15.5				X		4.23	4.89
		2-P	OP	610	12.2	2.3	14.5				X		2.14	3.30
		2-T	CP	610	10.7	2.3	13.0				X		2.40	8.99
		2-W	CP	610	12.2	2.3	14.5				X		3.22	5.20
	Site 3	3-C	OP	1067	30.6	0.0	30.6	X			X		3.49	4.00
		3-H	OP	1067	30.6	0.0	30.6				X		4.30	5.38
	Site 4	4-B	OP	610	18.3	2.8	21.1	X			X		1.11	-
		4-C	OP	610	18.3	2.8	21.1				X		2.15	-
		4-H	CP	610	18.3	2.8	21.1				X		2.36	5.00
		4-L	CP	610	19.5	2.8	22.3				X		2.85	4.69
		4-P	CP	610	17.1	2.8	19.9				X		1.56	3.46
4-T		OP	610	18.3	2.8	21.1				X		1.85	3.49	
		4-W	CP	610	18.3	2.8	21.1	X			X		1.42	4.26

Type Key:
OP – open-toed steel pipe pile
CP – closed-toed steel pipe pile
HP – steel H-pile
SC – solid precast concrete pile
HC – hollow precast concrete pile

2.4.3 Pile Types

2.4.3.1 Open-Toed Steel Pipe Piles

Sixty-nine of the 155 piles in this dataset are open-toed steel pipe piles. The piles range in diameter from 305 to 1830 mm with an average outside diameter of 570 mm. Nearly 50% of these piles are 610 mm in diameter. Only 7 of the piles are larger than 610 mm in diameter. Six have diameters of 1067 mm, and one has a diameter of 1829 mm. Though wall thickness ranges from 9.5 to 19.1 mm, the majority of piles have a wall thickness of 12.7 mm. There is no evidence that driving shoes were used on any of these piles.

2.4.3.2 Closed-Toed Steel Pipe Piles

Of the 155 test piles, 34 are closed-toed steel pipe piles. These piles range in diameter from 273 to 610 mm with an average diameter of 500 mm. The wall thickness ranges from 6.4 to 19.1 mm. Although detailed information on the toe plate, enclosing the pile toe, was generally not available, in the reported instances, the diameter of the toe plate was typically 12.7 mm larger than the outside diameter of the pile.

2.4.3.3 Steel H-Piles

Among its steel piles, the dataset includes 24 steel H-piles. In terms of H-sections, these 24 piles consist of 10x57, 12x74, 14x89 and 14x117 sections (English designations). The majority of the piles are 14x89, with 14x117 piles being the second largest group. These two sections, 14x89 and 14x117, have average widths of 362 and 370 mm, respectively.

2.4.3.4 Solid Precast Concrete Piles

Twenty-six of the piles are solid precast concrete piles. These are precast reinforced concrete piles with solid cross-sections, as opposed to the open-toed, hollow precast concrete piles described in the next paragraph. The solid precast concrete piles are typically pre-stressed in compression by tensioning the strands of heavy steel wire during casting. When the tensioned strands are unloaded, the elastic compression of the steel, which is now bonded to the surrounding concrete, compresses the concrete, effectively increasing the tensile strength of the pile. This increased tensile strength is required during both handling, especially lifting, and driving of the pile. All but three of these solid piles have square cross-sections. The other three piles, located at Bridges 46-0252, 46-0254 and 46-0255, have octagonal cross-sections with a width of 381 mm. The square piles have widths of either 305 or 356 mm. The majority are 356 mm in width.

2.4.3.5 Hollow Precast Concrete Piles

The dataset includes only two hollow precast concrete piles. These are basically open-toed concrete pipe piles. The two piles have an outside diameter of 1372 mm and a wall thickness of 178 mm. Both of these piles are located at Bridge 35-0038, which is Dumbarton Bridge, one of the three east-west bridges crossing San Francisco Bay. All of the concrete piles at this bridge were installed using jetting. These two piles are the only jetted piles in the dataset of 155 piles. Due to the limited number and the rather unique characteristics of these piles, the two hollow precast concrete piles were not included in the evaluation and development of predictive methods.

2.4.4 Methods of Installation

2.4.4.1 Impact Driving

In impact driving, the pile is advanced with a ram which is repeatedly lifted and dropped onto the head of the pile. In modern impact hammers, the ram is lifted by fluid pressure. This fluid pressure is typically generated either by the application of pressurized air (air hammer) or hydraulic fluid (hydraulic hammer) or by diesel combustion (diesel hammer). All three of these impact-hammer types were used to install the piles in Table 2.3.

2.4.4.2 Vibratory Driving

As an alternative to an impact hammer, a vibratory hammer can be used. A vibratory hammer contains two shafts provided with eccentric weights, such that rotation of the shafts causes centripetal acceleration of the weights. The component of the force produced in any direction is simple harmonic. The shafts are synchronized so the horizontal forces, for the two shafts taken together, are zero, while the vertical forces are additive. In some soil conditions, the pile cannot be advanced to the target toe elevation by vibratory driving alone. When this occurs, the vibratory hammer is dismounted, and an impact hammer is used to continue driving the pile to the target toe elevation. Twenty-two of the 155 piles in the dataset were installed with a vibratory hammer. In this dissertation, these are referred to as vibro-driven piles.

2.4.4.3 Jetting

Another means of advancing a driven pile is by jetting. In jetting, jets of water are used to remove soil at the pile toe, allowing the pile to advance under its own weight. For the two jetted piles in this dataset, pipes were installed within the walls of the hollow precast concrete piles, and water under high pressure was injected into these pipes during

pile installation. After being advanced by jetting to within a couple of meters of the target toe elevation, the jetting was terminated, and the piles were driven to the target toe elevation with an impact hammer.

2.4.4.4 Casing

Casing consists of a steel pipe which is set into the ground and through which the pile is installed. In most instances, a short section of casing, extending 1 to 3 m below the ground surface, is used to maintain a clean hole in which to center the pile. Casing was used for a large number of the 155 test piles in this dataset. For all but 18 of these piles, the casing was completely cleaned out prior to pile installation, and the use of casing should have no effect on the measured axial resistance of the pile.

However, for the 18 piles for which the casing was not completely cleaned out, the measured resistance could have been affected by the presence of the casing. In Table 2.3, these piles are identified by an "X" in the "Cased" column. In these instances, it is possible that, during the load test, some load could have been transferred from the pile to the casing through the soil in the annular space between the two. If this occurred, then the observed load-displacement behavior would be for a system consisting of both and the pile and the casing, not the pile alone.

The majority of these 18 piles are located at Bridge 57-0720 and the I-5/I-8 IPTP (Indicator Pile Test Program). At these locations, piles were installed through relatively long sections of casing to isolate them, during testing, from an upper stratum of potentially liquefiable sand. In design, Caltrans typically assumes that no resistance is mobilized in potentially liquefiable soils.

2.4.4.5 Predrilling

In predrilling, a pilot hole is drilled prior to pile driving to reduce the driving resistance. Although deeper holes are sometimes used, predrilling is most commonly used to penetrate near-surface soils through which a pile could not be driven. In predrilling, the diameter of the drilling bit is typically slightly less than or equal to the diameter of the pile. Of the 155 piles in the dataset, 29 were predrilled.

2.4.4.6 Relief Drilling

Relief drilling, like predrilling, is used to reduce driving resistance. However, unlike predrilling, relief drilling is performed during driving. In relief drilling, the soil plug, which forms in the interior of an open-toed pile during driving, is partially removed by drilling. Only four of the piles in the dataset were relief drilled. In Caltrans' practice, relief drilling is only used either when the available hammers cannot advance the pile to the target toe elevation or when the driving is so difficult ~~great~~ that continued driving without relief drilling would result in damage of the pile.

2.4.5 Soil Profiles

The compositions of the soil profiles in which the test piles were installed are described in Table 2.4. The soils in each profile are divided into four categories: clay (clay and clayey silt), sand (sand and sandy silt), gravel (gravel and cobbles) and rock. The rock is primarily sedimentary rock, although some of the piles in San Francisco are in serpentine, a weak metamorphic rock. For each profile, the percent composition of each of these four soil categories is provided in Table 2.4.

The setup times for the uplift and compressive tests are also provided in Table 2.4. A dash in one of these two columns indicates that the measured ultimate resistance for the particular direction of loading could not be determined, either because no test was

performed in this direction or because the test was not run to sufficient displacement for Fleming's extrapolation to be applied. A number of these tests have low setup times, less than 7 days. As discussed later, these piles with low setup times were not included in the evaluation and development of predictive methods.

The available site characterization data for each pile is also indicated in Table 2.4. Of the 155 test piles, all have standard penetration test (SPT) data over the full embedment, 96 have laboratory test data, 37 have CPTU data over the full embedment, and 31 have both laboratory test data and CPTU data. These site characterization data are described in Chapter 3.

Table 2.4 Soil Profiles of Test Piles

Bridge	Group	Pile	Setup (days)		Soil Profile (%)				Toe Soil	Soil Data		
			Uplift	Comp.	Clay	Sand	Gravel	Rock		SPT	Lab	CPTU
04-0017	Pier 2	72	1	-	0	0	0	100	Rock	X	X	
04-0017	Pier 3	108	1	-	0	0	23	77	Rock	X	X	
20-0251	Abutment 2R	28	-	2	37	50	13	0	Clay	X	X	
20-0254	Pier 3	14 (#1)	7	6	0	0	100	0	Gravel	X	X	
22-0032	Pier 37	2	-	5	68	32	0	0	Sand	X		
22-0062	Bent 2R	21	-	19	100	0	0	0	Clay	X		
28-0249	Bent 8	20	5	-	9	67	24	0	Gravel	X		
29-0013	Bent 6	1	-	21	0	100	0	0	Sand	X	X	
33-0025	Bent E28L	17	11	10	37	56	7	0	Sand	X	X	X
33-0025	Bent E31R	1	85	85	58	42	0	0	Sand	X		X
33-0393	Bent 3F	27	14	14	86	14	0	0	Sand	X	X	X
33-0611	Bent 13L	8	14	-	70	25	5	0	Sand	X		
33-0611	Bent 17R (LT)	17	15	17	91	9	0	0	Sand	X	X	X
33-0611	Bent 29R	23	14	14	94	3	3	0	Clay	X	X	X
33-0612	Bent 10NC1	3	29	28	75	21	4	0	Clay	X	X	X
33-0612	Bent 17NC1 (LT)	6	33	32	75	25	0	0	Clay	X	X	X
33-0612	Bent 27NC (RT)	9	30	29	77	19	4	0	Clay	X	X	X
33-0612	Bent 31NC (LT)	9	32	27	84	16	0	0	Clay	X	X	X
34-0046	Bent 34R	17	-	17	26	63	11	0	Sand	X		
34-0046	Bent 43AL	13	-	22	40	56	5	0	Sand	X		
34-0046	Bent 45AR	13	-	21	22	78	0	0	Sand	X		
34-0046	Bent 52C	21 (#1)	1	-	63	37	0	0	Sand	X		
34-0046	Bent 52C	21 (#2)	8	-	62	38	0	0	Sand	X		
34-0046	Bent 52R	15	3	-	69	31	0	0	Clay	X		
34-0046	Bent B-88	D	21	-	35	0	65	0	Clay	X		
34-0046	Bent SE-68	11	14	-	39	29	9	23	Rock	X		
34-0046	Bent SE-71	4	12	-	29	59	12	0	Sand	X		
34-0046	Tension Pile Test Site	48	169	168	100	0	0	0	Clay	X		
34-0046	Tension Pile Test Site	49	170	239	100	0	0	0	Clay	X		
34-0070	Bent WU-28	19	25	-	0	0	0	100	Rock	X	X	
34-0088	Site A	2	33	33	59	41	0	0	Sand	X		
34-0088	Site A	3	26	25	78	22	0	0	Sand	X		
34-0088	Site B	1	16	-	43	57	0	0	Sand	X		
34-0088	Site B	2	14	13	43	57	0	0	Sand	X		
34-0088	Site C	1	50	50	10	90	0	0	Sand	X	X	
34-0088	Site C	2	51	51	11	89	0	0	Sand	X	X	

Bridge	Group	Pile	Setup (days)		Soil Profile (%)				Toe Soil	Soil Data		
			Uplift	Comp.	Clay	Sand	Gravel	Rock		SPT	Lab	CPTU
34-0088	Site D	2	14	14	24	76	0	0	Clay	X	X	
34-0088	Site E	1	35	35	100	0	0	0	Clay	X	X	X
34-0088	Site E	2	33	33	100	0	0	0	Clay	X	X	X
34-0088	Site F	1	31	30	76	24	0	0	Sand	X	X	
34-0088	Site F	2	35	34	77	23	0	0	Sand	X	X	
34-0088	Site G	5	14	14	68	32	0	0	Clay	X	X	X
34-0100	Bent 20	14	40	-	55	45	0	0	Sand	X		
34-0100	Bent 22, Column 4	4	18	-	40	52	8	0	Sand	X		
34-0100	Bent 23, Column 4	5	11	-	64	28	8	0	Sand	X		
34-0100	Bent 29, Column 2	19	70	-	92	8	0	0	Sand	X		
34-0100	Site 2	2	23	-	40	59	0	1	Rock	X		
34-0100	Site 3	3	32	-	58	34	0	8	Rock	X		
34-0100	Site 4	4	53	-	71	25	4	0	Sand	X		
34-0100	Site 5	7	42	-	61	35	3	2	Rock	X		
34-0100	Site 6	8	36	-	69	29	2	0	Sand	X		
34-0100	Site 7	10	26	-	95	4	1	0	Clay	X		
35-0038	Pier 04	33	-	13	47	53	0	0	Sand	X		
35-0038	Pier 16	29	-	12	42	45	12	0	Sand	X		
35-0038	Pier 18	3	-	21	39	61	0	0	Clay	X		
35-0038	Pier 23	9	-	15	55	45	0	0	Clay	X		
35-0038	Pier 31	24	-	24	42	58	0	0	Sand	X		
35-0038	Pier 31	36	-	8	42	58	0	0	Sand	X		
35-0038	Pier 36	24	-	23	67	33	0	0	Clay	X		
35-0038	Pier 36	34	-	8	67	33	0	0	Clay	X		
35-0038	Pier 36	35	-	28	64	36	0	0	Sand	X		
35-0038	Pier 36	36	-	7	67	33	0	0	Clay	X		
35-0284	Bent 8B	3	-	4	86	14	0	0	Sand	X	X	
37-0011	Bent 4	8	-	7	65	15	21	0	Clay	X	X	X
37-0270	Line GC-4, Bent 14	25	6	5	54	29	17	0	Sand	X		
37-0270	Line GD-2, Bent 06	22 (#1)	1	1	75	25	0	0	Clay	X	X	X
37-0270	Line GD-2, Bent 06	22 (#2)	6	6	67	31	2	0	Gravel	X	X	
37-0270	Line GD-2, Bent 14	22	19	-	72	28	0	0	Clay	X	X	X
37-0270	Line GD-4, Bent 03	22	27	10	48	52	0	0	Clay	X		X
37-0279	Bent 3R-2	1	13	-	73	27	0	0	Sand	X		X
37-0279	Bent 6L-2	11	44	-	90	10	0	0	Clay	X	X	X
37-0410	Bent 3	34	-	6	78	22	0	0	Clay	X		
44-0030	Pier 2	13	7	6	0	0	0	100	Rock	X	X	
44-0030	Pier 3	13	8	-	0	0	0	100	Rock	X	X	
44-0216	Test Group	Test Pile	23	22	52	48	0	0	Sand	X	X	

Bridge	Group	Pile	Setup (days)		Soil Profile (%)				Toe Soil	Soil Data		
			Uplift	Comp.	Clay	Sand	Gravel	Rock		SPT	Lab	CPTU
46-0252	Bent 2	Test Pile	-	0	0	100	0	0	Sand	X	X	
46-0254	Bent 2	Test Pile	-	0	0	100	0	0	Sand	X	X	
46-0255	Bent 2	Test Pile	-	0	0	100	0	0	Sand	X	X	
49-0133	Bent 2, Column 1	11	4	-	0	100	0	0	Sand	X	X	
51-0273	Station 20+04	Test Pile	0	1	38	62	0	0	Sand	X		
51-0273	Station 22+58	2	13	-	0	100	0	0	Sand	X	X	
51-0276	Bent 5	907	7	-	72	21	8	0	Rock	X		
52-0118	Pier 02	25	2	1	0	0	100	0	Gravel	X	X	
52-0118	Pier 11	406	16	15	0	0	26	74	Rock	X	X	
52-0178	Abutment 3	113	-	7	0	100	0	0	Sand	X	X	
52-0217	Bent 6	101	-	6	93	7	0	0	Clay	X		
52-0271	Bent 3	24	-	5	0	100	0	0	Sand	X	X	
53-0527	Ramp 7, Bent 10	31	0	-	18	82	0	0	Sand	X	X	
53-0527	Ramp 7, Bent 10	35	0	-	21	79	0	0	Sand	X	X	
53-0527	Ramp 8, Bent 04	27	21	-	7	75	18	0	Gravel	X		
53-1181	Bent 5	25	25	-	0	59	41	0	Gravel	X	X	
53-1193	Bent 6	5	2	-	40	60	0	0	Sand	X		X
53-1424	Ramp 18, Bent 5	8	0	-	8	92	0	0	Sand	X		
53-1851	Bent 21, Footing A	2	13	-	48	52	0	0	Sand	X	X	
53-2733	Bent 02	36	-	4	55	45	0	0	Sand	X	X	X
53-2733	Bent 20	Test Pile	-	1	0	100	0	0	Sand	X	X	
53-2791	Bent 5	71	1	-	43	57	0	0	Sand	X	X	
54-0823	Smooth Pile Group	#1-2	-	232	26	0	74	0	Gravel	X		
54-0823	Smooth Pile Group	#1-4	1	232	36	0	64	0	Gravel	X		
54-0967	Bent 09	Test Pile	19	-	0	0	100	0	Gravel	X	X	
54-0967	Bent 13	Test Pile	17	17	0	63	37	0	Gravel	X	X	
55-0438	Bent 9	22	2	-	9	91	0	0	Sand	X		
55-0642	Bent 6	18	6	-	35	65	0	0	Sand	X		X
55-0642	Bent 6	21	-	5	35	65	0	0	Sand	X		X
55-0681	Bent 5	1C	16	-	21	71	9	0	Gravel	X		
55-0681	Bent 5	3C	-	14	32	52	16	0	Sand	X		
55-0681	Bent 5	4S	-	4	29	56	15	0	Sand	X		
55-0689	Bent 16	16	-	4	29	66	5	0	Clay	X	X	X
55-0689	Bent 16	21	6	-	29	66	5	0	Clay	X	X	X
55-0794	Bent 8	23	6	1	0	76	24	0	Sand	X	X	

Bridge	Group	Pile	Setup (days)		Soil Profile (%)				Toe Soil	Soil Data		
			Uplift	Comp.	Clay	Sand	Gravel	Rock		SPT	Lab	CPTU
55-0794	Bent 8	47	2	2	0	78	22	0	Sand	X	X	
55-0794	Bent 8	48	2	-	0	76	24	0	Sand	X	X	
57-0488	Test Group	Test Pile	2	1	0	100	0	0	Sand	X	X	
57-0720	Control Location 01	5	2	-	0	51	0	49	Rock	X	X	
57-0720	Control Location 02	5	8	8	0	47	53	0	Gravel	X	X	
57-0720	Control Location 03	5	15	-	0	31	38	32	Rock	X	X	
57-0720	Control Location 06	5	1	-	0	0	40	60	Rock	X	X	
57-0720	Control Location 07	5	18	14	0	41	51	8	Rock	X	X	
57-0720	Control Location 08	5	13	13	0	17	0	83	Rock	X	X	
57-0720	Control Location 10	5	15	9	0	29	17	54	Rock	X	X	
57-0720	Ramp 3, Bent 11	7	112	-	0	85	15	0	Gravel	X	X	
57-0720	Ramp 5, Bent 11	2	98	-	0	82	18	0	Sand	X	X	
57-0720	Ramp 7, Bent 19	7	126	-	0	78	22	0	Gravel	X	X	
57-0783	Bent 5	18	1	-	65	35	0	0	Sand	X	X	X
57-0982	Pier 2L	48	1	-	0	64	28	8	Rock	X	X	
57-0989	Bent 4L	8	2	1	15	85	0	0	Sand	X		
57-1017	Abutment 7R	5	-	7	0	100	0	0	Sand	X	X	X
57-1017	Bent 2L	5	8	8	0	100	0	0	Sand	X	X	X
57-1017	Retaining Wall 179	5	-	9	0	100	0	0	Sand	X	X	X
I-5/I-8 ITP	Site 1	1C	6	5	0	100	0	0	Sand	X	X	
I-5/I-8 ITP	Site 1	1D	6	-	0	93	7	0	Sand	X	X	
I-5/I-8 ITP	Site 1	1E	7	-	0	92	8	0	Sand	X	X	
I-5/I-8 ITP	Site 1	1F	6	6	0	100	0	0	Sand	X	X	
I-5/I-8 ITP	Site 2	2C	4	4	41	59	0	0	Sand	X	X	
I-5/I-8 ITP	Site 2	2D	2	-	21	74	5	0	Sand	X	X	
I-5/I-8 ITP	Site 2	2E	3	-	22	72	6	0	Sand	X	X	
I-5/I-8 ITP	Site 2	2F	8	8	47	53	0	0	Sand	X	X	

Bridge	Group	Pile	Setup (days)		Soil Profile (%)				Toe Soil	Soil Data		
			Uplift	Comp.	Clay	Sand	Gravel	Rock		SPT	Lab	CPTU
I-880 ITP	Site 1	1B	40	-	0	100	0	0	Sand	X	X	
I-880 ITP	Site 1	1C	38	-	0	100	0	0	Sand	X	X	
I-880 ITP	Site 1	1J	36	76	0	100	0	0	Sand	X	X	
I-880 ITP	Site 1	1U	47	42	0	100	0	0	Sand	X	X	
I-880 ITP	Site 2	2-H	31	30	41	59	0	0	Sand	X	X	
I-880 ITP	Site 2	2-L	29	28	45	55	0	0	Clay	X	X	
I-880 ITP	Site 2	2-P	25	24	41	59	0	0	Sand	X	X	
I-880 ITP	Site 2	2-T	20	17	47	53	0	0	Sand	X	X	
I-880 ITP	Site 2	2-W	21	20	41	59	0	0	Sand	X	X	
I-880 ITP	Site 3	3-C	28	26	63	37	0	0	Sand	X	X	X
I-880 ITP	Site 3	3-H	60	55	63	37	0	0	Sand	X	X	X
I-880 ITP	Site 4	4-B	56	-	76	19	4	0	Sand	X	X	X
I-880 ITP	Site 4	4-C	62	-	76	19	4	0	Sand	X	X	X
I-880 ITP	Site 4	4-H	43	42	76	19	4	0	Sand	X	X	X
I-880 ITP	Site 4	4-L	43	42	71	24	4	0	Sand	X	X	X
I-880 ITP	Site 4	4-P	49	49	82	14	5	0	Sand	X	X	X
I-880 ITP	Site 4	4-T	41	38	76	19	4	0	Sand	X	X	X
I-880 ITP	Site 4	4-W	42	41	76	19	4	0	Sand	X	X	X

2.4.5.1 Profile Compositions

A graphical description of the soil profile compositions is provided in Figure 2.7. For each of the four soil categories, this clustered-column chart gives the number of piles with soil profiles having a percent composition greater than 0, 25, 50 and 75 % and equal to 100%. Some aspects of the data shown in Figure 2.7 should be noted. First, these profiles are predominantly interstratified. Only 31 of 155 profiles derive 100% of their composition from a single soil category (5 clay, 19 sand, 3 gravel and 4 rock). Second, 14% of the average profile is composed of gravel, cobbles or rock. These are materials which are difficult to characterize adequately. CPTU soundings cannot be made in these materials, and SPT measurements and sieve analyses are of little value when the average particle size is greater than the sampler diameter. Clearly, these profiles are not ideal for research, but they are those encountered by Caltrans.

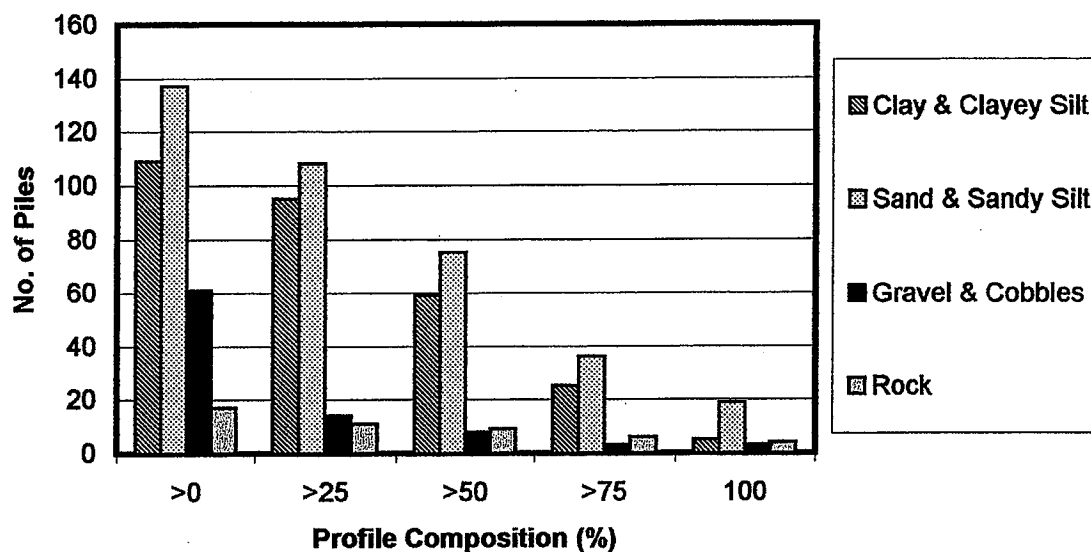


Figure 2.7 Profile Compositions of Test Piles

2.4.5.2 Geology

In northern California, specifically in the Bay Area, the soil profiles typically consist of hydraulically-placed sand fill overlying Quaternary alluvial deposits. The Quaternary alluvial deposits generally consist of normally consolidated Holocene clays above interbedded overconsolidated Pleistocene sands and clays. In San Francisco, where the depth to bedrock can vary drastically, piles are often driven through these alluvial deposits into the underlying bedrock, either sedimentary rock or serpentine. Groundwater is usually encountered at the base of the fill, close to sea level. In southern California, the soil profiles typically consist of coarse-grained fluvial deposits overlying sedimentary rock, with the fluvial deposits generally becoming coarser with depth. The coarse-grained fluvial deposits range in size from sands to boulders and in age from Holocene to Pliocene.

2.4.6 Setup Times

Setup time is the elapsed time between the end of pile installation and the start of load testing. The setup times for the test piles are provided in Table 2.4. It should be noted that during this period between installation and testing some of the test piles were re-struck as part of a dynamic pile test with the Pile Driving Analyzer (PDA) or load tested in compression. The results of a statistical analysis of the setup times for all test piles and for test piles in predominantly clay profiles are presented in Figure 2.8. For these two sets of test piles, the median setup times are 14 and 28 days, respectively. In , the median setup time corresponds to a cumulative percentage of load tests equal to 50%. The effect of setup time on axial resistance in clay is examined later in this dissertation.

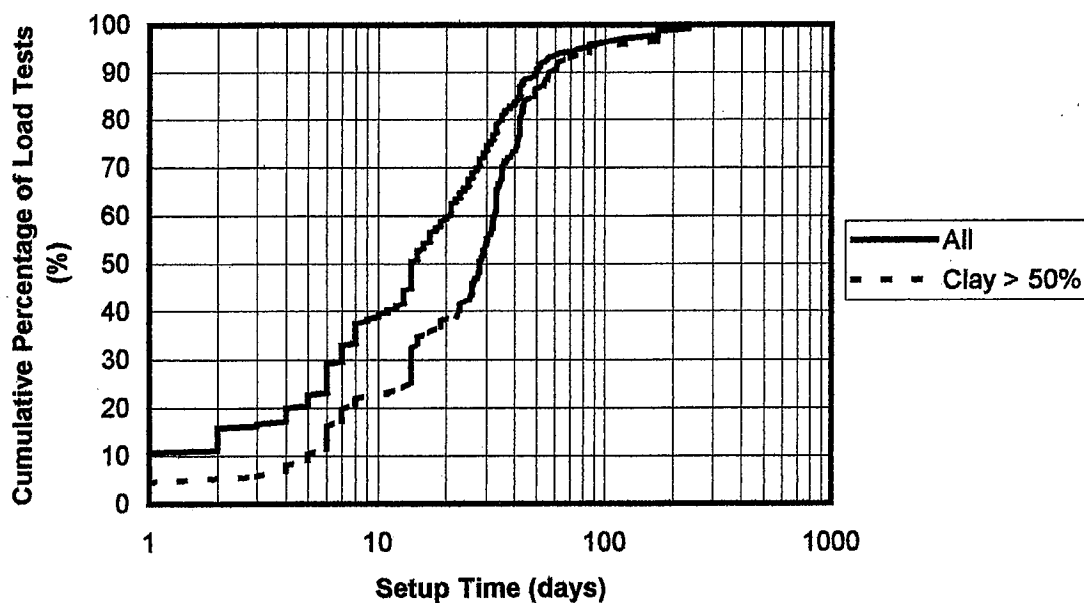


Figure 2.8 Cumulative Probability Plot of Setup Times

2.4.7 Load Test Procedures

On examination of the load test data, no standard test procedure is evident. However, the uplift and compression tests were generally performed in accordance with ASTM D 3689 and D 1143, respectively, (ASTM 1999) using the quick load test method with the load applied by a hydraulic jack acting against an anchored reaction frame. In the quick load test method currently used by Caltrans, each load is held for 5 min during loading and 1 min during unloading. Although most of the tests were run in this manner, a few of the older tests were run at slower rates with loads sometimes held for 24 h. The database includes tests from the 1970s, 1980s and 1990s. In the past 30 years, Caltrans has increased the rate of loading, moving from ASTM's standard loading procedure to ASTM's quick load test method, and increased the level of sophistication of the instrumentation used to measure pile-head load and displacement, moving from dial gages and pressure gages to electronic displacement transducers and load cells. As stated previously, the only measurements made in any of these tests were of pile-head load and displacement.

2.5 CONCLUSION

In this chapter, the data for the 155 test piles included in the analyses were summarized. Four aspects of these data have implications for the subsequent analyses to evaluate existing methods and develop improved methods of predicting axial resistance.

First, only pile-head load and displacement measurements are available. This means that the analyses will focus on the prediction of total ultimate uplift and compressive resistances rather than on the distribution of these resistances on the side and toe of the pile. The lack of toe load measurements makes the study of toe behavior and the evaluation and development of toe resistance methods somewhat difficult. For this

reason, the primary focus of this dissertation is the evaluation and development of side resistance methods based on the uplift tests.

Second, all but 31 of the 155 test piles are in interstratified profiles. When studying pile behavior and developing predictive methods, researchers typically avoid using piles in interstratified profiles. The use of such piles complicates analyses and makes it more difficult to isolate and study pile behavior in a particular material, like clay or sand. Given these circumstances, it is unlikely that this dissertation will lead to new understandings of fundamental pile behavior. However, having a dataset of piles in interstratified soils does provide the opportunity to evaluate existing methods, developed in relatively ideal profiles, against the varied conditions encountered in actual practice.

Third, 73% of the piles in this dataset are steel pipe piles. This means that the effects on side resistance and toe resistance of plugging in open-toed piles will be of interest in the evaluation and development of predictive methods. Since roughly a quarter of these steel pipe piles were installed with a vibratory hammer, the effects of vibratory installation will also be of interest in the analyses.

Fourth, 51 of the 155 test piles have both uplift and compressive tests. Lacking toe load measurements, these test piles offer the best opportunity for examining toe resistance. By assuming that side resistance in compression is equal to the measured uplift resistance times some side resistance ratio and by then subtracting this estimated compressive side resistance from the total compressive resistance, an estimate of the mobilized toe resistance can also be made.

Some of these points will be touched on again in Chapter 4, which contains some of the author's observations regarding the load test results for these 155 test piles, especially those in groups with multiple tests. However, in the next chapter, prior to these observations, the site characterization data will be discussed in Chapter 3.

3. SITE CHARACTERIZATION DATA

3.1 INTRODUCTION

In terms of site characterization data, Caltrans' archives provided data from numerous borings, with the data consisting primarily of visual classifications and standard penetration test (SPT) results. However, since many modern predictive methods rely on data from other in situ or laboratory tests, it was necessary to collect additional data as part of the author's project. In the project's field exploration phase, 46 borings and 56 piezocone penetration test (CPTU) soundings were made to provide additional site characterization data needed for the evaluation and development of predictive methods. Both pushed samples and driven SPT samples were obtained from these borings. Laboratory tests were performed on these samples. The laboratory testing included unconsolidated-undrained triaxial compression (UU) tests, one-dimensional vertical consolidation tests, Atterberg liquid (LL) and plastic limit (PL) determinations, and sieve analyses. In this chapter, the borings made in the project's field exploration phase are referred to as project borings. The older borings, from Caltrans' archives, are referred to as pre-project borings.

3.2 DRILLING AND SAMPLING

The project borings were made using wet-rotary methods. In southern California, a wire-line system for drilling and sampling was used in the borings in which only driven SPT samples were to be taken. The pushed samples were taken using 76-mm diameter thin-walled sample tubes. These samples were generally obtained through normal open-tube sampling. However, piston samplers and Pitcher samplers were used when the soils

were either too soft or too stiff, respectively, for normal open-tube sampling. In pre-project borings, the use of wet-rotary methods was also predominant. Although a variety of driven samplers were used in these older borings, the majority of samples were SPT samples. In this dissertation, the only data used from the driven non-SPT samples were the visual classifications.

3.3 STANDARD PENETRATION TESTING

In the project borings, SPT was used to sample and characterize the cohesionless soils. The pre-project borings, also relied heavily on SPT as a means of sampling and characterizing both cohesionless and cohesive soils. For many of the piles, the only available site characterization data are from these previous borings. Due to the widespread use of SPT in geotechnical engineering practice, both in California and throughout the U.S., and the availability of SPT data for these piles, the evaluation and development of predictive methods based on SPT is a major component of this dissertation.

3.3.1 Equipment and Procedures

3.3.1.1 Drive-Weight Assembly

Although various types of dynamic penetration tests are available and have been used by Caltrans in the past, only the SPT results were included in the site characterization data used in the analyses in this dissertation. The standard penetration test is described in ASTM D 1586 (ASTM 1999). In the SPT, a 63.5-kg hammer is lifted from an anvil, which is attached to the sampling rods, to a height of 0.76 m and then released, falling 0.76 m to the anvil below. This impact is used to drive a sampler at the bottom of the sampling rod string. In SPT, the sampler is driven 450 mm in three 150-

mm increments. The number of blows required to advance the sampler the final 300 mm is the standard penetration resistance (N).

3.3.1.2 Hammer Drop Systems

In the U.S., the hammer is usually lifted and released using either an automatic hammer or the cathead-and-rope method. The cathead is "the rotating drum or windless in the rope-cathead lift system around which the operator wraps a rope to lift and drop the hammer by successively tightening and loosening the rope turns around the drum" (ASTM 1999). According to ASTM D 1586, the cathead should be 150 to 250 mm in diameter, and no more than $2\frac{3}{4}$ rope turns should be used on the cathead. Generally, $1\frac{3}{4}$ to $2\frac{3}{4}$ turns are used depending on the direction of rotation of the cathead. The two contractor's used in the project's field exploration phase were Taber Consultants and Pitcher Drilling. Taber Consultants used two automatic hammers manufactured by Diedrich Drill, Inc. An automatic hammer incorporates a motorized system to lift and drop the hammer. Pitcher Drilling used safety hammers in conjunction with the rope-cathead lift system. A safety hammer is a drop hammer configuration in which the hammer and anvil are enclosed.

3.3.1.3 Sampling Rods

For SPT, typically either A rods or N rods have been used in the recent past. Today, W series A and N rods (AW, AWJ, NW and NWJ) are most often used. Taber Consultants uses AW rods. However, Pitcher Drilling uses larger diameter N, NW or NWJ rods. The specifications of these rod sizes are given in Table 3.1.

Table 3.1 Sampling Rod Specifications

Rod Size	Outside Diameter (mm)	Wall Thickness (mm)	Coupling Bore (mm)	No. Threads/ 25.4 mm
A	41.275	6.350	14.288	3
AW	44.450	6.125	15.875	3
AWJ	44.450	4.763	15.875	5
N	60.325	4.763	25.400	4
NW	66.675	4.763	34.925	3
NWJ	66.675	4.763	28.575	4

3.3.1.4 Sampler

In the project borings, a split-barrel sampler with an inside diameter of 35 mm and an outside diameter of 51 mm was used in the SPT. This sampler was not designed to accommodate a liner. Sample retainer baskets were used in this sampler for some, though not all, of the SPT samples in the project borings. However, the field logs of the borings do not indicate when a sample retainer basket was or was not used. It was assumed that a similar sampler was used in the pre-project borings as well.

3.3.2 SPT Energy Correction

In the project borings, both safety hammers and automatic hammers were used in the SPT. For lack of better information, it has been assumed that safety hammers were also used in the SPT in the pre-project borings. However, safety hammers and automatic hammers do not deliver the same energy to the sampling rod string. Therefore, to use these data together the measured N -values must be normalized to a standard rod energy. In the U.S., it is generally accepted that the standard rod energy is 60% of the theoretical free-fall energy of 475 J. The N -value corresponding to this standard rod energy is referred to as N_{60} . More important than the energy delivered to the top of the rod string is the energy delivered to the sampler at the bottom of the rod string. In an attempt to

normalize the measured N -values to account for energy losses in both the hammer drop system and the sampling rod string itself, Skempton (1986) evaluated the influence of the following factors:

- Rod energy ratio
- Rod length
- Borehole diameter

3.3.2.1 Rod Energy Ratio

The rod energy ratio (ER_r) is the ratio of the delivered energy (E_r) to the theoretical free-fall energy (E_x) and is defined by Equation 3.1.

$$ER_r = E_r / E_x \quad (3.1)$$

Based primarily on the findings of Schmertmann and Palacios (1979), Skempton concluded that the typical ER_r for safety hammers is 55%. This value is based on U.S. practice using a cathead approximately 200 mm in diameter with a two-turn slip-rope release.

For the automatic hammers which were used on the project, the ER_r was taken as 81%. This value is based on measurements made by Abe and Teferra (1998) of Goble Rausche Likins and Associates, Inc. (GRL) on one of Taber Consultants' hammers. In this evaluation, AW rods were used, and tests were made at depths ranging from 1.8 to 13.7 m. During the evaluation of this hammer, the hammer rate, the rate at which the hammer was operating, ranged from 34 to 42 bpm. In a previous evaluation of a Diedrich automatic hammer, Frost (1992) using the same model of hammer as Abe and Teferra, found the average ER_r to be 64% and 89% with AW and NWJ rods, respectively, at a hammer rate of 14 bpm. Frost found that ER_r increased by 8% when the hammer rate was increased to 35 bpm. Clearly, the findings of Frost do not agree with those of Abe and Teferra. However, since the calibration of Abe and Teferra was done on one of the

hammers actually used on the project, it was decided to use an ER_r of 81%. Ideally, the author would have liked to have had both of Taber Consultants' automatic hammers re-evaluated to confirm this rod energy ratio, but this was not possible.

In both of these studies of automatic hammers, the delivered energy was calculated using the force velocity method rather than the force squared method. The rod energy ratios and correction factors ($ER_r/60\%$) used to correct measured N values are provided in Table 3.2.

Table 3.2 Rod Energy Ratio

Hammer	ER_r (%)	$ER_r/60\%$
Automatic	81	1.35
Safety	55	0.92

3.3.2.2 Effect of Rod Length

Again relying on the work of Schmertmann and Palacios (1979), Skempton noted that the energy delivered to the sampler is less than E_r when the rod length is less than 10 m. His proposed corrections to measured N -values are provided in Table 3.3. In this dissertation, these rod length correction factors were used in the calculation of N_{60} .

Table 3.3 Correction Factors for Rod Length (Skempton 1986)

Rod Length (m)	Correction Factor
> 10	1.00
6-10	0.95
4-6	0.85
3-4	0.75

Schmertmann and Palacios attempt to explain the decrease of energy in shorter rods using wave theory. They state that with a shorter rod string the hammer remains in contact with the rod string for a shorter period of time and therefore imparts less of its

energy to the rod string. In the model Schmertmann and Palacios present, it is assumed that the initial compressive wave in a given hammer blow is reflected as a tensile wave at the bottom of the rod string. This reflected tensile wave is then reflected as a compressive wave at the top of the rod string. According to Schmertmann and Palacios, when the reflected compressive wave begins traveling down the rod string, the top of the rod string moves downward ahead of the hammer, causing a loss of contact between the two. This event is referred to as the "tension cutoff of hammer energy." In a shorter rod string, the time between initial impact and tension cutoff is less than it is in a longer rod string.

One problem with this model is the assumption that the bottom of the rod string is free. This assumption is only correct when the soil resistance is very low, as it is in soft clay. Fortunately, Skempton's correction factors are based on actual data rather than the model of Schmertmann and Palacios. However, the behavior observed in these data is not adequately explained by either Skempton or Schmertmann and Palacios.

3.3.2.3 *Effect of Borehole Diameter*

Skempton also determined, based on work of Lake (1974, cited by Skempton 1986) and Sanglerat and Sanglerat (1982), that in cohesionless soils, but not in cohesive soils, the use of boreholes with diameters greater than 115 mm does result in lower N -values. Skempton proposed the admittedly conservative correction factors in Table 3.4. To correct a measured N -value to obtain N_{60} , the measured N -value is multiplied by the appropriate value of $ER_r/60\%$ and by the correction factors for rod length and borehole diameter. In this dissertation, N_{60} is used exclusively in all analyses requiring an N -value.

Table 3.4 Correction Factors for Borehole Diameter (Skempton 1986)

Borehole Diameter (mm)	Correction Factor
65-115	1.00
150	1.05
200	1.15

3.3.2.4 Other Factors

Skempton concluded from the research of Brown (1977) and Matsumoto and Matsubara (1982) that the diameter and cross-section of the sampling rods have little effect on the energy delivered to the sampler. Frost's findings would seem to contradict the conclusion of Skempton. However, unlike Matsumoto and Matsubara, Frost measured energy at the top rather than at the bottom of the sampling rod string, and Brown, more appropriately, relied on actual *N*-values rather than energy measurements. In light of this, the author decided to consider only those factors which Skempton identified as significant.

3.4 PIEZOCONE PENETRATION TESTING

In the project's field exploration phase, CPTU soundings were made at 45 locations. However, only 33 of these soundings could be advanced to the pile toe. In northern California, soundings often met refusal in very dense overconsolidated sands interbedded with overconsolidated clays. In southern California, soundings could not be advanced due to the presence of gravel and cobbles. The data from CPTU soundings from the project's field exploration phase were the only CPT/CPTU data included in the analyses. Unfortunately, the data from the CPT soundings used in Caltrans' 1989 study were not available in a format which could be readily used. x

3.4.1 Equipment and Procedures

All of the CPTU soundings were made using cones with a projected area of 10 cm² and an apex angle of 60° and sleeves with a surface area of 150 cm². All of these soundings were made at a penetration rate of 20 mm/s. For the CPTU, pore pressure was measured behind the cone (u_2), and the cones had a cone area ratio (a) of 0.8. This equipment and these procedures are in agreement with ASTM D 5778 (ASTM 1999). All of the CPTU equipment used was manufactured by Hogentogler.

3.4.2 CPTU/SPT Correlations

To supplement the SPT data from poorly tested borings, the available CPTU measurements were converted into equivalent values of N_{60} using the correlation of Jeffries and Davies (1993). Taber Consultants (Skaug 1998) performed an evaluation of this correlation for a previous project and found that it performed reasonably well. This evaluation was actually performed using the CPTU rig and one of the automatic SPT hammers used by Taber Consultants on the author's project. The correlation of Jeffries and Davies is based on their previous CPTU soil behavior type classification chart (1991).

In the correlation of Jeffries and Davies, the soil behavior type is indicated by the soil behavior type index (I_c) defined by Equation 3.2.

$$I_c = \sqrt{\left\{3 - \log\left[Q_t(1 - B_q)\right]\right\}^2 + \left[1.5 + 1.3(\log F_r)\right]^2} \quad (3.2)$$

The dimensionless parameters of normalized cone resistance (Q_t), normalized friction ratio (F_r), and pore pressure ratio (B_q) used in Equation 3.2 are defined in the following equations:

$$Q_t = \frac{q_t - \sigma_{vo}}{\sigma'_{vo}} \quad (3.3)$$

$$F_r = \frac{f_s}{q_t - \sigma_{vo}} \quad (3.4)$$

$$B_q = \frac{u_2 - u_o}{q_t - \sigma_{vo}} \quad (3.5)$$

where,

q_t = corrected unit cone resistance

σ_{vo} = free-field vertical total stress

σ'_{vo} = free-field vertical effective stress

f_s = unit sleeve friction resistance

u_2 = pore pressure measured behind cone

u_o = free-field pore pressure

To calculate q_t , the force of the water pressure (u_2) acting behind the cone is subtracted from the total force acting on the face of the cone, and this adjusted force is divided by the projected area of the cone (A_c). Because the pore pressure filter occupies only the annular space surrounding the load-cell or shaft to which the cone is attached, u_2 only acts on an area equal to A_c minus A_n , which is the cross-sectional area of the load-cell or shaft. The corrected cone resistance is defined using Equation 8.1, in which a is equal to A_n divided by A_c .

$$q_t = q_c + u_2(1-a) \quad (3.6)$$

Using I_c from this soil behavior type classification system, Jeffries and Davies developed the CPTU-SPT ratio defined in Equation 3.7. It should be noted that this ratio incorporates q_c , the measured unit cone resistance in MPa, rather than q_t .

$$q_c / N_{60} = 0.85(1 - I_c / 4.75) \quad (3.7)$$

Table 3.5 Soil Behavior Type

Soil Behavior Type	Zone	I_c
Gravelly sand	7	< 1.25
Sands – clean sand to silty sand	6	1.25 – 1.90
Sand mixtures – silty sand to sandy silt	5	1.90 – 2.54
Silt mixtures – clayey silt to silty clay	4	2.54 – 2.82
Clays	3	2.82 – 3.22
Organic soils – peats	2	> 3.22

3.5 LABORATORY TESTING

Primarily, the laboratory tests included unconsolidated-undrained triaxial compression (UU) tests and Atterberg liquid (LL) and plastic limit (PL) determinations on cohesive soils and sieve analyses on cohesionless soils. The laboratory tests also included some one-dimensional vertical consolidation tests on cohesive soils, but these data are not used directly in this dissertation. The only consolidation test parameter used in this dissertation is the overconsolidation ratio (*OCR*), and where it is needed, site-specific correlations are employed to obtain *OCR* from UU test results. The development of these correlations is presented in this dissertation.

All of the UU tests used specimens from 76-mm diameter pushed samples. The UU tests were performed on both untrimmed specimens and 51-mm diameter trimmed specimens. Generally, the UU tests were run with a cell pressure equal to the estimated free-field vertical total stress. However, one set of UU tests by a subcontracted commercial laboratory were accidentally run with a cell pressure of 200 kPa regardless of

the sample depth. Fortunately, the effect of this error was not substantial enough to warrant the exclusion of these UU test results.

3.6 CONCLUSION

In this chapter, the site characterization data for the test piles presented in the previous chapter were described. These data included the results from both laboratory and in situ testing. The laboratory testing included unconsolidated-undrained triaxial compression (UU) tests, one-dimensional vertical consolidation tests, Atterberg liquid (LL) and plastic limit (PL) determinations, and sieve analyses. The in situ testing consisted of SPT and CPTU. In the field exploration phase of the author's project, it was found that in many cases CPTU soundings could not be advanced to the toe elevation of the surrounding test piles. This led the author to concentrate more heavily on predictive methods based on SPT and laboratory testing than originally intended. The existing side resistance methods evaluated in this dissertation are described in Chapter 5. These methods include methods based on CPTU, SPT and laboratory testing, especially UU tests. Prior to the description of these existing methods, various aspects of pile behavior which are relevant to these predictive method are discussed in the next chapter.

4. OBSERVATIONS ON PILE BEHAVIOR

4.1 INTRODUCTION

In reviewing the load test reports furnished by Caltrans, the author made several observations regarding the effects of method of installation (impact vs. vibratory) and toe condition (closed vs. open) on axial resistance. These observations were based on the results of load tests made on piles in seven groups at two bridges in Oakland and San Francisco. In this chapter, the data from these pile groups is presented, followed by the author's observations. The observations are discussed in comparison with the findings of other researchers. Additionally, the effect of a prior compressive test on the uplift resistance measured in a subsequent test, the effect of setup time on axial resistance in clay, and the relationship between uplift side resistance and compressive side resistance are also discussed based on the findings of other researchers.

4.2 CALTRANS' TESTS

The load tests examined in this chapter were made in seven pile groups at two bridges in Oakland and San Francisco. These two bridges are Bridge 34-0088 and the I-880 IPTP (Indicator Pile Test Program).

4.2.1 Bridge 34-0048 (Bayshore Freeway Viaduct)

Bridge 34-0088 is more commonly known as Bayshore Freeway Viaduct. It is a segment of I-80 in San Francisco. In the fall of 1997, Caltrans conducted the Bayshore Freeway Viaduct Pile Indicator Test Program (PITP). This program was initiated to evaluate various pile installation methods for use in the seismic retrofit of Bayshore

Freeway Viaduct. Since the piles for the retrofit would be installed below existing bridge decks, Caltrans was interested in the performance of various pile installation methods, particularly vibratory driving, in low-overhead conditions.

The load test results from Sites B, C, E and F provide four cases for evaluating the effect of vibratory driving on uplift and compressive resistances. The results from each of these groups are presented below. The impact-driven piles at these sites were installed with a Menck MHF 5-10 hydraulic impact hammer, and the vibro-driven piles were installed with an APE 400 vibratory hammer. The cross-sectional dimensions of the open-toed steel pipe piles and the compositions of the soil profiles at these sites are provided in Table 4.1.

Table 4.1 Bayshore Freeway Viaduct Sites

Site	Diameter (mm)	Wall Thickness (mm)	Side Soil (%)				Toe Soil
			Clay	Sand	Gravel	Rock	
B	610	19.1	43	57	0	0	Sand
C	406	15.5	10	90	0	0	Sand
E	610	19.1	100	0	0	0	Clay
F	610	19.1	76	24	0	0	Sand

As indicated in Table 4.1, the soil conditions at each of these four sites are quite different. At Site B, the piles were driven through 7 m of soft to medium stiff clay into very dense sand. At Site C, the piles were driven through 8 m of dense to very dense sand into interbedded stiff clay, dense silty sand and very dense clean sand. At Site E, the entire profile is composed of medium stiff clay. At Site F, the piles were driven through 5.5 m of medium stiff clay into interbedded very stiff clay and very dense sand.

The results of the load tests are presented in Table 4.2. The reduction factor for vibro-driven piles (F_v) is equal to the measured ultimate resistance (Q_m) of the vibro-driven pile divided by Q_m of the impact-driven pile. At Site B, the compressive test on Pile 1 was run to a maximum load of 4.44 MN, but the maximum displacement was only

11.2 mm, not sufficient for the application of either Caltrans' offset-limit or Fleming's extrapolation. With or without the compressive tests at Site B, the average value of F_v for these four sites is approximately 0.65.

Table 4.2 Results of Bayshore Freeway Viaduct Tests

Site	Pile	Hammer	Embded. (m)	Depth Range (m)		Setup (days)		Q_m (MN)		F_v	
						Uplift	Comp.	Uplift	Comp.	Uplift	Comp.
B	1	Impact	15.7	3.7	19.4	16	16	3.60	4.44*	0.18	<0.50
	2	Vibratory	15.5	3.7	19.2	14	13	0.64	2.22		
C	1	Impact	16.0	2.1	18.1	50	50	1.78	4.24	0.86	0.66
	2	Vibratory	15.8	2.1	18.0	51	51	1.53	2.78		
E	1	Impact	24.1	4.3	28.3	35	35	0.90	0.95	0.96	0.85
	2	Vibratory	23.8	4.3	28.0	33	33	0.86	0.81		
F	1	Impact	14.9	5.5	20.4	31	30	2.00	4.02	0.45	0.64
	2	Vibratory	14.8	5.5	20.3	35	34	0.89	2.58		

* - Peak load. Q_m unknown.

4.2.2 I-880 IPTP

In early 1994 Caltrans conducted the Indicator Pile Test Program (IPTP) on the I-880 Replacement Project. The structure being replaced was the Cypress Expressway which collapsed in the Loma Prieta earthquake of 1989. The IPTP was initiated to investigate the behavior of steel pipe piles, which would be used in the replacement project.

The load test results at Sites 1, 2 and 4 provide a number of cases for evaluating the effects of (1) method of installation on axial resistance, (2) toe condition on axial resistance, and (3) a prior compressive test on uplift resistance. The cross-sectional dimensions of the piles and the compositions of the soil profiles at these sites are provided in Table 4.3

Table 4.3 I-880 IPTP Sites

Site	Diameter (mm)	Wall Thickness (mm)	Side Soil (%)				Toe Soil
			Clay	Sand	Gravel	Rock	
1	610	19.1	0	100	0	0	Sand
2	610	19.1	41	59	0	0	Sand
4	610	19.1	76	19	4	0	Sand

Like the sites in the Bayshore Freeway Viaduct PITP, the sites in the I-880 IPTP also display a variety of soil conditions. At Site 1, the piles were driven through 4 m of medium dense silty sand into very dense sand. At Sites 2 and 4, the piles were driven through a stratum of medium stiff clay into a stratum of interbedded very stiff clay and very dense sand. At Site 2 the medium stiff clay stratum is only 4 m thick, while at Site 4 it is 9 m thick. At both sites, the piles are tipped in a layer of very dense sand. The results of the load tests from these sites are presented in Table 4.4.

Table 4.4 Results of I-880 IPTP Tests

Site	Pile	Toe	Hammer	Embedd. (m)	Depth Range (m)		Setup (days)		Q_m (MN)	
							Uplift	Comp.	Uplift	Comp.
1	1-B	Closed	Impact	8.6	2.3	10.9	40	-	3.36	-
	1-C	Open	Impact	8.5	2.3	10.8	38	-	1.65	-
	1-J	Open	Impact	8.5	2.3	10.8	36	76	4.60	7.81
	1-M	Open	Impact	8.5	2.3	10.8	42	42	5.00	4.47*
	1-R	Closed	Impact	8.5	2.3	10.8	40	40	5.34	7.01
	1-U	Open	Vibratory	8.5	2.3	10.8	47	42	1.19	3.34
2	2-H	Open	Vibratory	12.2	2.3	14.5	31	30	1.25	1.61
	2-P	Open	Impact	12.2	2.3	14.5	25	24	2.14	3.30
	2-W	Closed	Impact	12.2	2.3	14.5	21	20	3.22	5.20
4	4-B	Open	Vibratory	18.3	2.8	21.1	56	-	1.11	-
	4-C	Open	Impact	18.3	2.8	21.1	62	-	2.15	-
	4-H	Closed	Impact	18.3	2.8	21.1	43	42	2.36	5.00
	4-T	Open	Impact	18.3	2.8	21.1	41	38	1.85	3.49
	4-W	Closed	Vibratory/ Impact	18.3	2.8	21.1	42	41	1.42	4.26

* - Peak load. Q_m unknown.

4.2.2.1 Effects of Method of Installation on Axial Resistance

The effects of method of installation (vibratory vs. impact) on axial resistance are shown in Table 4.5. At the I-880 IPTP sites, there is a marked reduction in axial resistance when the pile is installed with a vibratory hammer rather than with an impact hammer, just as was observed at Bayshore Freeway Viaduct. At Site 1, the average values of F_v in compression and uplift are 0.25 and 0.43, respectively, ignoring the compressive test on Pile 1-M for which Q_m is unknown. For the one case at Site 2, the values of F_v in compression and uplift are 0.58 and 0.49, respectively. Assuming that uplift resistance is proportional to compressive side resistance, the lower value of F_v in compression relative to uplift could be an indication that toe resistance is also reduced by vibratory driving. At Site 4, the average values of F_v in compression and uplift are 0.56 and 0.85, respectively. The data from Site 4, like that from Site 1, with a higher value of F_v in compression than in uplift, seem to indicate that the toe resistance is not greatly affected by vibratory driving. With conflicting results in the I-880 IPTP data, it is difficult to draw any conclusions regarding the effect of vibratory driving on toe resistance. The same situation exists for the data from Bayshore Freeway Viaduct.

Table 4.5 Effects of Method of Installation at I-880 IPTP

Site	Piles		F_v	
	Vibratory	Impact	Uplift	Comp.
1	1-U	1-J	0.26	0.43
		1-M	0.24	<0.75
2	2-H	2-P	0.58	0.49
4	4-B	4-C	0.52	-
	4-W*	4-H	0.60	0.85

*- Re-struck with impact-hammer.

4.2.2.2 Effects of Toe Condition on Axial Resistance

The effects of toe condition (open vs. closed) on axial resistance is demonstrated by the results given in Table 4.6. In this table, the multiplier for closed-toed piles (F_t) is equal to Q_m of the closed-toed pile divided by Q_m of the open-toed pile.

Table 4.6 Effects of Toe Condition at I-880 IPTP

Site	Piles		F_t	
	Open	Closed	Uplift	Comp.
1	1-C	1-B	2.04	-
	1-J	1-R	1.16	0.90
	1-M	1-R	1.09	<1.56
2	2-P	2-W	1.50	1.59
4	4-T	4-H	1.28	1.43

Regarding the effects of toe condition on axial resistance, the I-880 test results demonstrate that the side resistance of open-toed piles is lower than that of closed-toed piles. In uplift, the average value of F_t in Table 4.6 is 1.41. In compression, the average value of F_t is 1.30. However, at Site 1 the compressive resistance of the open-toed pile is actually higher than that of the closed-toed pile, while at Sites 2 and 4 the reverse is true. The presence of interbedded clay layers in the predominantly sand, bearing stratum at Sites 2 and 4 could explain this difference.

4.2.2.3 Effect of Prior Compression Test on Uplift Resistance

The final effect examined in the I-880 IPTP data, is the effect of a prior compressive test on the uplift resistance measured in a subsequent test. In Table 4.7, the effect of a prior compressive test on the uplift resistance measured in a subsequent test is shown. In this table, F_c is equal to Q_m in uplift of the pile with a prior compressive test divided by Q_m in uplift of the pile without a prior compressive test.

Table 4.7 Effect of Prior Compressive Test on Uplift Test at I-880 IPTP

Site	Toe	Piles		F_c
		w/o Comp.	w/ Comp.	
1	Closed	1-B	1-R	1.59
	Open	1-C	1-J	2.78
			1-M	3.03
4	Open	4-C	4-T	0.86

The values of F_c for Site 1 in Table 4.7 indicate that uplift resistance is higher when measured following a prior compressive test. However, it must be noted that the uplift test piles without a prior compressive test were all located on the perimeter of the test pile group while the test piles with prior compression tests were located in the interior of the group. It is possible that the sand at the interior of the Site 1 group was more heavily densified during driving of the group's piles than was the sand at the perimeter of the group. This phenomenon could explain the lower resistance of the uplift test piles on the perimeter. Given this alternative explanation for the behavior at Site 1 and the F_c value of 0.86 at Site 4, it is not possible to draw from these data definitive conclusions regarding the effect of a prior compressive test.

4.3 OBSERVATIONS

4.3.1 General

For each of the effects discussed in this section of the chapter, comparisons are made between the data from Caltrans' tests and data from other researchers. For the most part, the tests performed by these other researchers were in sand. Although, a number of the profiles in the Bayshore Freeway Viaduct PITP and the I-880 IPTP contain clay, all of the piles, with the exception of those at Site E of the Bayshore Freeway Viaduct PITP, are tipped in sand and derive a large percentage of their resistance in sand.

4.3.2 Effects of Method of Installation on Axial Resistance

4.3.2.1 Findings from Caltrans' Tests

In the Bayshore Freeway Viaduct PITP and the I-880 IPTP, the average values of F_v in uplift and compression were 0.51 and 0.61, respectively. These values were for piles driven entirely with a vibratory hammer. For piles re-struck with an impact hammer prior to loading, the case from Site 4 of the I-880 IPTP gave values of F_v of 0.60 and 0.85 in uplift and compression, respectively. These findings indicate that (1) the reduction in toe resistance due to vibratory driving is less than the reduction in side resistance and (2) re-striking a vibro-driven pile with an impact hammer prior to loading mitigates the reduction in resistance to some extent.

4.3.2.2 O'Neill et al. 1990

In 1990, O'Neill, Vipulanandan and Wong (1990) at the University of Houston, conducted laboratory model tests on both impact-driven and vibro-driven piles in saturated sand. An instrumented closed-toed steel pipe pile was used in these tests. This pile had an outside diameter of 102 mm and a wall thickness of 5.1 mm. The tests were performed in a cylindrical chamber with a height of 2.54 m and an inside diameter of 0.76 m. Uplift and compressive tests were performed at relative densities (D_r) of 65 and 90% and effective horizontal chamber pressures (σ'_h) of 69 and 138 kPa using both San Jacinto River sand and blasting sand.

Table 4.8 contains values of unit side resistance (f_s) measured in tests in blasting sand at D_r of 90% and σ'_h of 69 kPa. These values of f_s correspond to approximately 25 mm of local displacement, the maximum displacement in the tests. In Table 4.8, side resistance of the vibro-driven pile divided by side resistance of the impact-driven pile is referred to as F_{vs} . For these tests, the average values of F_{vs} in uplift and compression are

0.91 and 1.21, respectively. In these same tests, the measured unit toe resistances at 25 mm of local displacement were 8.6 MPa for the vibro-driven pile and 5.7 MPa for the impact driven pile, with the toe resistance of the vibro-driven pile being 50% greater than that of the impact-driven pile. For these two piles, the ultimate compressive resistance of the vibro-driven pile was approximately 60% greater than the that of the impact-driven pile, resulting in an F_v -value of 1.6.

Table 4.8 Unit Side Resistance from Laboratory Model Tests (O'Neill et al. 1990)

Depth (mm)	Hammer	f_s (kPa)		F_v	
		Uplift	Comp.	Uplift	Comp.
0.51	Vibratory	38	91	0.53	1.47
	Impact	72	62		
1.52	Vibratory	124	105	1.29	0.95
	Impact	96	110		

In the finer San Jacinto river sand, compressive tests at 65 and 95% relative density produced F_v -values of 0.8 and 1.2, respectively. However, for the test at 65% relative density the vibro-driven pile was re-struck with an impact-hammer prior to the compressive test. This test was the only comparison made at 65% relative density.

4.3.2.3 Conclusions

For vibro-driven piles relative to impact-driven piles, the University of Houston tests do not show the general reduction in axial resistance observed in Caltrans' tests. The University of Houston's tests yielded F_v -values of 0.9 in uplift and 1.2 to 1.6 in compression at 90% relative density and 0.8 in compression at 65% relative density. In contrast, Caltrans' tests yielded average F_v -values of 0.5 and 0.6 in uplift and compression, respectively. However, it should be noted that the University of Houston's tests were performed on closed-toed piles while Caltrans' tests, with exception of the Site 4 tests, were performed on open-toed piles. This could explain the differences between these two sets of tests. In any case, the author believes that the lower axial resistances

observed for vibro-driven piles in Caltrans' tests are valid and representative of Caltrans' practice with regard to the use of vibratory driving, which is primarily used by Caltrans to install open-toed piles and H-piles. Based on this, the author has included reduction factors for vibro-driven piles in the predictive methods developed and presented in this dissertation.

4.3.3 Effects of Toe Condition on Axial Resistance

4.3.3.1 Findings from Caltrans' Tests

In the I-880 IPTP, uplift and compressive resistances of closed-toed piles were found to be greater than those of open-toed piles, with average F_r -values of 1.41 and 1.30 in uplift and compression, respectively. The only exception to this general trend was one compressive case at Site 1 with an F_r -value of 0.90.

4.3.3.2 O'Neill and Raines 1991

Using an experimental arrangement similar to that used by O'Neill, Vipulanadan and Wong (1990), O'Neill and Raines (1991) conducted laboratory model tests to examine the behavior of open- and closed-toed steel pipe piles in dense sand. In these tests, San Jacinto river sand with an average relative density of 89% was used. From these tests, O'Neill and Raines found side resistance was not affected by the toe condition. However, they did find that on average the toe resistance of closed-toed piles was 50% greater than that of open-toed piles. This evaluation of toe resistance corresponds to a pile-head displacement equal to 10% of the pile diameter. O'Neill and Raines attributed this reduction in toe resistance to the greater compressibility of the soil plug in the open-toed pile relative to the more rigid toe of the closed-toed pile.

4.3.3.3 *De Nicola and Randolph 1999*

In 100-g centrifuge modeling of steel pipe piles in saturated sand at the University of Western Australia, De Nicola and Randolph (1999) examined this issue among others. From tests on open- and closed-toed piles, De Nicola and Randolph found that on average the side resistance and toe resistance of closed-toed piles were, respectively, 37 and 52% greater than those of open-toed piles. This evaluation of toe resistance, like that of O'Neill and Raines, corresponds to a pile-head displacement equal to 10% of the pile diameter. The higher side resistance of closed-toed piles was observed to be due to the higher horizontal effective stresses which developed near the toe.

4.3.3.4 *Conclusions*

The results of O'Neill and Raines (1991) and De Nicola and Randolph (1999) generally agree with those from Caltrans' tests. The Caltrans' tests show that the uplift side resistance of closed-toed piles is 41% higher than that of open-toed piles. This agrees well with the 37% increase found by De Nicola and Randolph. O'Neill and Raines did not find any real difference in side resistance between open- and closed-toed piles. This was probably due to the fact that in the tests of O'Neill and Raines unit side resistance decreased near the toe of both open- and closed-toed piles. This decrease, like the increase observed by De Nicola and Randolph, was attributed to interference of the pile toe.

In terms of toe resistance, the tests from the University of Houston and the University of Western Australia both indicate that at a displacement equal to 10% of the pile diameter the toe resistance of closed-toed piles is 50% greater than that of open-toed piles. If the side and toe resistances of closed-toed piles are 40 and 50% greater than those of open-toed piles, then the compressive resistance, which is the sum of the side and toe resistances, would be 40 to 50% greater than that of open-toed piles, depending

on the relative distribution of resistance on the side and the toe. For the Caltrans' tests, ignoring the anomalous compressive case at Site 1, the average value of F_r is 1.51, which falls on the upper end of this range.

To account for the lower toe resistance of open-toed piles, the author has included a plug mobilization factor for both open-toed piles and H-piles in the improved methods for predicting axial resistance presented in this dissertation. Likewise, the author has also chosen to include a side resistance multiplier to account for the higher side resistance of closed-toed piles relative to open-toed piles, which comprise the majority of the test piles used in the development of these predictive method.

4.3.4 Effect of Prior Compression Test on Uplift Resistance

4.3.4.1 Findings from Caltrans' Tests

In the I-880 IPTP, the tests at Site 1 appear to indicate that a prior compressive test increases the uplift resistance measured in a subsequent test by almost 60 to 200%, while the tests at Site 4 indicate that a prior compressive test decreases the subsequently measured uplift resistance by 14% relative to the uplift resistance measured in a test with no prior compressive test.

4.3.4.2 De Nicola and Randolph 1999

In addition to examining the effects of toe condition on axial resistance, De Nicola and Randolph (1999) also conducted five sets of tests to evaluate the effect of a prior compression test on the uplift resistance measured in a subsequent test. In each set, one uplift-compression-uplift series and one compression-uplift-compression series were conducted. From these tests, it was found that a prior compressive test actually reduces uplift resistance by 5%. De Nicola and Randolph attribute this reduction to a degradation of side resistance caused by a reversal of the direction of loading.

4.3.4.3 Conclusions

De Nicola and Randolph's finding that a prior compressive test reduces subsequent uplift resistance by 5% is in relative agreement with the data from Site 4 of the I-880 IPTP, which showed a reduction of 14%. Despite the contrary results from Site 1, the results of De Nicola and Randolph and the results from Site 4 lead the author to believe that a prior compressive test has little effect on the uplift resistance measured in a subsequent test. Based on this conclusion, the author has used compression-uplift series together with independent uplift tests in the development of the predictive methods presented later in this dissertation.

4.4 OTHER EFFECTS OF INTEREST

4.4.1 Effect of Direction of Loading on Side Resistance

Since the Caltrans' tests only provide pile-head load and displacement measurements, preventing the separation of side and toe resistance in compressive tests, the author had to rely on the findings of other researchers in evaluating the effect of direction of loading on side resistance. For behavior in clay, the author relied upon the findings of Lehane and Jardine (1994) in lightly overconsolidated clay and Bond and Jardine (1995) in heavily overconsolidated clay. In clay, the tests of these researchers has shown that ultimate side resistance is not greatly dependent on the direction of loading. In the lightly overconsolidated, estuarine/shallow-marine clays at Bothkennar, Scotland, Lehane and Jardine conducted one comparison and found that the average peak unit side resistance in uplift was 8% lower than that in compression. In the heavily overconsolidated London clay at the Canons Park test site in northern London, Bond and Jardine found that the average side resistance in uplift was actually 13% higher than that in compression.

For behavior in sands the author relied on the findings of O'Neill and Raines (1991), De Nicola and Randolph (1999) and Lehane, Jardine, Bond and Frank (1993). O'Neill and Raines, using laboratory model tests, and Lehane et al., using small-scale instrumented piles in dune sands at the Labenne test site near Bayonne, France, both concluded that side resistance in uplift is approximately 20% lower than that in compression. Similarly, De Nicola and Randolph's centrifuge tests indicated that side resistance in uplift is on average 32% lower than that in compression.

The tests in clay, lead the author to believe that the effect of direction of loading on side resistance is negligible in clay. However, the tests in sand clearly show a dependence on the direction of loading, with side resistance in uplift ranging from 70 to 80% of that in compression. Based on these findings, the author has included a side resistance ratio to relate side resistance in uplift and compression in the predictive methods developed as part of this dissertation.

4.4.2 Effect of Setup Time on Axial Resistance in Clay

The setup times for the 155 tests piles in the dataset presented in Chapter 2 range from 0 to 239 days. For this range of setup times, the axial load tests furnished by Caltrans contain no cases useful in evaluating the effect of setup time on axial resistance in clay. However, this effect is clearly demonstrated by the data from Seed and Reese (1957, cited by Vesic 1977) shown in Figure 4.1. The results plotted in Figure 4.1 are from tests on 152-mm diameter steel pipe piles in soft clay in San Francisco. The test piles had a length of 6.7 m. These data indicate that resistance continues to increase during the first month following installation. At 7 days, the resistance is approximately 80% of the maximum resistance.

In normally consolidated and lightly overconsolidated clay, the increase in resistance with time is due largely to the dissipation of excess pore pressures generated

by pile installation. For a group of 610-mm diameter piles, the time required for excess pore pressures to dissipate in these same soils would probably be greater than one month. Nevertheless, due to this effect, the author, in the development of predictive methods, has decided to exclude axial load tests with setup times less than 7 days in profiles containing clay. The inclusion of these tests in the calibration of a predictive method would result in a method which would under-predict axial resistance in profiles containing normally consolidated and lightly overconsolidated clay.

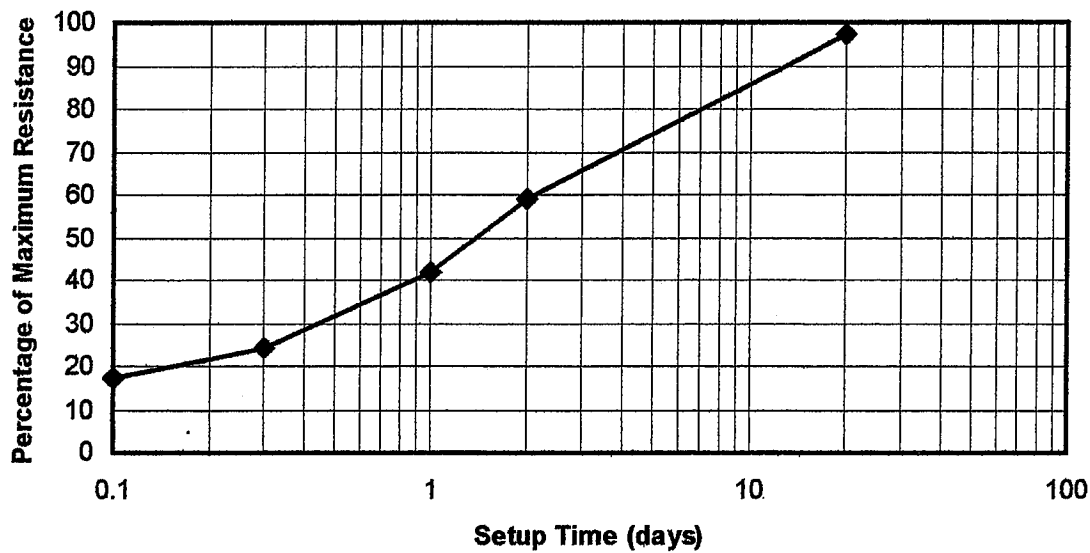


Figure 4.1 Effect of Setup Time on Axial Resistance in Clay (Seed and Reese 1957, cited by Vesic 1977)

4.5 CONCLUSION

In this chapter, a number of aspects of pile behavior were examined in light of both Caltrans' data and the data collected by other researchers. These aspects included the effects of:

- Method of installation on axial resistance,
- Toe condition on axial resistance,
- Prior compressive test on uplift resistance,
- Direction of loading on side resistance, and
- Setup time on axial resistance in clay.

The examination of these effects, led the author to conclude that (1) vibro-driven piles have lower axial resistance than do impact-driven piles; (2) open-toed piles have lower side and toe resistances than do closed-toed piles; (3) a prior compressive test does not significantly affect the uplift resistance measured in a subsequent test; (4) side resistance in sand, but not in clay, is lower in uplift than in compression; and (5) axial resistance in normally consolidated and lightly overconsolidated clay increases with time. These general conclusions are reflected in the formulation of the improved predictive methods presented in Chapters 7 and 8.

In the next two chapters, several existing methods for the prediction of side resistance are first described (Chapter 5) and then evaluated against the author's uplift test pile database (Chapter 6). The purpose of this evaluation is to identify a candidate from which to develop the improved side resistance method presented in Chapter 7.

5. DESCRIPTION OF SIDE RESISTANCE METHODS

5.1 INTRODUCTION

Twelve existing methods, based on standard penetration testing (SPT) and laboratory testing, are evaluated against the uplift test pile database. These methods included the three methods currently used by Caltrans, five methods developed using the American Petroleum Institute (API) database compiled by Olson and Dennis (1982), two methods based on instrumented load tests conducted in the 1990s under the sponsorship of major oil companies, and two other methods: an SPT method (Decourt 1982) and a revised λ -method (Kraft et al. 1981).

In addition to these 12 methods, four existing methods based on electric cone penetration testing (CPT) and piezocone penetration testing (CPTU) are evaluated against the uplift test pile database. These methods include the two CPT-methods which performed the best for driven piles in Caltrans' 1989 study (Richman and Speer 1989) and two recently developed CPTU-methods.

5.2 METHODS BASED ON SPT AND LABORATORY TESTS

5.2.1 Caltrans/FHWA Methods

Caltrans now uses the methods recommended by the U.S. Department of Transportation, Federal Highway Administration (FHWA) and incorporated in the DOS program SPILE and the Microsoft Windows program DRIVEN. These programs were developed by FHWA for the calculation of ultimate axial resistance. For the calculation of side resistance, FHWA uses two methods developed by Tomlinson (Tomlinson 1971,

Hannigan et al. 1997) in cohesive soils and Nordlund's (1963) method in cohesionless soils.

5.2.1.1 Tomlinson 1971

Tomlinson's (1971) method provides adhesion factors (α) based on (1) the composition of the strata overlying the clay stratum of interest and (2) the thickness of the clay stratum, as indicated in Figure 5.1, Figure 5.2 and Figure 5.3. In these figures, the variable L represents the length of pile embedded in the underlying clay stratum. Once α is determined from these charts, the unit side resistance is computed using Equation 5.1, where s_u is the undrained shearing strength measured in unconsolidated-undrained triaxial compression (UU) tests or unconfined compression (UC) tests. In this dissertation, UU test results are used unless otherwise noted.

$$f_s = \alpha s_u \quad (5.1)$$

Tomlinson's method is based on 94 load tests. In the development of the adhesion factors for Cases I, II and III, Tomlinson used 31, 31 and 32 tests, respectively. In his analyses, Tomlinson defined Q_m as the pile-head load at a pile-head displacement equal to 10% of the pile diameter. The side resistance in the clay stratum was estimated by subtracting from Q_m both the side resistance in the overlying strata and the toe resistance in the clay stratum. The unit toe resistance was assumed to be equal to 9 times s_u of the clay at the pile toe. For Case I, the side resistance in the overlying sand strata was generally estimated using Nordlund's method. For Case II, the side resistance in the overlying soft clay strata was calculated using Equation 5.1 with α equal to 1.0.

Case I: Piles Driven through Overlying Sands or Sandy Gravels

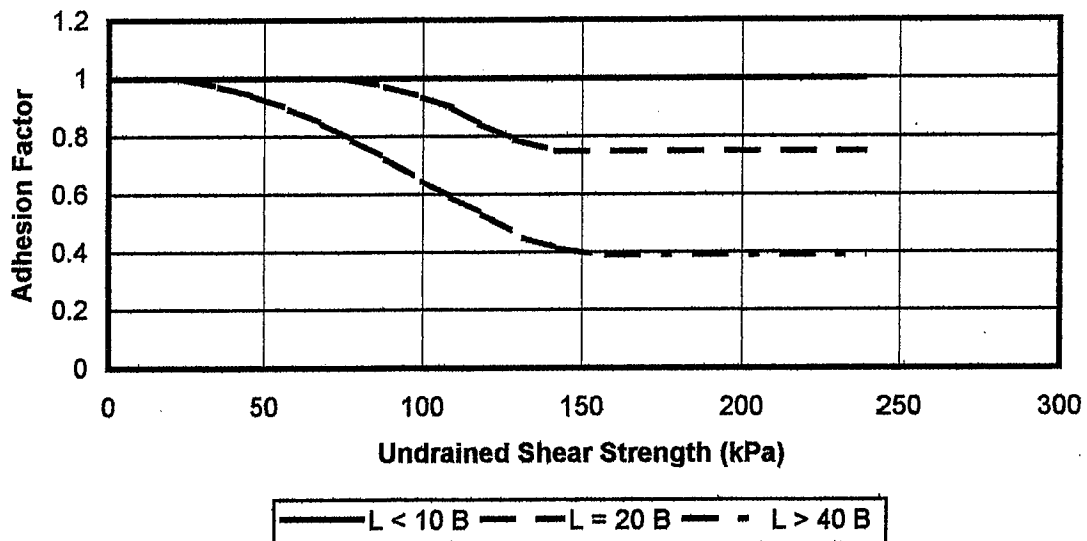


Figure 5.1. Adhesion Factors for Piles in Clay: Case I (Tomlinson 1971)

Case II: Piles Driven through Weak Clay

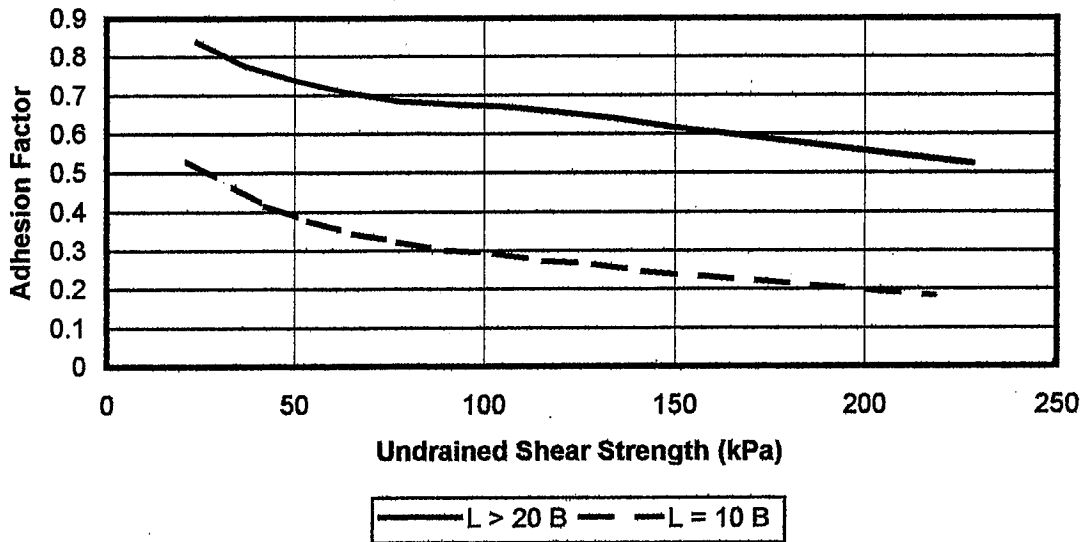


Figure 5.2. Adhesion Factors for Piles in Clay: Case II (Tomlinson 1971)

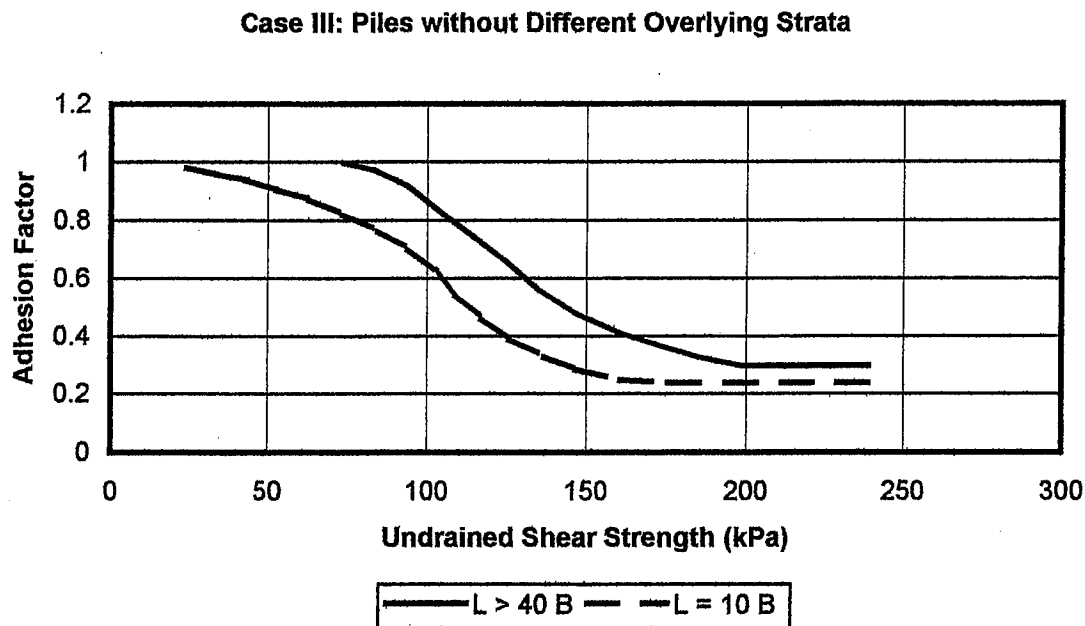


Figure 5.3 Adhesion Factors for Piles in Clay: Case III (Tomlinson 1971)

5.2.1.2 Tomlinson 1979

In this method attributed to Tomlinson (Hannigan et al. 1997), unit side resistance (pile adhesion) is determined directly from Figure 5.4. Unlike Tomlinson's 1971 method, which did not consider pile material, this method uses separate curves for concrete and steel piles. The adhesion values for concrete piles correspond to the adhesion factors in Figure 5.3. Oddly, Hannigan et al. do not provide a reference to the original source of this method. It appears to be similar to Tomlinson's (1957) original α -method. However, in Figure 5.4, the pronounced reduction in pile adhesion at undrained shear strengths above 150 kPa is not reflected in the data presented by Tomlinson (1957).

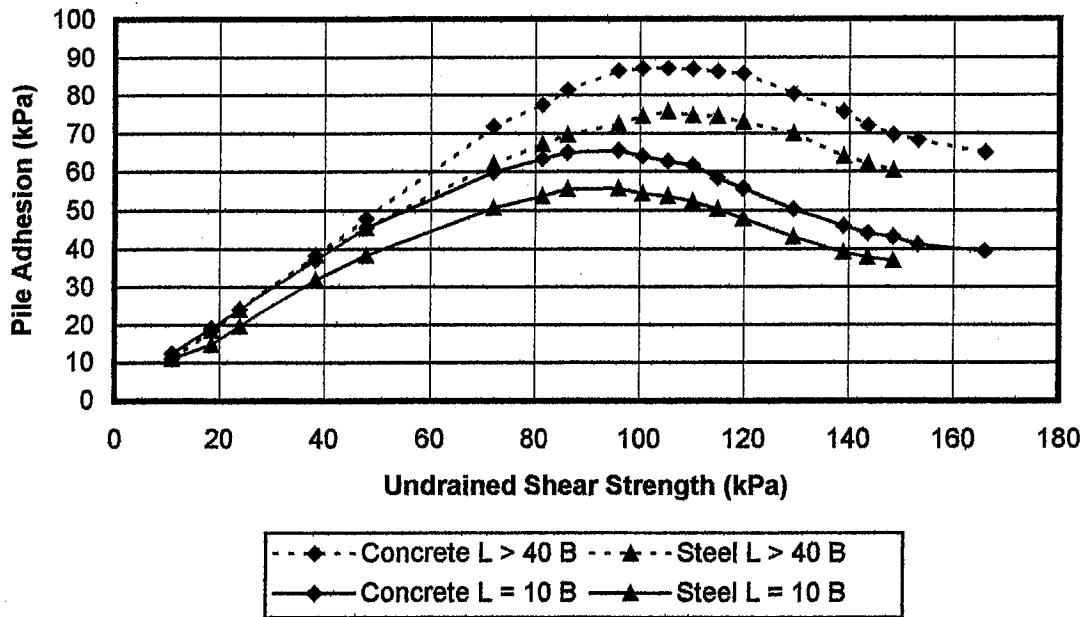


Figure 5.4 Adhesion Values for Piles in Cohesive Soils (Hannigan et al. 1997)

5.2.1.3 Nordlund 1963

According to Nordlund, unit side resistance in cohesionless soils is affected by the free-field vertical effective stress (σ'_{vo}), the internal friction angle of the soil (ϕ), the interface friction angle between the soil and the pile (δ), and the volume of soil displaced per unit length of pile, which is simply the cross-sectional area of the pile (A). Unit side resistance is calculated using Equation 5.2.

$$f_s = K_\delta \sigma'_{vo} \sin(\delta) \quad (5.2)$$

The value of δ is typically determined using Figure 5.5 with a correlation used to obtain ϕ from the corrected SPT resistance (N_{corr}). To obtain ϕ from N_{corr} , FHWA, uses the correlation presented by Peck et al. (1974) shown in Figure 5.6. The value of N_{corr} is computed by multiplying the measured value of N by the dimensionless factor C_N defined

1400 2000 3000

in Equation 5.3. This equation is applicable for σ'_{vo} less than or equal to 23.9 kPa (Peck et al. 1974). In this dissertation, all measured values of N were first converted to N_{60} as described in Chapter 3. Regarding Figure 5.5, in the evaluation of this method the curve for closed-toed piles is also used for open-toed steel pipe piles, which are assumed to be closed-toed.

$$C_N = 0.77 \log \left(\frac{1.92 \text{ MPa}}{\sigma'_{vo}} \right) \quad (5.3)$$

Once estimates of ϕ and δ have been obtained, K_δ for δ equal to ϕ is determined from Figure 5.7. When δ is not equal to ϕ , this value of K_δ is corrected using the appropriate multiplier from Figure 5.8. In the development of this method, Nordlund used estimated values of ϕ in gravel, in which he considered N -values to be misleadingly high. Unfortunately, Nordlund did not specify how the ϕ -values in gravel were estimated.

Nordlund's method was developed in a relatively subjective manner, even for an empirical method. Figure 5.5 and Figure 5.7 were developed using data from only 41 load tests. In Figure 5.5, a curve for precast concrete piles is provided despite the fact that Nordlund's database did not include any data for precast concrete piles. The curves for closed-toed steel pipe piles and steel H-piles are based on only 11 and 4 load tests, respectively. Of the 7 closed-toed steel pipe piles and 2 steel H-piles documented by Nordlund, all but one of the closed-toed steel pipe piles are 324 mm in diameter, and the steel H-piles are both 10x42 (English designation). For reference, a 324-mm diameter closed-toed steel pipe has a cross-sectional area of 0.082 m², while a 10x42 steel H-pile has a cross-sectional area of 0.008 m².

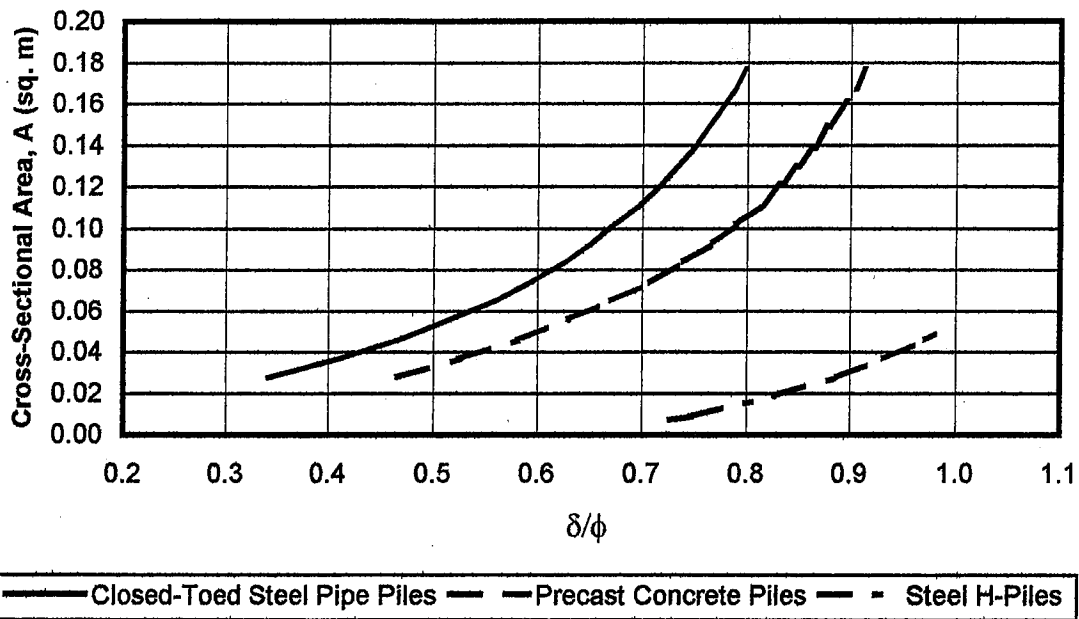


Figure 5.5. Relationship between A and δ/ϕ (Nordlund 1963)

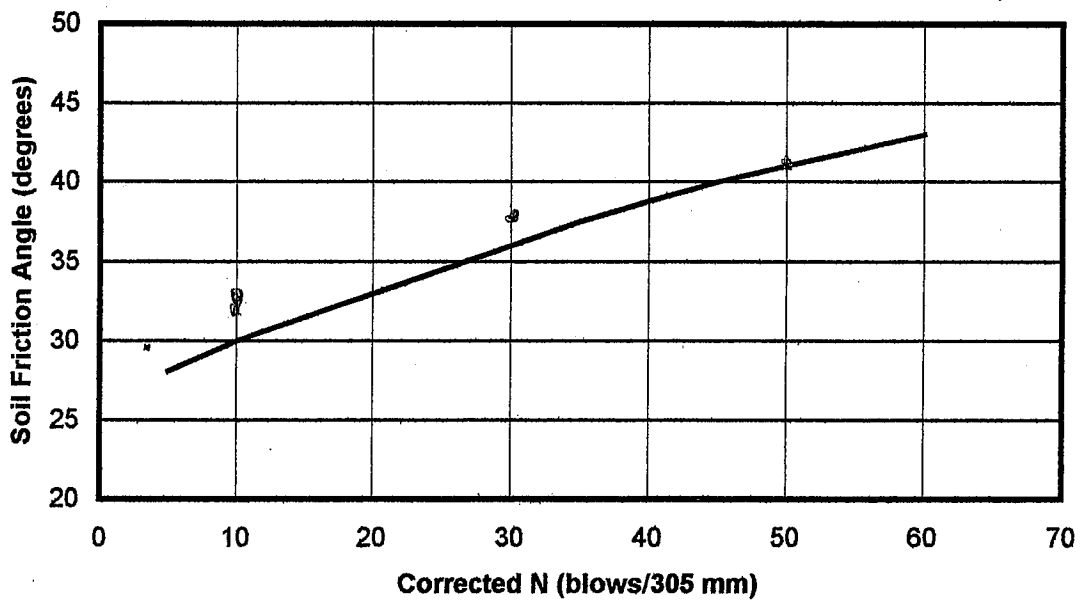


Figure 5.6. Relationship between N_{corr} and ϕ (Peck et al. 1974)

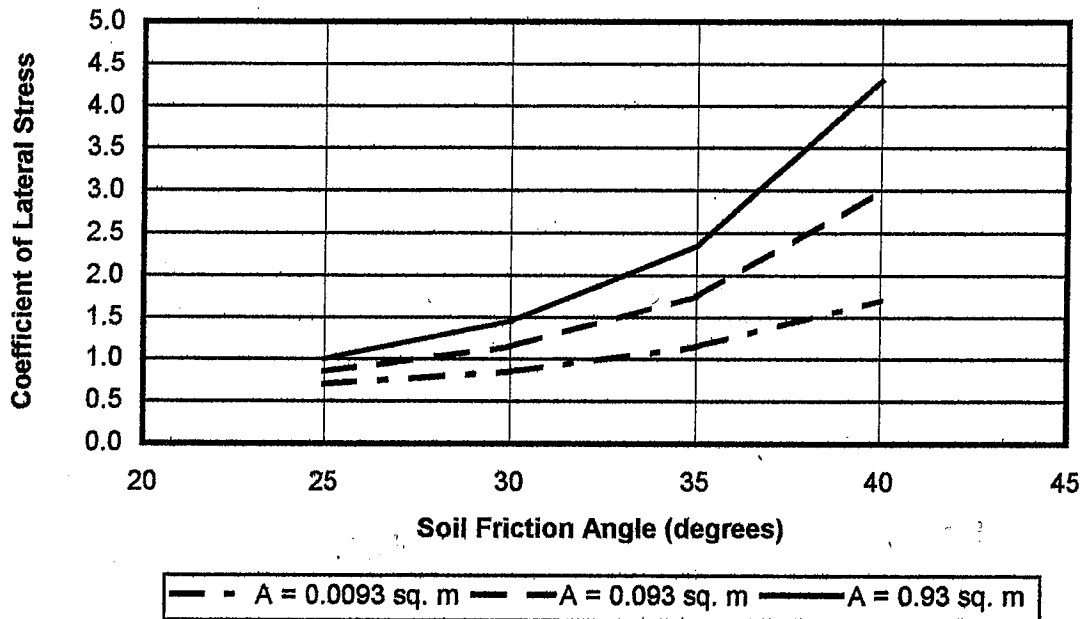


Figure 5.7. Design Curve for Evaluating K_{δ} where $\delta = \phi$ (Nordlund 1963)

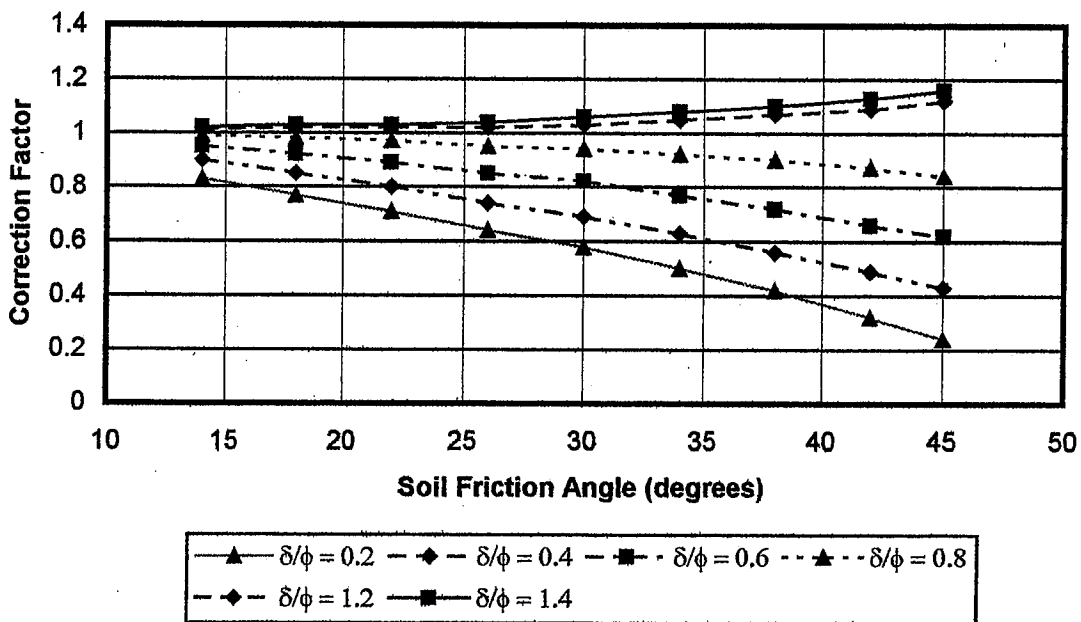


Figure 5.8. Correction Factor for K_{δ} when $\delta \neq \phi$ (Nordlund 1963)

5.2.2 API Methods

In the early 1980s, Olson and Dennis (1982), sponsored by API, conducted a project similar to the author's current project. In this project, Olson and Dennis compiled a database of published axial load test results and used these results to evaluate existing methods and develop improved methods of predicting ultimate axial resistance. In their evaluation and development of predictive methods for steel pipe piles, Olson and Dennis used 116 uplift and compressive tests in cohesive soils and 108 tests in cohesionless soils. Like the author, Olson and Dennis were primarily interested in steel pipe piles. In addition to the methods developed by the original researchers (Dennis and Olson 1983a, Dennis and Olson 1983b, Olson 1990), a number of other researchers subsequently used this database to develop methods for use by API. Two of the most prominent of these are the method of Randolph and Murphy (1985) for use in cohesive soils and the method of Toolan, Lings and Mirza (1990) for use in cohesionless soils. The current API RP 2A guidelines (1993) incorporate a modification of Randolph and Murphy's method in cohesive soils and a modification of Dennis and Olson's (1983b) earlier method in cohesionless soils. A detailed discussion of the evolution of API RP 2A is provided by Pelletier, Murff, and Young (1993).

5.2.2.1 API - Clay

The current API method for piles in clay is a modification of the method developed by Randolph and Murphy (1985). In this α -method, side resistance is calculated using Equation 5.1. However, in the API method, α is correlated with s_u/σ'_{vo} rather than s_u as in Tomlinson's α -methods. In Randolph and Murphy's method, the equations for calculating α take the general form of Equations 5.4 and 5.5,

$$\alpha = \psi_{nc}^{0.5} \psi^{-0.5} \quad \text{for } \psi \leq 1.0 \quad (5.4)$$

$$\alpha = \psi_{nc}^{0.5} \psi^{-0.25} \quad \text{for } \psi > 1.0 \quad (5.5)$$

with the constraint that $\alpha \leq 1.0$, where,

$$\psi = s_u / \sigma'_{vo} \quad \text{for the point of interest}$$

$$\psi_{nc} = s_u / \sigma'_{vo} \quad \text{for normally consolidated soil}$$

In the API method, ψ_{nc} is assumed to be 0.25. This is a reasonable value for the marine clays in which the API method is intended to be used, but in San Francisco bay mud ψ_{nc} is typically taken to be 0.33. In the evaluation of the API method, two trials were performed: one with ψ_{nc} as 0.25 and one with ψ_{nc} as 0.33.

5.2.2.2 Dennis and Olson 1983 – Clay

Dennis and Olson's (1983a) method for piles in clay is an α -method in the style of Tomlinson, with α correlated to s_u as indicated in Figure 5.9. Unit side resistance is calculated using Equation 5.6. In this equation, F_L is a correction factor for pile penetration from Figure 5.10. This method also incorporates a correction factor to account for the manner in which s_u is measured. However, the s_u measurements in this dissertation were from UU tests, for which a correction factor of 1.0 would be applied. This method of Dennis and Olson was developed using 27 uplift tests and 57 compressive tests on steel pipe piles.

$$f_s = \alpha s_u F_L \quad (5.6)$$

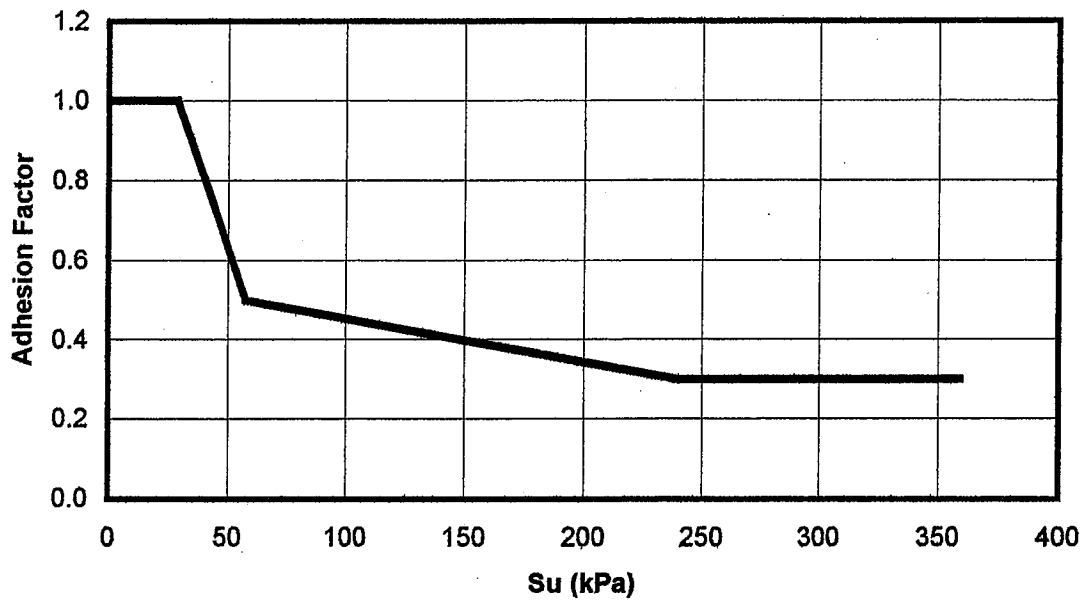


Figure 5.9 Adhesion Factors for Piles in Clay (Dennis and Olson 1983a)

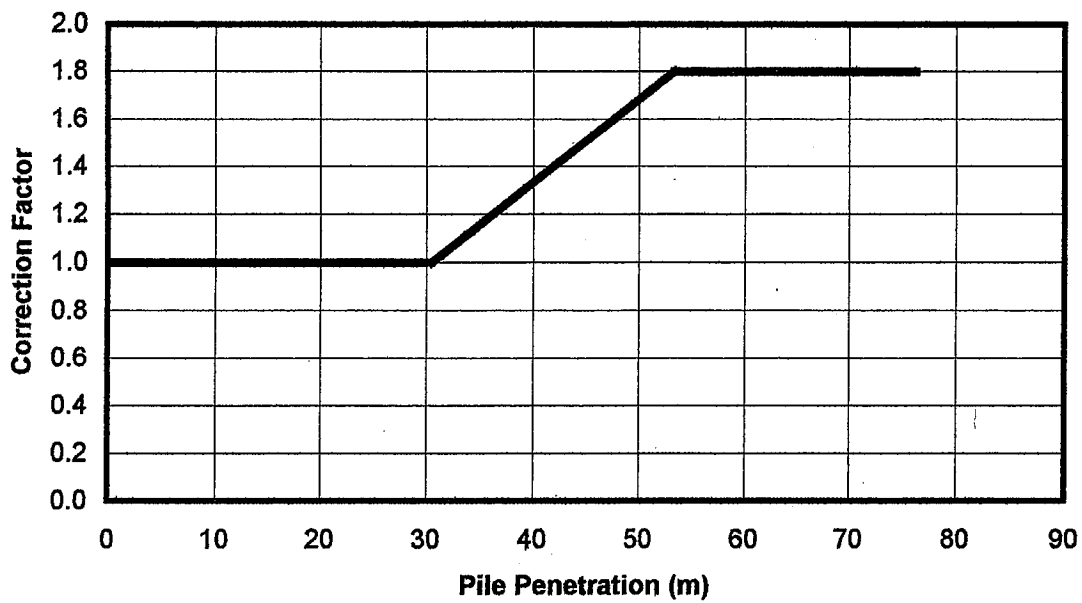


Figure 5.10 Correction Factor F_L for Pile Penetration (Dennis and Olson 1983a)

5.2.2.3 API – Sand

The current API method for piles in sand is a modification of Dennis and Olson's (1983b) method for piles in sand. Unit side resistance is calculated using Equation 5.7. For open-toed steel pipe piles driven unplugged, K is 0.8. For open-toed piles driven plugged and closed-toed piles K is 1.0. In the evaluation of this method, all open-toed piles were assumed to be driven unplugged. Although relatively few in number, the observations of plugging behavior available in Caltrans' archives supports this assumption.

Properly, the value of δ and the limiting value of f_s are determined using Table 5.1. However, since no objective means of evaluating density is provided, a modified form of Table 5.1 was used in this dissertation. In Table 5.2, density is replaced with N_{corr} as defined in Equation 5.3. This table was originally used by Olson (1990) to evaluate the performance of this API method.

$$f_s = K \sigma'_{vo} \tan(\delta) \quad (5.7)$$

Table 5.1 Design Parameters for Cohesionless Siliceous Soil (API 1993)

Density	Soil Description	δ (degrees)	Limit f_s (kPa)
Very Loose Loose Medium	Sand Sand-Silt Silt	15	47.8
Loose Medium Dense	Sand Sand-Silt Silt	20	67.0
Medium Dense	Sand Sand-Silt	25	81.3
Dense Very Dense	Sand Sand-Silt	30	95.7
Dense Very Dense	Gravel Sand	35	114.8

Table 5.2 Soil Properties Assumed for RP 2A Analyses (Olson 1990)

Soil Type	Range of N_{corr} (blows/305 mm)	δ (degrees)	Limit f_s (kPa)
Gravel	0 – 4	20	67.0
	5 – 10	25	81.3
	11 – 30	30	95.7
	over 30	35	114.8
Sand/Gravel	0 – 4	20	67.0
	5 – 10	25	81.3
	11 – 30	30	95.7
	over 30	35	114.8
Sand	0 – 4	15	47.8
	5 – 10	20	67.0
	11 – 30	25	81.3
	31 – 50	30	95.7
	over 50	35	114.8
Sand/Silt	0 – 4	0	0.0
	5 – 10	15	47.8
	11 – 30	20	67.0
	31 – 50	25	81.3
	over 50	30	95.7
Silt	0 – 10	0	0.0
	11 – 30	15	47.8
	over 30	20	67.0

5.2.2.4 Olson 1990

Olson's 1990 method is actually a revision of the API method for piles in sand, which itself was developed from Dennis and Olson's (1983b) earlier work on piles in sand. Olson's method follows the same pattern as the API method, using Equation 5.7 for the calculation of unit side resistance. However, K is determined as a function of N_{corr} using Equations 5.8 and 5.9 for non-displacement and full-displacement piles, respectively, and the design parameters differ as indicated in Table 5.3. This method was developed using 31 tests on steel pipe piles.

$$K = 0.16 + 0.15N_{corr} \quad \text{for non-displacement piles} \quad (5.8)$$

$$K = 0.7 + 0.15N_{corr} \quad \text{for full-displacement piles} \quad (5.9)$$

Table 5.3 Soil Properties (Olson 1990)

Soil Type	Range of N_{corr} (blows/305 mm)	δ (degrees)	Limit f_s (kPa)
Gravel	0 - 4	20	67.0
	5 - 10	25	81.3
	11 - 30	30	95.7
	over 30	35	114.8
Sand/Gravel	0 - 4	20	67.0
	5 - 10	25	81.3
	11 - 30	30	95.7
	over 30	35	114.8
Sand	0 - 4	20	47.8
	5 - 10	30	52.7
	11 - 30	35	91.0
	31 - 50	40	124.5
	51 - 100	40	177.2
over 100	40	181.9	
Sand/Silt	0 - 4	10	47.8
	5 - 10	10	47.8
	11 - 30	15	67.0
	31 - 50	20	95.7
	51 - 100	30	95.7
over 100	34	95.7	
Silt	0 - 4	10	47.8
	5 - 10	15	47.8
	11 - 30	20	47.8
	31 - 50	20	67.0
	over 50	25	67.0

5.2.2.5 Toolan et al. 1990

The method of Toolan, Lings, and Mirza (1990) is a proposed revision to the API method for piles in sand. Instead of using the design parameters in Table 5.1, Toolan et al. proposed to determine unit side resistance based solely on relative density using the values given in Table 5.4. For the purpose of evaluating the method in this dissertation, relative density was correlated with N_{corr} as indicated in Table 5.5 in a manner similar to that used by Olson (1990) for the evaluation of the API method.

Table 5.4 Values of Skin Friction in Revised Method (Toolan et al. 1990)

Description	Relative Density (%)	f_s (kPa)
Loose	15	24
Medium Dense	25	40
Dense	50	80
Very Dense	100	160

Table 5.5 Correlation between Density Descriptions and N_{corr} (Peck et al. 1974)

N_{corr}	Description
0 – 10	Loose
11 – 30	Medium Dense
31 – 50	Dense
over 50	Very Dense

5.2.3 Methods Based on Recent Instrumented Tests

In the 1990s, a number of small- and large-scale instrumented axial load tests were conducted at sites in Norway, the U.K. and the U.S. The majority of these tests were performed by Imperial College (IC) and the Norwegian Geotechnical Institute (NGI). At Imperial College, Jardine and his students have used these results to develop methods for both piles in clay and piles in sand (Jardine and Chow 1996). The method

for piles in clay is described below. At NGI, Karlsrud and his colleagues have developed a series of methods for piles in clay. The β -method currently recommended by NGI is also described below.

5.2.3.1 *Jardine and Chow 1996 – Clay (Imperial College)*

Jardine and Chow's (1996) method for piles in clay was developed based on data collected from small-scale instrumented axial load tests at four sites in the U.K.: Canons Park, Cowden, Bothkennar and Pentre. The piles used were 102-mm diameter closed-toed steel pipe piles ranging from 6 to 20 m in length. The piles were installed by fast jacking. Unit side resistance is calculated according to Equation 5.10.

$$f_s = 0.8K_c \sigma'_{vo} \tan(\delta_f). \quad (5.10)$$

Here K_c defined as,

$$K_c = [2.2 + 0.016OCR - 0.87 \log(S_t)] OCR^{0.42} (h/R)^{-0.20} \quad (5.11)$$

with the constraint that,

$$h/R \geq 8 \quad (5.12)$$

where,

$OCR = \sigma'_p / \sigma'_{vo}$, overconsolidation ratio

σ'_p = apparent preconsolidation pressure

S_t = soil sensitivity

h = distance above pile toe

R = pile radius.

For open-toed piles, R is calculated as,

$$R^* = (R_{outer}^2 - R_{inner}^2)^{0.5} \quad (5.13)$$

The constraint in Equation 5.12 specifies that where h/R is less than 8, close to the toe of the pile, a value of 8 should be used for h/R in Equation 5.11.

Jardine and Chow indicate that the interface angle of friction at failure δ_f in Equation 5.10 is an intermediate value between the peak and ultimate interface angles of friction as measured in an IC interface ring shear test. Unfortunately, the author does not have access to an IC interface ring shear device. For the purpose of evaluating the method as part of this dissertation, the value of $\tan(\delta_f)$ was determined using a correlation between $\tan(\delta_{ultimate})$ and plasticity index (PI) presented by Jardine and Chow (Figure 5.11).

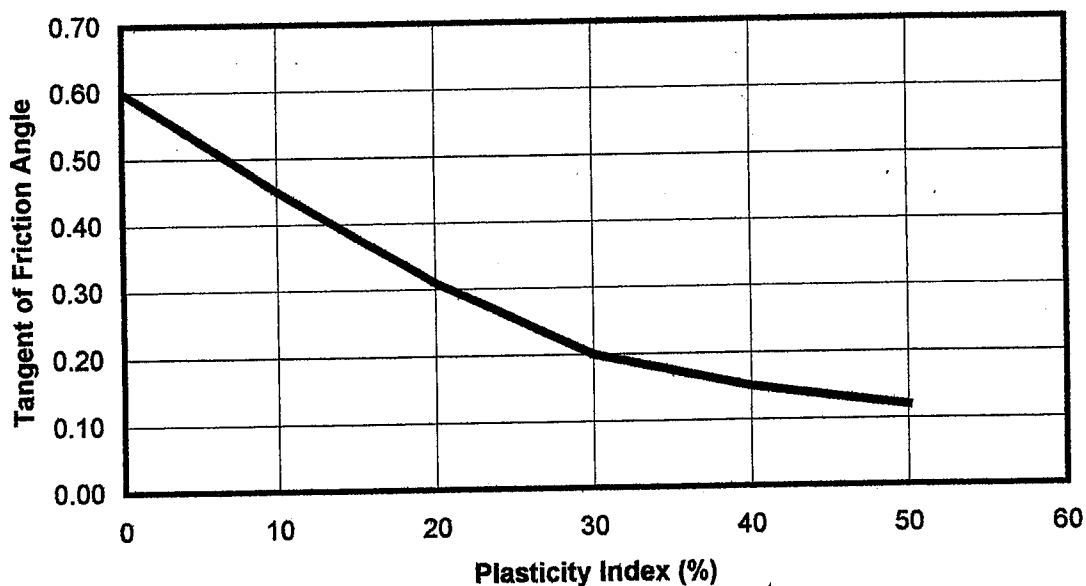


Figure 5.11 Trend for $\tan(\delta_{ultimate})$ Values from IC Ring Shear Tests on North Sea Clays (Jardine and Chow 1996)

The author also used a correlation to determine soil sensitivity (S_t). Jardine and Chow recommend evaluating S_t using parameters from a pair of consolidation tests: one test on an undisturbed sample and one test on a reconstituted sample at a water content of 1.25 times the Atterberg liquid limit. However, since this recommended testing was beyond the author's means, S_t was determined using the correlation with liquidity index LI suggested by Jardine and Chow. This correlation is incorporated in Equation 5.14, in which s_u is measured in a UU test.

$$S_t = 1.7 \left[10^{2(1-LI)} \right] \sqrt{s_u} \quad (5.14)$$

In this dissertation, the overconsolidation ratio (OCR) was also determined from a correlation rather than from a consolidation test on an undisturbed sample. On the pushed samples obtained from the project borings, 83 consolidation tests were performed. Unfortunately, most of the samples were too disturbed for the apparent preconsolidation pressure to be evaluated from the consolidation test. However, from the 35 consolidation tests showing the least sample disturbance the author has developed the site-specific correlation between ψ and OCR in Equation 5.15. This correlation is shown with the actual data in Figure 5.12. The scatter at lower OCR s is the result of sample disturbance, which can make it impossible to determine the apparent preconsolidation from the consolidation test results. The correlation recommended by Ladd, Foott, Ishihara, Schlosser and Poulos (1977) is also provided for comparison. In Equation 5.16, a value of 0.33 for ψ_{nc} is used in the correlation of Ladd et al. In evaluating this method, two trials were performed: one using the site-specific correlation and one using the correlation of Ladd et. al.

$$OCR = \left(\frac{\psi}{0.28} \right)^{1.02} \text{ Site-Specific} \quad (5.15)$$

$$OCR = \left(\frac{\psi}{\psi_{nc}} \right)^{1.25} \quad \text{Ladd et. al (1977)} \quad (5.16)$$

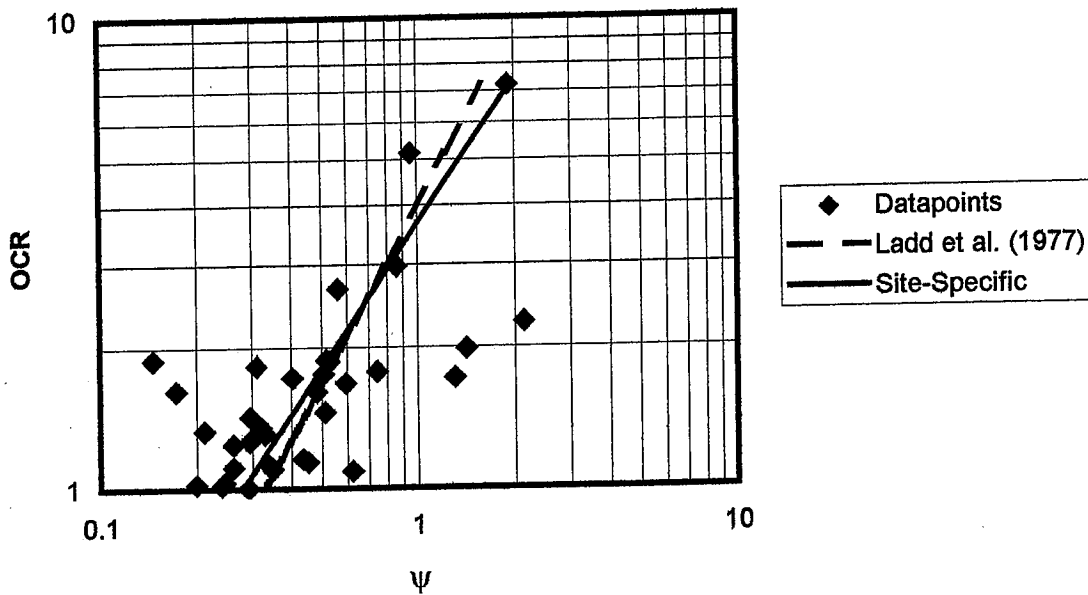


Figure 5.12 Relationship between ψ and OCR

5.2.3.2 Karlsrud 1999 (NGI)

The method for piles in clay currently recommended by NGI is a β -method, in which unit side resistance is defined using Equation 5.17 (Karlsrud 1999). In NGI's β -method, β is determined from OCR using the relationship in Figure 5.13. In this dissertation, OCR is determined from the correlations with ψ given in Equations 5.15 and 5.16.

$$f_s = \beta \sigma'_{vo} \quad (5.17)$$

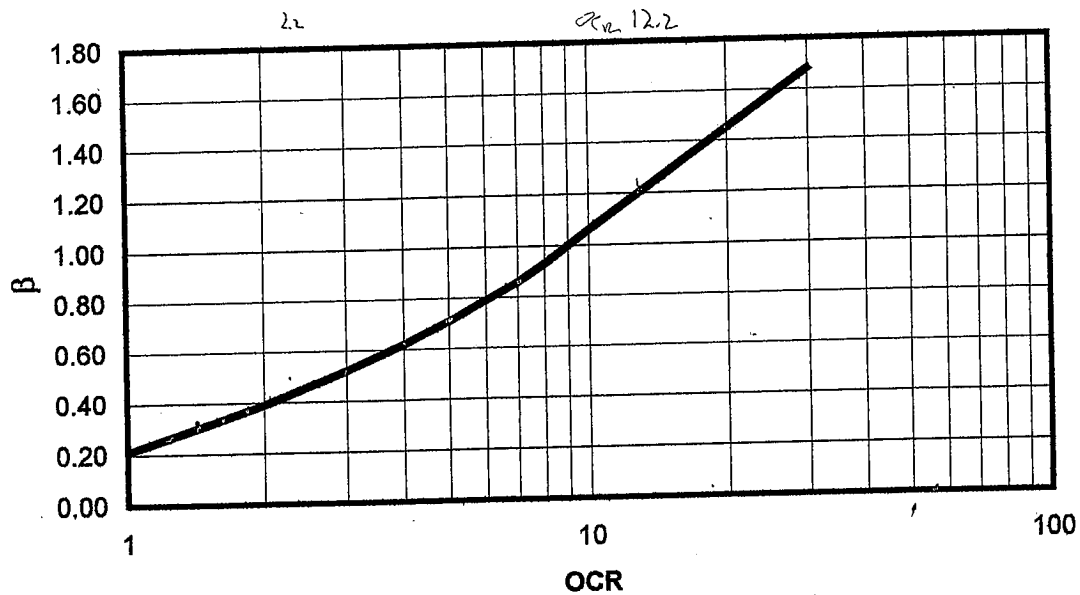


Figure 5.13 Relationship between β and OCR (Karlsrud 1999)

Karlsrud's correlation between OCR and β is based on data collected from instrumented axial load tests on both closed- and open-toed steel pipe piles at 10 sites: Haga, University of Houston, West Delta, Onsøy, Lierstranda, Pentre, Tilbrooke, Canons Park, Cowden and Bothkennar. These sites include the four used by Jardine and Chow (1996). The piles range in diameter from 154 to 812 mm and in length from 5.5 to 71.3 m.

5.2.4 Other Methods

5.2.4.1 Decourt 1982

Decourt (1982) presents a simple SPT-based method for the prediction of side resistance in both clays and sand. Unit side resistance is calculated using Equation 5.18 with lower and upper limits on N of 3 and 50 blows/305 mm. This method was developed based on data collected by Decourt and Quaresma in their respective

consulting practices in Brazil. Their original database included a variety of bored and driven piles in both alluvial and residual soils.

$$f_s = 3.3 N + 10 \text{ in kPa} \quad (5.18)$$

5.2.4.2 Kraft et al. 1981 – Revised λ -Method

In the early 1970s, as an alternative to earlier α -methods, Vijayvergiya and Focht (1972) proposed the λ -method, in which unit side resistance is calculated using Equation 5.19. In this equation, λ is an empirical coefficient correlated to pile penetration with the value of λ decreasing with increasing pile penetration.

$$f_s = \lambda(\sigma'_{vo} + 2s_u) \quad (5.19)$$

In the early 1980s, Kraft, Focht and Amerasinghe (1981) developed a revised λ -method, replacing Vijayvergiya and Focht's correlation with separate correlations between λ and pile penetration (L) for normally consolidated and overconsolidated soils. These two correlations are provided in Equations 5.20 and 5.21. Kraft et al. define overconsolidated soils as those with ψ greater than 0.4.

$$\lambda = 0.296 - 0.032 \ln(L) \text{ for } \psi \leq 0.4 \quad (5.20)$$

$$\lambda = 0.488 - 0.078 \ln(L) \text{ for } \psi > 0.4 \quad (5.21)$$

5.2.5 Application of Methods

For these methods, uplift resistance (Q_o) was calculated using Equation 5.22 on a layer-by-layer basis. The weight of the pile was ignored. For the 155 piles used in this dissertation, the pile weight is negligible when compared to the measured ultimate resistance. However, for larger piles, especially precast concrete piles or concrete-filled

steel pipe piles, it could be unconservative in compression or uneconomical in uplift to ignore the weight of the pile.

$$Q_c = P \sum_{i=1}^n f_{si} H_i \quad (5.22)$$

where,

Q_c = calculated uplift resistance

P = exterior perimeter of pile

f_{si} = unit side resistance in layer i

H_i = height of layer i

5.3 METHODS BASED ON CPT AND CPTU

5.3.1 CPT-Methods from Caltrans' 1989 Study

In Caltrans' 1989 study, Richman and Speer evaluated six existing CPT-methods against a database of 32 compressive tests on 19 bored piles and 13 driven piles. The performance of these six methods against the 13 driven piles is summarized in Table 5.6. In this table, the sample mean (E), sample standard deviation (σ) and coefficient of variation (COV) of the ratio of calculated resistance (Q_c) to measured resistance (Q_m) are given for each of the six methods.

Table 5.6 Performance of CPT-Methods for 13 Driven Piles (Richman and Speer 1989)

Method	Reference	E	σ	COV
Cone-M	Tumay and Fakhroo 1981	1.12	0.52	0.47
Schmertmann	Schmertmann 1978	0.96	0.36	0.37
Bustamante	Bustamante and Ganeselli 1982	0.79	0.28	0.36
LPC Cone	Briaud et al. 1985	1.01	0.45	0.45
Direct Cone	Briaud et al. 1985	1.97	1.01	0.51
European	De Ruiter and Beringen 1979	1.19	0.60	0.51

Based on the COV 's in Table 5.6, the methods of Bustamante (Bustamante and Ganeselli 1982) and Schmertmann (1978, cited by Briaud and Miran 1992) performed much better than the other four methods. For this reason, these two methods were included in the evaluation of existing methods in this dissertation.

5.3.1.1 *Bustamante and Ganeselli 1982*

In the 1960s, methods using CPT and pressuremeter measurements to predict pile resistance were introduced. In 1964, the laboratories of the French counterpart of FHWA, Laboratoires des Ponts et Chaussées (LPC), began research to experimentally verify these methods. In 1972, prior to the completion of this research, LPC adopted such methods for the design of highway structures. The research involved in development of the CPT-method is described by Bustamante and Ganeselli (1982).

This research involved 197 compressive and uplift tests. These tests were performed on 96 piles at 48 sites in France in soil profiles consisting of "clay, silt, and gravel or even weathered rock, but also mud, peat, more or less weathered chalk, and marl."

The distribution of pile types included in this study is given in Table 5.7. Bored piles included "plain bored piles, totally or partially cased piles, mud or fresh-water bored

piles using a wide variety of tools (augers, buckets, hammergrabs, bits, valves).” Driven piles included steel H-piles, closed-toed steel pipe piles, and precast reinforced concrete piles. No description of grouted piles, barrettes, or piers is given.

In the axial load tests, the piles were loaded in equal increments with durations of 60 or 90 min. without intermediate unloading. Of the 96 piles, 57 piles, apparently bored piles, on 31 sites were instrumented to measure separately the resistance mobilized on the side and on the toe. This method was calibrated to predict an allowable resistance, rather than an ultimate resistance. In the calculation of allowable resistance, the measured ultimate resistance was defined using the creep method, which is described by Fellenius (1996).

Table 5.7 Distribution of Pile Types (Bustamante and Gianceselli 1982)

Pile Type	Number	Diameter (cm)	Length (m)
Bored	55	42 – 150	6 – 44
Driven	31	30 – 64	6 – 45
Grouted	8	11 – 70	10 – 31
Barrettes	1	60 x 220	30
Piers	1	200	12

Two types of cone penetrometers were used in this study: a Parez-type cone penetrometer and an electric cone penetrometer. The cone penetrometer developed by Parez consisted of a conical point connected to the piston of a small hydraulic jack at the base of a rod. An oil pressure line transmitted the pressure to manometers located at the surface (Lunne et al. 1997). The Parez-type cone penetrometer used a 45-mm diameter (15 cm²) cone. The electric cone penetrometer used a 36-mm diameter (10 cm²) cone. CPT was only performed on 30 of the 39 sites investigated in the development of CPT- and pressuremeter-methods. On nine of the sites, shallow refusal occurred during testing. Of the remaining 21 sites tested, the CPT results from only 12 sites were considered “utilizable or representative.”

Unit side resistance (f_s) is calculated using Equation 5.23. Values of α and $f_{s,max}$ are obtained from Table 5.8. Different values of α are given for concrete and steel piles.

$$f_s = q_c / \alpha \leq f_{s,max} \quad (5.23)$$

where,

q_c = unit cone resistance

α = factor from Table 5.8

$f_{s,max}$ = maximum f_s from Table 5.8

Table 5.8 Design Parameters for Side Resistance (Bustamante and Ganeselli 1982)

Soil	q_c (MPa)	α		$f_{s,max}$ (kPa)
		Concrete	Steel	
Soft clay and mud	<1	30	30	15
Moderately compact clay	1 – 5	40	80	35
Compact to stiff clay and compact silt	>5	60	120	35
Silt and loose sand	≤5	60	120	35
Moderately compact sand and gravel	5 – 12	100	200	80
Compact to very compact sand and gravel	>12	150	200	120

5.3.1.2 Schmertmann 1978

Schmertmann's method (Schmertmann 1978, cited by Briaud and Miran 1992) is slightly more complicated than the method of Bustamante and Ganeselli. In the calculation of unit side resistance (f_s) in both clay and sand, Schmertmann first calculates two or three alternative values of f_s and then defines f_s as the minimum of these values.

In clay, f_s is calculated as the minimum of f_1 and f_2 as defined by Equations 5.24 through 5.26. Since, for Equation 5.24, a correlation between q_c and s_u is not specified by Briaud and Miran, the author chose to use the one defined in Equation 5.27. This equation is based on the recommendations of Lunne, Robertson and Powell (1997).

$$f_1 = \alpha s_u \quad (5.24)$$

$$f_2 = \alpha \frac{l}{8D} q_s \quad \text{for } l < 8D \quad (5.25)$$

$$f_2 = \alpha q_s \quad \text{for } l \geq 8D \quad (5.26)$$

where,

$$s_u = q_c / 17.5 \quad (5.27)$$

α = adhesion factor from Figure 5.14

l = depth of point of interest below mudline

D = total pile embedment

q_s = unit sleeve friction

In sand, f_s is calculated as the minimum of f_1 , f_2 and f_3 as defined in Equations 5.28 through 5.31.

$$f_1 = K \frac{l}{8D} q_s \quad \text{for } l < 8D \quad (5.28)$$

$$f_1 = K q_s \quad \text{for } l \geq 8D \quad (5.29)$$

$$f_2 = 0.12 \text{ MPa} \quad (5.30)$$

$$f_3 = c q_c \quad (5.31)$$

where,

K = adhesion factor from Figure 5.15

c = coefficient from Table 5.9

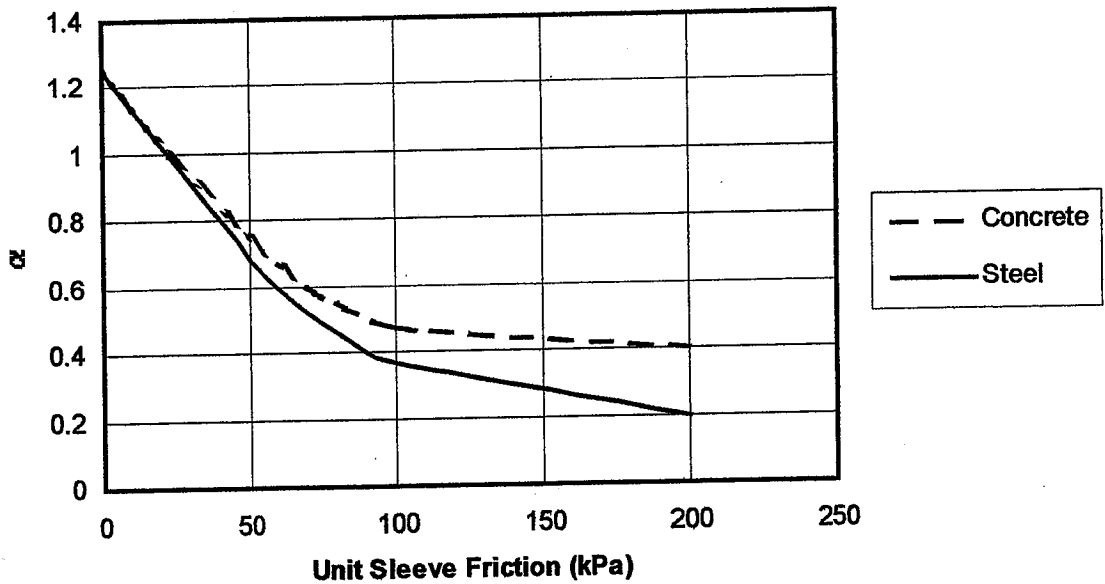


Figure 5.14 Adhesion Factors for Piles in Clay (Briaud and Miran 1978)

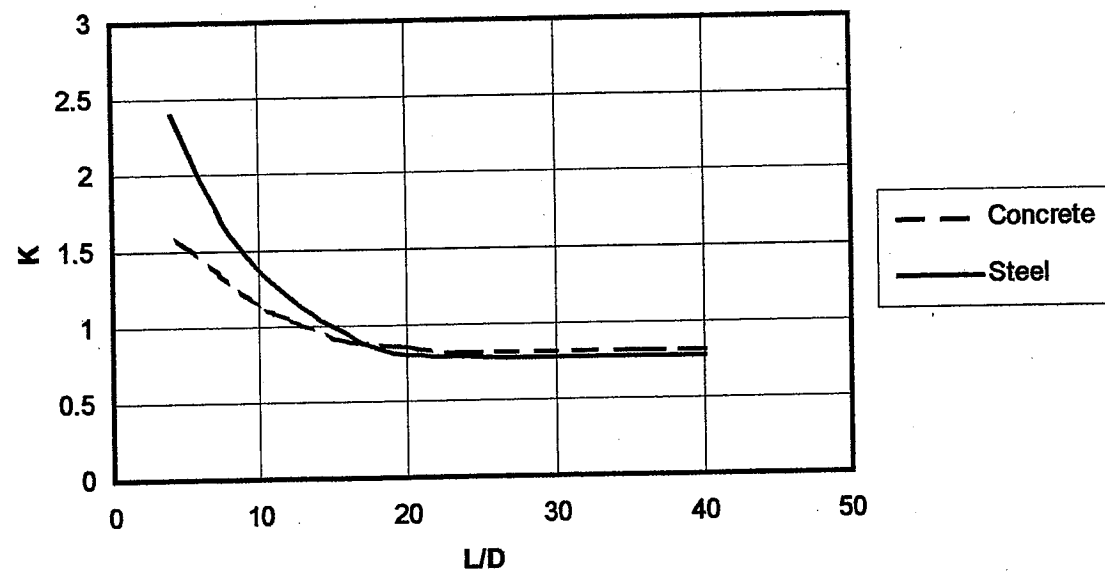


Figure 5.15 Adhesion Factors for Piles in Sand (Briaud and Miran 1992)

Table 5.9 Coefficients for Side Resistance in Sand (Briaud and Miran 1992)

Pile Type	<i>c</i>
Solid precast concrete	0.012
Closed-toed steel pipe pile	0.012
Open-toed steel pipe pile	0.008

5.3.2 Recent CPTU-Methods

Since the advent of CPTU in the early 1970s, researchers have been modifying earlier CPT-based correlations to make use of the measurement of pore pressure in CPTU. In the 1990s, a few researchers developed CPTU-methods for the prediction of pile resistance. Two of these methods, which can be used in the variety of soils encountered by Caltrans, are evaluated in this dissertation: Eslami and Fellenius (1997) and Takesue, Sasao and Matsumoto (1998).

5.3.2.1 Eslami and Fellenius 1997

Eslami and Fellenius (1997) collected 102 published cases of axial load tests with CPT or CPTU measurements. Ninety-two of these cases involved driven piles. In addition to steel pipe piles and steel H-piles, the pile types included square, octagonal, round and triangular precast concrete piles. The pile embedment lengths ranged from 5 to 67 m; the pile widths ranged from 200 to 900 mm; and the measured ultimate resistances ranged from 0.08 to 8 MN.

The 102 cases were divided into three groups. Group I contained 24 cases: 14 compressive tests with toe load measurements and 10 uplift tests; Group II contained 53 cases: 34 compressive tests with no toe load measurements and 19 uplift tests without CPT sleeve friction measurements; and Group III contained 25 cases in which the maximum pile-head displacement was too small to determine the measured ultimate

resistance. In these 25 cases, the measured ultimate resistance was apparently estimated by extrapolating the load-displacement curve to higher displacements.

Of the 102 cases, 80% included electric CPT measurements. The other 20% included only mechanical CPT measurements. Although all of the CPT readings in silt and clay included pore pressure measurements, not all of the readings in coarse-grained soils included such pore pressure measurements.

Eslami and Fellenius calculate unit side resistance using Equation 5.32. This equation includes a coefficient (C_s) based on the soil classification, which is determined from Figure 5.16. The cone area ratio (α) is 0.8 for all the cones used in the project soundings.

$$f_s = C_s q_E \quad (5.32)$$

$$q_E = q_t - u_2 \quad (5.33)$$

$$q_t = q_c + u_2(1 - \alpha) \quad (5.34)$$

where,

C_s = coefficient from Table 5.10

q_E = effective unit cone resistance

q_t = corrected unit cone resistance

u_2 = pore pressure measured behind cone

α = cone area ratio

Table 5.10 Adhesion Factors from Soil Type (Eslami and Fellenius 1997)

Zone	Soil Type	C_s
1	Soft sensitive soils	0.080
2	Clay	0.050
3	Stiff clay and mixture of clay and silt	0.025
4	Mixture of silt and sand	0.010
5	Sand	0.004

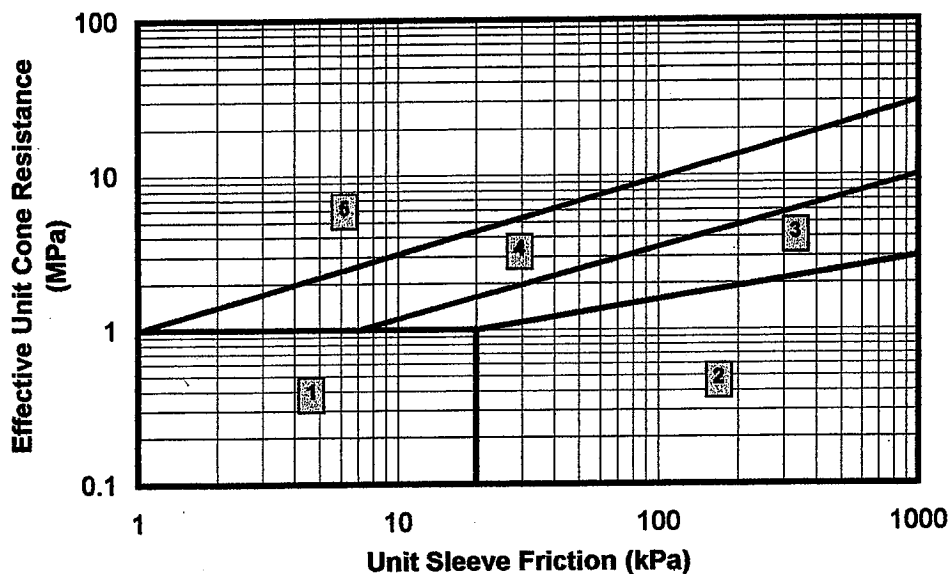


Figure 5.16 Soil Classification Chart (Eslami and Fellenius 1997)

5.3.2.2 Takesue et al. 1998

In evaluating the results of six instrumented axial load tests, Takesue, Sasao and Matsumoto (1998) discovered a correlation between the excess pore pressure Δu and the ratio of unit side resistance to unit sleeve resistance, which is referred to as an adhesion factor (α). The correlation between Δu and α is shown in Figure 5.17. Excess pore pressure Δu is defined in Equation 5.35, in which u_0 is the free-field pore pressure. Unit side resistance is calculated using Equation 5.36.

$$\Delta u = u_2 - u_0 \quad (5.35)$$

$$f_s = \alpha q_s \quad (5.36)$$

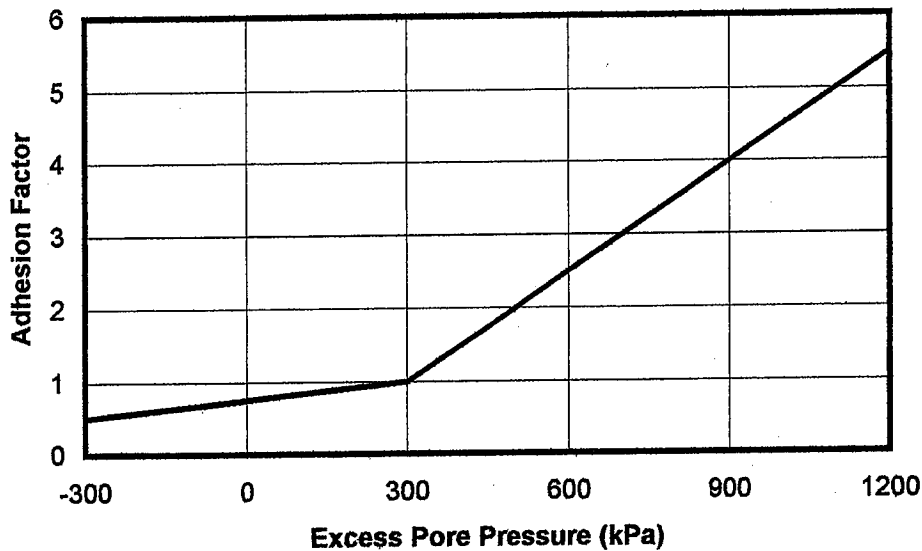


Figure 5.17 Adhesion Factors from Δu (Takesue et al. 1998)

Three of the six tests were on bored cast-in-situ concrete piles. The other three tests were on driven steel pipe piles. Three of the piles were installed in unusual soils: one bored pile in *Shirasu* sand, which is a volcanic sand, and two driven piles in diatomaceous mudstone. The piles and soils used in the development of this method are very different from those in the author's database. For this reason, this method was not expected to perform well in the author's evaluation, but it was evaluated because of its simplicity and its uniqueness in using pore pressure measurements directly.

5.3.3 Application of CPT/CPTU-Methods

For all four of these methods, uplift resistance (Q_c) was calculated using Equation 5.37. To simplify the use of these methods, Q_c was calculated on a reading-by-reading

basis directly from the CPTU measurements rather than on a layer-by-layer basis, as was done for the methods based on SPT and laboratory tests. The weight of the pile was ignored.

$$Q_c = \frac{PL}{n} \sum_{i=1}^n f_{si} \quad (5.37)$$

where:

P = external pile perimeter

L = pile embedment

n = number of CPTU readings between pile mudline and pile toe

f_{si} = calculated unit side resistance for reading i

The method of Eslami and Fellenius is intended to be used in this manner, and the method of Takesue et al. is easily adapted to this approach since prior soil classification is not required for its application. However, for the method of Bustamante and Gianeselli and the method of Schmertmann, a prior soil classification is required before unit side resistance can be calculated. Fortunately, both of these methods only require that the soil be classified as either clay or sand. For this purpose, the author used the soil classification chart of Douglas and Olsen (1981). This chart, rather than other more recent charts, was used because it does not require a design stratigraphy with estimated soil unit weights. The soil can be classified using only the CPTU measurements. The clay and sand zones used by the author are shown in Figure 5.18. The dividing line between the zones is the boundary between "non-cohesive coarse-grained" soils and "non-cohesive coarse- and fine-grained soils" on Douglas and Olsen's 1981 chart. The stratigraphy provided by this classification system was found to agree reasonably well with the borings made adjacent to the CPTU soundings used in this dissertation.

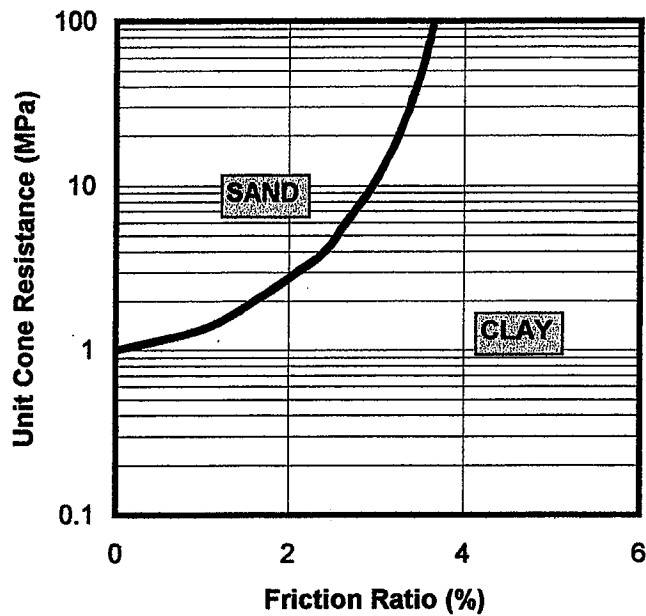


Figure 5.18 Soil Classification Chart (Douglas and Olsen 1981)

5.4 CONCLUSION

In this chapter, sixteen existing methods for the prediction of ultimate side resistance were described. In the next chapter, these methods are evaluated against the author's uplift test pile database to identify a candidate from which to develop the improved side resistance method presented in Chapter 7.

6. EVALUATION OF SIDE RESISTANCE METHODS

6.1 INTRODUCTION

In this chapter, the sixteen side resistance methods described in the previous chapter are evaluated against the uplift test pile database to select an initial format from which to develop an improved method for Caltrans' use. The twelve methods based on standard penetration tests (SPT) and laboratory tests are evaluated first, followed by the four methods based on electric cone penetration testing (CPT) and piezocone penetration testing (CPTU). The evaluation of existing methods was done using a Microsoft Visual Basic 6.0 program VBPILE created by the author.

6.2 STATISTICAL INTERPRETATION

In statistically evaluating these methods, the ratio of the calculated ultimate resistance (Q_c) to the measured ultimate resistance defined by Fleming's extrapolation (Q_m) was used to evaluate the performance of each method or combination of methods. No statistical distribution was assumed for Q_c/Q_m . In each case, the sample mean (E), variance (Var), standard deviation (σ), and coefficient of variation (COV) of Q_c/Q_m were calculated using Equations 6.1 through 6.4 (Ang and Tang 1975).

$$E = \frac{1}{n} \sum_{i=1}^n (Q_c/Q_m)_i \quad (6.1)$$

$$Var = \frac{1}{n-1} \sum_{i=1}^n [(Q_c/Q_m)_i - E]^2 \quad (6.2)$$

$$\sigma = \sqrt{Var} \quad (6.3)$$

$$COV = \frac{\sigma}{E} \quad (6.4)$$

In terms of selecting an existing method for further improvement, *COV* was considered to be the most important measure. The accuracy of the existing method, measured by *E*, was considered to be secondary to its precision, measured by *COV*.

6.3 METHODS BASED ON SPT AND LABORATORY TESTS

6.3.1 Against 26 Uplift Test Piles in Clay/Sand Profiles

The twelve methods based on SPT and laboratory tests were first evaluated against 26 of the 118 piles in the uplift test pile database. The results of the evaluation are provided in Table 6.1. These 26 piles were those satisfying the criteria listed below:

- Both Q_{CT} (Caltrans' offset-limit) and Q_m (Fleming's extrapolation) are known.
- The soil profile (in contact with the side of the pile) is composed of clay and/or sand.
- If the soil profile contains clay, the setup time is greater than or equal to 7 days.
- There are UU test results and Atterberg limits in the clay layers and SPT measurements in both the clay and sand layers
- The pile is either steel pipe or solid precast concrete.
- The pile was installed with an impact hammer.
- The pile was not relief drilled.

Table 6.1 Evaluation of Existing Methods

Clay Method \ Sand Method	API ($\psi_{nc} = 0.25$)	API ($\psi_{nc} = 0.33$)	Decourt	Dennis & Olson	Jardine (OCR - Ladd)	Jardine (OCR - Site)	Karlsrud (OCR - Ladd)	Karlsrud (OCR - Site)	Kraft et al.	Tomlinson 1971	Tomlinson 1979
$E(Q_c/Q_m)$											
API	0.87	0.92	0.77	0.79	0.69	0.69	0.87	0.87	0.85	0.95	0.88
Decourt	1.30	1.36	1.20	1.23	1.13	1.13	1.30	1.31	1.29	1.39	1.32
Nordlund	0.87	0.93	0.77	0.80	0.70	0.70	0.87	0.88	0.86	0.96	0.89
Olson	0.88	0.94	0.79	0.81	0.71	0.71	0.89	0.89	0.87	0.97	0.90
Toolan et al.	0.74	0.79	0.64	0.66	0.56	0.56	0.74	0.74	0.72	0.82	0.75
$\alpha(Q_c/Q_m)$											
API	0.41	0.46	0.37	0.35	0.34	0.35	0.41	0.41	0.40	0.46	0.48
Decourt	0.40	0.41	0.43	0.39	0.43	0.43	0.39	0.40	0.40	0.42	0.43
Nordlund	0.46	0.50	0.42	0.40	0.39	0.40	0.46	0.46	0.44	0.50	0.50
Olson	0.37	0.41	0.34	0.31	0.31	0.31	0.36	0.37	0.36	0.42	0.44
Toolan et al.	0.38	0.44	0.32	0.30	0.27	0.27	0.38	0.38	0.36	0.45	0.46
$COV(Q_c/Q_m)$											
API	0.48	0.50	0.48	0.45	0.50	0.50	0.47	0.47	0.47	0.48	0.54
Decourt	0.30	0.30	0.35	0.32	0.38	0.38	0.30	0.30	0.31	0.30	0.33
Nordlund	0.52	0.54	0.54	0.50	0.56	0.57	0.52	0.52	0.51	0.52	0.57
Olson	0.41	0.44	0.43	0.39	0.44	0.44	0.41	0.41	0.41	0.43	0.49
Toolan et al.	0.52	0.55	0.50	0.46	0.48	0.48	0.51	0.51	0.50	0.54	0.61

In the evaluation of these twelve methods against 26 uplift test piles, it was found that Decourt's method had the lowest *COV* of the sand methods in all cases. For this particular dataset, the clay methods, with the exception of Jardine and Chow's method, yielded comparable *COVs*. However, since in this dataset only 30% of the calculated resistance was derived from clay, this was not an adequate evaluation of the clay methods, and further examination of the clay methods was in order. To accomplish this,

a second evaluation was performed pairing each clay method with Decourt's sand method. The author suspects that Decourt's sand method performed with less variability than the other sand methods because it uses N -values directly while the others rely on estimates of ϕ or relative density obtained through correlations with N -values.

6.3.2 Against 11 Piles in Predominantly Clay Profiles

In this second evaluation, the eight clay methods were evaluated against 11 of the previous 26 uplift test piles. These 11 piles were those in profiles of at least 50% clay. In this dataset, 70% of the calculated resistance was derived from clay, the reverse of the previous dataset. The results of this second evaluation are provided in Table 6.2.

Table 6.2 Evaluation of Clay Methods with Decourt's Sand Method

Clay Method	E	σ	COV
API ($\psi_{nc} = 0.25$)	1.41	0.24	0.17
API ($\psi_{nc} = 0.33$)	1.52	0.24	0.15
Decourt	1.18	0.35	0.29
Dennis & Olson	1.24	0.26	0.21
Jardine (OCR - Ladd)	1.02	0.39	0.38
Jardine (OCR - Site)	1.02	0.39	0.38
Karlsrud (OCR - Ladd)	0.40	0.24	0.17
Karlsrud (OCR - Site)	1.41	0.24	0.17
Kraft et. al	1.36	0.24	0.18
Tomlinson 1971	1.54	0.28	0.18
Tomlinson 1979	1.46	0.29	0.20

This evaluation of the clay methods reinforces the results of the previous evaluation. From these two evaluations, it is clear that the majority of variability or lack of precision in the methods based on SPT and laboratory tests is due to the poor performance of the methods in sand.

6.4 METHODS BASED ON CPT AND CPTU

The four CPT- and CPTU-methods were evaluated against 22 uplift test piles in profiles of clay and/or sand. These 22 piles satisfy the criteria in the evaluation of methods based on SPT and laboratory tests. The results of this evaluation are provided in Table 6.3. Decourt's SPT-method was included for comparison.

Table 6.3 Evaluation of CPT/CPTU-Methods

Method	μ	σ	<i>COV</i>
Bustamante & Gianceselli	0.84	0.35	0.41
Decourt (SPT)	1.08	0.31	0.29
Eslami & Fellenius	1.37	0.45	0.33
Schmertmann	1.03	0.38	0.37
Takesue et al.	2.29	1.49	0.65

Surprisingly, Decourt's SPT-method had a lower *COV* than the CPT/CPTU-methods. The values of *E* and *COV* for Bustamante and Gianceselli's and Schmertmann's methods were similar to those from Caltrans' 1989 study (Richman and Speer 1989). As expected, the method of Takesue et al. performed rather poorly. Of the CPT/CPTU-methods, the method of Eslami and Fellenius had the least variability as indicated by the *COV*, although it over-predicted significantly.

6.5 CONCLUSION

From these evaluations, three primary findings emerge. First, for this dataset Decourt's method is clearly the best of the SPT-based sand methods. Second, the majority of variability in the methods based on SPT and laboratory tests is derived from the predictions in sand not clay. Third, for this dataset Decourt's SPT-method performs better than the CPT/CPTU-methods in profiles of clay and/or sand.

Given these three findings, the author concluded that the best opportunity for improving Caltrans' prediction of side resistance lay in modifying Decourt's method for piles in sand and clay. For the author's database, Decourt's method is clearly the best choice for piles in sand, and it also works reasonably well for piles in clay. In addition, Decourt's method does not require the additional sampling and testing on which the α - and β -methods rely. In the field exploration phase of the author's project, it was found that the number of drilling contractors and commercial laboratories which routinely perform undisturbed sampling and UU testing properly is rather limited. This makes an SPT-method for piles in clay attractive, even though the SPT-method would, due to the variability in SPT measurements, have a somewhat greater variability than would an α - or β -method based on UU tests. Additionally, an SPT-method would provide better coverage of the available axial load test data. If an α - or β - method were used in clay, only 70 uplift test piles could be included in the regression analyses to develop improved side resistance methods. This number of piles is significantly less than the 97 piles which could be included if an SPT-method were used in clay.

The next chapter covers regression analyses to develop an improved version of Decourt's method. Using the improved SPT-method for piles in sand and clay, regression analyses are then performed to develop a simple method for predicting the side resistance of piles in gravel, cobbles and rock. Regression analyses are also used to expand the method to accommodate vibro-driven piles.

7. DEVELOPMENT OF SIDE RESISTANCE METHOD

7.1 INTRODUCTION

In the previous chapter, sixteen existing methods of predicting side resistance were evaluated against the uplift test pile database. In sand, Decourt's (1982) method produced the lowest *COV*. Decourt's method, in both clay and sand, also performed better than the four CPT/CPTU-methods evaluated. In this chapter, the performance of Decourt's method is more closely examined, and an improved version, calibrated to the uplift test pile database, is developed. The improved method is also expanded to cover vibro-driven piles and piles in gravel, cobbles, boulders and rock.

7.2 REGRESSION ANALYSES

7.2.1 Methodology

The regression analyses used in the development of the improved method were conducted using the Microsoft Visual Basic 6.0 program VBPIle, which was created by the author. The general regression model is provided in Equation 7.1.

$$f_s = F_v (A + B N_{60}) \quad (7.1)$$

with the constraint,

$$L \leq N_{60} \leq U$$

where,

$$f_s = \text{unit side resistance in kPa}$$

N_{60} = SPT resistance in blows/305 mm normalized to 60% of theoretical energy

F_v = reduction factor for vibro-driven piles

A, B = dimensionless model parameters

L, U = limiting values of N_{60} in blows/305 mm

Why Limit? Or why so low.

The model parameters A, B, L, U and F_v were fitted to the uplift test pile database using an automated trial-and-error approach in which various values were tried for each parameter. The adopted combination of parameter values was that with the lowest COV and a mean Q_c/Q_m of approximately 1.0. An example of this approach is given later in this chapter.

The regression analyses were performed in four major stages. In Stage 1, the model was fitted to 35 uplift test piles. These 35 piles are impact-driven piles in profiles of clay and/or sand. In Stage 2, the model was fitted to 45 piles, consisting of the previous 35 piles plus 10 vibro-driven piles in profiles of clay and/or sand. In Stage 3, the model was fitted to 35 piles in profiles containing gravel but no rock. In Stage 4, the model was fitted to 17 piles in profiles containing rock. Each of these stages is discussed separately below.

7.2.2 Uplift Test Piles

Out of the 118 uplift test piles described in Chapter 2, 97 were included in the regression analyses. The composition of the uplift test piles used in the regression analyses is given in Table 7.1.

Stage 1 sand/clay uplift
2 + 10 vibro
3 gravels, etc
4 rock.

Table 7.1 Uplift Test Piles in Regression Analyses for SPT-Method

Pile Type	Hammer	Clay & Sand only	with Gravel	with Rock	with Gravel & Rock	All Soils	
Open-Toed Steel Pipe	Impact	20	16	9	4	39	53
	Vibratory	9	3	0	0	12	
Closed-Toed Steel Pipe	Impact	11	7	1	1	18	19
	Vibratory	0	1	0	0	1	
Steel H-Pile	Impact	1	10	4	3	12	19
	Vibratory	1	5	3	2	7	
Solid Precast Concrete	Impact	3	3	0	0	6	6
All Piles	Impact	35	36	14	8	77	97
	Vibratory	10	9	3	2	20	
	Total	45	45	17	10	97	97

Twenty-one piles with setup times less than 7 days in profiles containing clay were excluded. A plot of Q_m/Q_c (not Q_c/Q_m) vs. setup time is provided in Figure 7.1. The values of Q_c were calculated using the final model parameters presented later in the chapter. In this plot, for setup times less than 7 days there are eight uplift tests piles with Q_m/Q_c -values less than 0.6, while for setup times greater than or equal to 7 days there is only one pile with a value of Q_m/Q_c less than 0.6. Clearly, 6 days is insufficient time for the excess pore pressures generated by installation to dissipate. The inclusion of these piles, with setup times less than 7 days, in the regression analyses would have resulted in a final model which under-predicted at higher setup times.

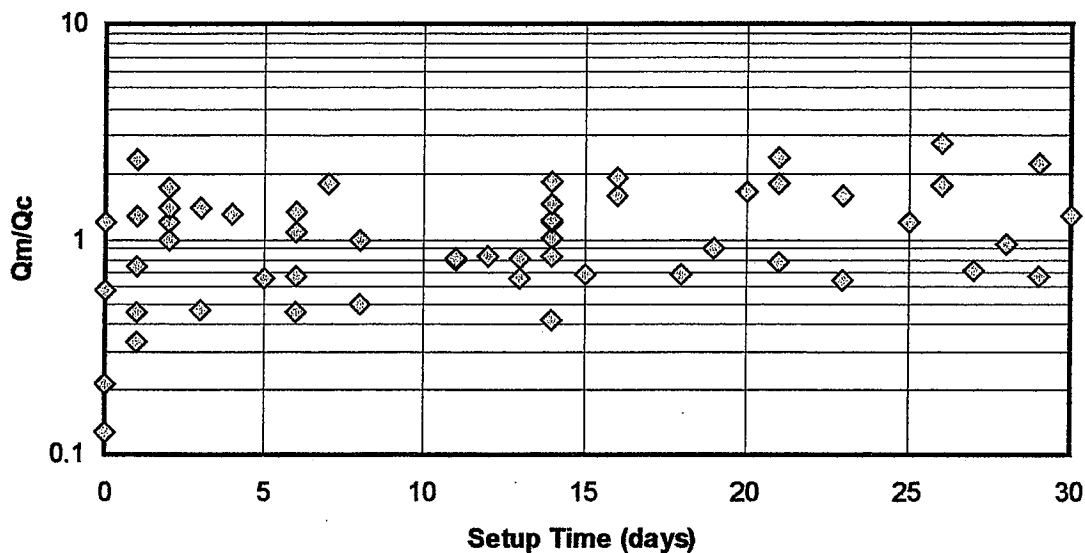


Figure 7.1 Effect of Setup Time on Q_m/Q_c in Profiles Containing Clay (Final Model)

7.2.3 Stage 1

In Stage 1, the model parameters A , B , L and U were fitted to 35 impact-driven, uplift test piles in profiles of clay and/or sand. A single set of parameters for both clay and sand, in the manner of Decourt's original method, was first determined. Once this was done, two sets of parameters, one for clay and one for sand, were then determined to evaluate the benefit of separating clay and sand in the model. The results of Stage 1 are given in Table 7.2. The parameter F_v was assumed equal to 1.0 in these analyses. Set 0 is Decourt's original method, which over-predicts slightly with a mean of 1.14. The COV s for Sets 1 and 2, both 0.38, indicate that no benefit, no reduction in variability, is derived from separating clay and sand in the model.

Table 7.2 Stage 1 Results

Set	Material	A	B	L	U	E	σ	COV
0	Clay/Sand	10	3.3	3	50	1.14	0.48	0.42
1	Clay/Sand	23	2.0	3	50	1.01	0.39	0.38
2	Clay	26	1.4	3	30	1.00	0.38	0.38
	Sand	19	2.1	0	50			

As an example of the methodology used in the regression analyses, the trials used to optimize the parameters in Set 1 are provided in Table 7.3. For each trial, the upper row contains the search parameters, and the lower row contains the results.

Table 7.3 Set 1 Trials

Trial	A			B			L			U			Qc/Qm	
	Max.	Min.	Step	E	COV									
1	0	50	5	0	5	0.5	0	5	1	20	100	20	1.983	0.383
	40			4.5			4			40				
2	10	30	2	1.3	3.3	0.2	0	5	1	20	60	10	0.967	0.381
	22			1.9			3			50				
3	17	27	1	1.4	2.4	0.1	0	5	1	30	60	5	0.919	0.381
	21			1.8			3			50				
4	18	28	1	1.5	2.5	0.1	3	3	0	45	55	2	1.149	0.381
	26			2.3			3			48				
5	18	28	1	1.5	2.5	0.1	3	3	0	46	50	1	1.149	0.381
	26			2.3			3			48				
6	23	23	0	2.0	2.0	0	3	3	0	50	50	0	1.014	0.381
	23			2.0			3			50				

In Trial 1, a coarse search was performed to cover the range of reasonable values for each of the four model parameters. In this initial trial, 3630 combinations of model parameters were evaluated. In each trial, the combination with the lowest COV of Q_c/Q_m was selected. If multiple combinations had the same COV, the one with the mean of Q_c/Q_m closest to 1.0 was selected. Since Trial 1 resulted in a mean of 1.983, the ranges of A and B in Trial 2 were reduced in an effort to shift E closer to 1.0, and the search was narrowed by decreasing the step from 5 to 1. This process was repeated through Trial 5. By Trial 4, it was apparent that the optimum value of L was 3. So L was fixed at 3 for the remaining trials to reduce run-time. In Trial 5, an optimal combination had been reached

with respect to COV , but E was still 1.149. To correct this, in Trial 6 the values of A and B were reduced. In this trial, U was also rounded to 50. The purpose of this final trial, in which only one combination was evaluated, was simply to confirm that E had been adjusted as desired without increasing COV .

7.2.4 Stage 2

In Stage 2, 10 vibro-driven piles were added to the dataset used in Stage 1. In this stage, the parameters determined in Set 1 were revised slightly to fit the larger dataset, and the parameter F_v was introduced as a reduction factor for vibro-driven piles. The results of Stage 2 are provided in Table 7.4.

Table 7.4 Stage 2 Results

Set	Material	A	B	L	U	F_v	E	σ	COV
0	Clay/Sand	10	3.3	3	50	1.00	1.30	0.71	0.55
1	Clay/Sand	23	2.0	3	50	1.00	1.13	0.54	0.48
3	Clay/Sand	25	1.8	3	50	0.68	1.00	0.41	0.41

lowest

What is set 3

By comparing the performance of Set 1 and Set 3, it is clear that the introduction of the reduction factor F_v for vibro-driven piles provides a significant improvement when such piles are included. The performance of Set 3 for various subsets of the 45-pile dataset is provided in Table 7.5. From this table, it is clear that when a reduction factor is applied for vibro-driven piles the model has very little bias, in terms of E , with regard to either toe condition or method of installation. A scatter diagram for Set 3 is given in Figure 7.2. In the scatter diagram, the middle diagonal line represents Q_d/Q_m of 1.0. The upper and lower diagonal lines represent Q_d/Q_m of 2.0 and 0.5, respectively.

Table 7.5 Set 3 Performance by Subset

Subset	No. Piles	E	σ	COV
H-Piles	2	0.81	-	-
Open-Toed Piles	29	1.02	0.41	0.40
Closed-Toed Piles	14	0.98	0.46	0.47
Vibro-Driven Piles	10	1.01	0.53	0.52
Impact-Driven Piles	35	1.00	0.38	0.38

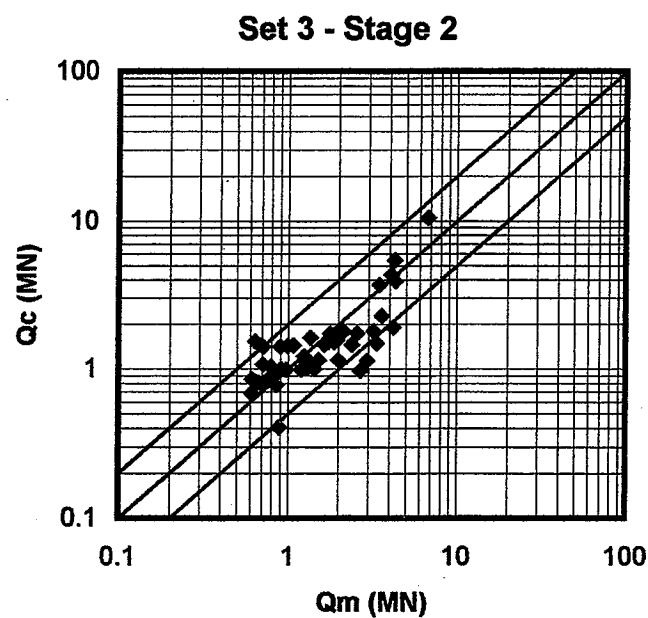


Figure 7.2 Scatter Diagram for Set 3 in Stage 2

A cumulative probability plot of Set 3 in Stage 2 is provided in Figure 7.3. To create the cumulative probability plot, each data point is arranged in order from the lowest to the highest Q_c/Q_m and numbered from 1 to n . The cumulative probability (CP) is defined in Equation 7.2, in which m is the point number ranging from 1 to n in order of increasing Q_c/Q_m (Ang and Tang 1975). For a specified value of Q_c/Q_m , the corresponding CP is the probability that Q_c/Q_m will not exceed this specified value.

$$CP = \frac{m}{n+1} \quad (7.2)$$

The relatively high *COV* of Set 3 is due largely to the inclusion of the piles represented by the six points with Q_c/Q_m values less than 0.5 and greater than 2.0. If these six points were excluded, the *COV* would decrease from 0.41 to 0.30. The points in the tails of the curve represent tests which are not well predicted by the model.

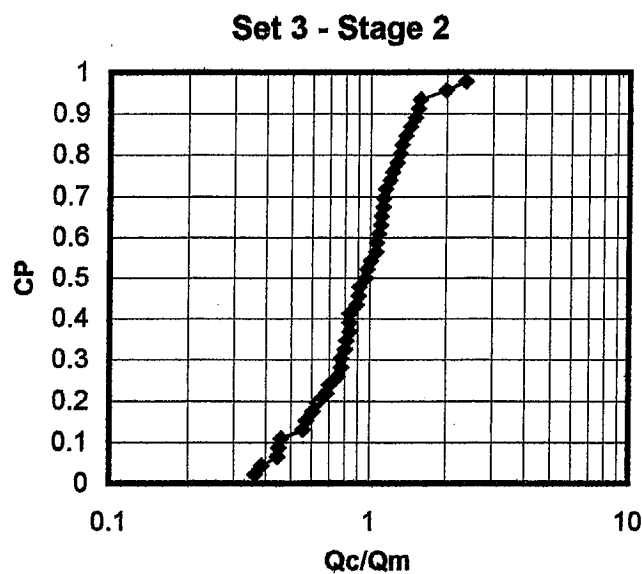


Figure 7.3 Cumulative Probability Plot of Set 3 in Stage 2

The optimal value of F_v in Stage 2 was 0.68. *How is this determined?* This value is somewhat higher than the F_v -value of 0.51 observed in the uplift tests at the Bayshore Freeway Viaduct PITP and the I-880 IPTP presented in Chapter 4. With regard to the effects of toe condition on axial resistance, which was also discussed in Chapter 4, such an effect is not noticeable in Table 7.5. The mean values of Q_c/Q_m for open-toed and closed-toed piles are 1.02 and 0.98, respectively.

7.2.5 Stage 3

In Stage 3, 35 piles in profiles containing gravel, cobbles and boulders were considered. In this stage, the Set 3 model parameters were used for clay and sand. For gravel, cobbles and boulders, the optimum value of the parameter B was found to be zero. Physically, this is due to the fact that the particles in these very coarse materials are larger than the 35-mm inside diameter of the SPT sampler. When the sampler is driven into a matrix of particles of this size, the penetration resistance is no longer a reliable indicator of the relative density or the state of stress of the matrix, making the N -value useless as an index of unit side resistance. In gravel, cobbles and boulders, only the parameter A was used in the model. All of these materials are referred to as gravel in the table below. A scatter diagram and cumulative probability plot of Set 4 in Stage 3 are presented in Figure 7.4 and Figure 7.5, respectively.

Table 7.6 Stage 3 Results

Set	Material	A	B	L	U	F_v	E	σ	COV
0	Clay/Sand/Gravel	10	3.3	3	50	1.00	1.25	0.62	0.50
4	Clay/Sand	25	1.8	3	50	0.68	1.01	0.47	0.47
	Gravel	40	-	-	-	0.68			

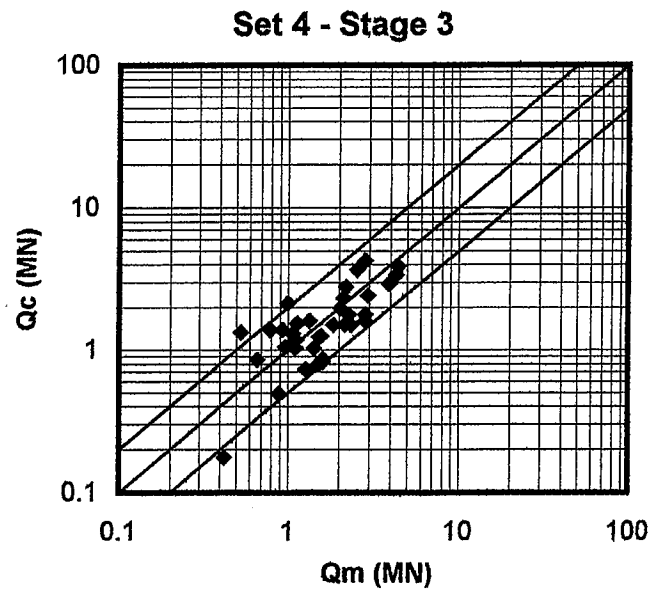


Figure 7.4 Scatter Diagram of Set 4 in Stage 3

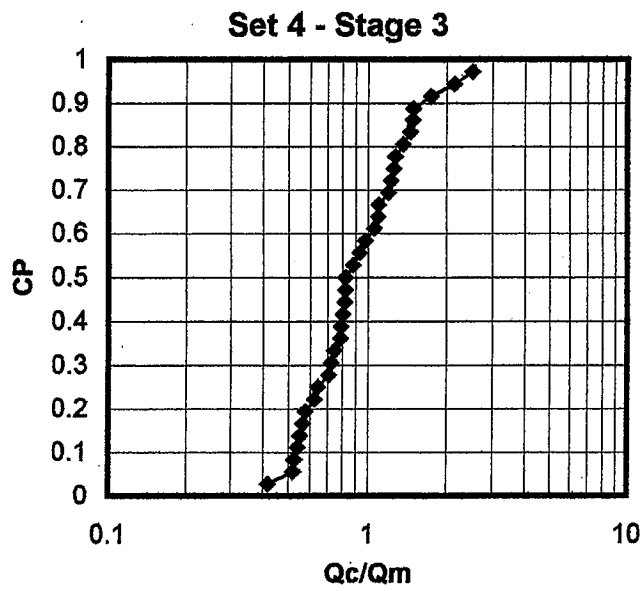


Figure 7.5 Cumulative Probability Plot for Set 4 in Stage 3

7.2.6 Stage 4

In Stage 4, 17 piles in profiles containing rock were examined. In this stage the Set 4 model parameters were used for materials other than rock. As with gravel, cobbles and boulders, for rock only the parameter A was used in the model. The parameter F_v is not applied to rock because a vibratory hammer would not be used to install piles into rock. A scatter diagram and cumulative probability plot of Set 5 in Stage 4 are presented in Figure 7.6 and Figure 7.7, respectively.

Table 7.7 Stage 4 Results

Set	Material	A	B	L	U	F_v	E	σ	COV
0	Clay/Sand/Gravel/Rock	10	3.3	3	50	1.00	1.17	0.63	0.54
5	Clay/Sand	25	1.8	3	50	0.68	1.00	0.47	0.47
	Gravel	40	-	-	-	0.68			
	Rock	130	-	-	-	1.00			

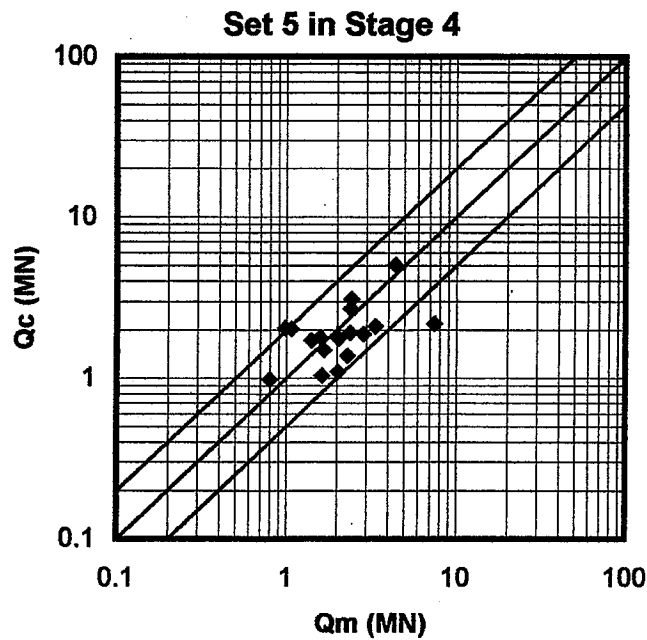


Figure 7.6 Scatter Diagram of Set 5 in Stage 4

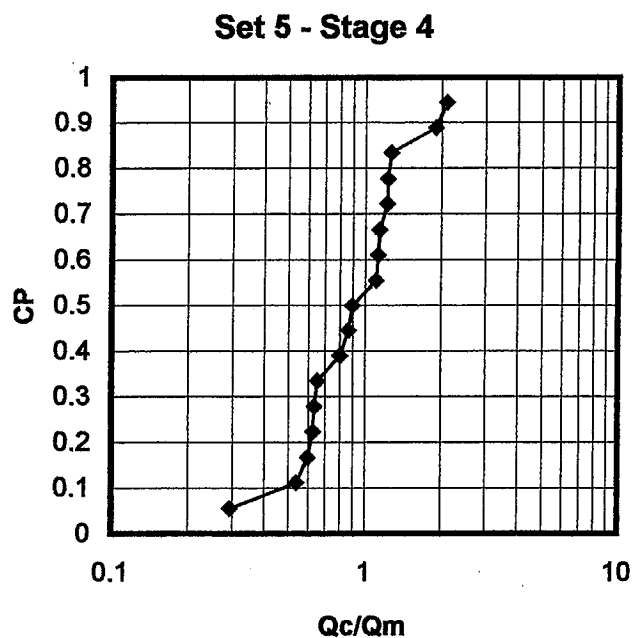


Figure 7.7 Cumulative Probability Plot for Set 5 in Stage 4

The performance of Set 5 by subset is given in Table 7.8. The 6 precast concrete piles are included in the subset with closed-toed steel pipe piles. In Table 7.8, the performance of Set 5 appears to be relatively consistent across the various subsets, with $E(Q_c/Q_m)$ remaining close to 1.0 and $COV(Q_c/Q_m)$ remaining between 0.41 and 0.48.

Table 7.8 Performance of Improved Side Resistance Method by Subset

Subset		No. Piles	E	σ	COV
All		97	1.00	0.44	0.44
Pile Type	Open-Toed	53	1.01	0.42	0.41
	Closed-Toed	25	0.93	0.44	0.47
	H-Pile	19	1.08	0.52	0.48
Hammer	Impact	77	1.02	0.45	0.44
	Vibratory	20	0.94	0.40	0.42

7.3 IMPROVED SPT-METHOD

7.3.1 Description

In the improved method, ultimate uplift resistance (Q_{cu}) is calculated using Equation 7.3 on a layer-by-layer basis. The weight of the pile is ignored.

$$Q_{cu} = P \sum_{i=1}^n F_{vs} f_{si} H_i \quad (7.3)$$

where,

Q_{cu} = ultimate uplift resistance

P = exterior perimeter of pile

f_{si} = unit side resistance (f_s) in layer i

H_i = height of layer i

F_{vs} = 0.68 for vibro-driven piles; 1.00 for impact-driven piles

The equations used in the method to calculate unit side resistance are provided below. In clay, silt and sand,

$$f_s = 25 + 1.8 N_{60} \text{ in kPa} \quad (7.4)$$

with the constraint that,

$$3 \leq N_{60} \leq 50 \text{ with } N_{60} \text{ in blows/305 mm.} \quad (7.5)$$

In gravel, cobbles and boulders,

$$f_s = 40 \text{ kPa.} \quad (7.6)$$

In intact rock, both weathered and unweathered,

$$f_s = 130 \text{ kPa.} \quad (7.7)$$

7.3.2 Potential Bias

Some of the poorly predicted cases led the author to evaluate the effect of embedment on Q_c/Q_m in an attempt to develop an embedment correction factor. However, as shown in Figure 7.8, the method does not show any bias with respect to this parameter.

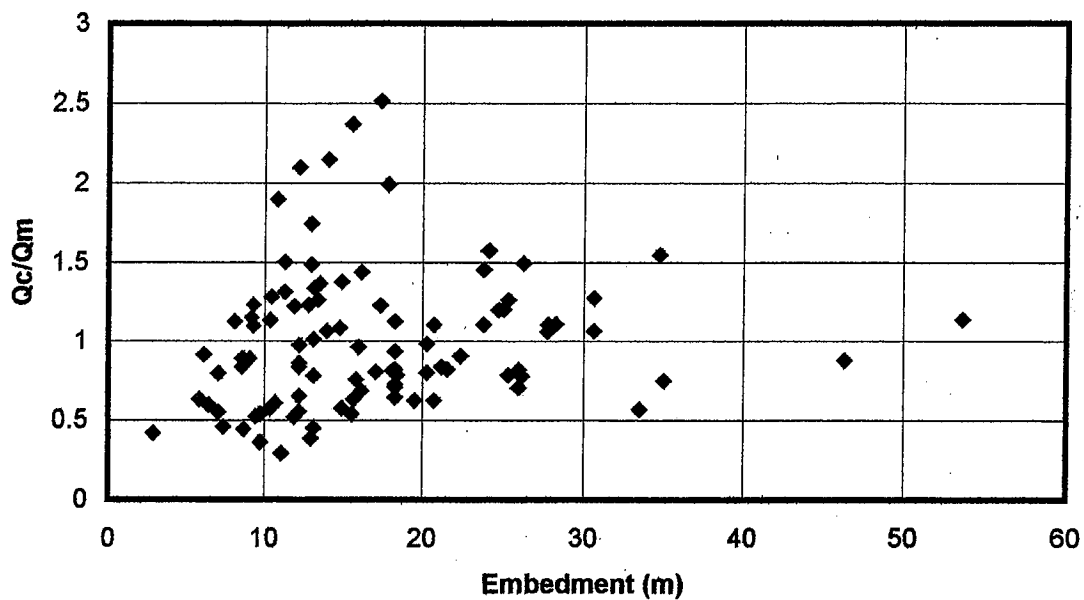


Figure 7.8 Effect of Embedment on Q_c/Q_m

7.3.3 Alternative Method in Clay

7.3.3.1 Re-Evaluation of UU-Based Clay Methods

In an attempt to further reduce the variability of the improved method, the author re-evaluated the clay methods from Chapters 4 and 5 for possible use as an alternative to the improved method in cohesive soils. The clay methods, based on unconsolidated-undrained triaxial compression (UU) tests, paired with the improved method in

cohesionless soils and rock, were evaluated against the 35 uplift test piles with UU tests in clay. The results of this evaluation are provided in Table 6.2.

Table 7.9 Evaluation of Clay Methods with Improved Sand Method

Clay Method	E	σ	COV
Improved Clay Method	0.98	0.30	0.31
API ($\psi_{nc} = 0.25$)	1.13	0.36	0.32
API ($\psi_{nc} = 0.33$)	1.21	0.40	0.33
Dennis & Olson	1.03	0.31	0.30
Jardine (OCR - Ladd)	0.81	0.29	0.36
Karlsrud (OCR - Ladd)	1.14	0.35	0.31
Kraft et. al	1.10	0.34	0.31
Tomlinson 1971	1.24	0.46	0.37
Tomlinson 1979	1.10	0.41	0.38

The only clay method that performed as well or better than the improved clay method was the method of Dennis and Olson (1983a). In subsequent analyses, the author found that the performance of Dennis and Olson's clay method against this dataset was improved when the calculated unit side resistance of vibro-driven piles was factored by 0.68, as in the improved method. The performance of Dennis and Olson's clay method, both with and without the reduction factor for vibro-driven piles F_v , against various subsets of the 35-pile dataset is given in Table 7.10. The performance of the improved clay method is also provided for comparison.

They are all very close.

Table 7.10 Performance of Dennis and Olson's Clay Method by Subset

Subset	No. Piles	Dennis & Olson				Improved Method	
		$F_v = 1.00$		$F_v = 0.68$		E	COV
		E	COV	E	COV		
All	35	1.03	0.30	0.98	0.28	0.98	0.31
Open-Toed Piles	23	1.12	0.26	1.06	0.24	1.06	0.27
Closed-Toed Piles	12	0.85	0.30	0.83	0.30	0.82	0.35
Vibro-Driven Piles	8	1.16	0.28	0.95	0.21	0.92	0.19
Impact-Driven Piles	27	0.99	0.30	0.99	0.30	1.00	0.33

7.3.3.2 Modified α -Method

The results in Table 7.10 show that the replacement of the improved clay method with a modified version of Dennis and Olson's (1983a) α -method reduces variability without significantly altering the mean values of Q_c/Q_m . In the modified α -method, unit side resistance is calculated using Equation 7.8. The adhesion factors α are determined from Figure 7.9. The value of s_u is determined from a UU test.

$$f_s = \alpha s_u \quad (7.8)$$

Note that Equation 7.8 does not include the correction factor for pile penetration from included in the original method. This correction, which only applies to piles with an embedment greater than 30.5 m, was not found to very relevant to the piles used in the re-evaluation of the clay methods. Only one pile in this dataset has an embedment greater than 30.5 m, and it is only 34.7 m.

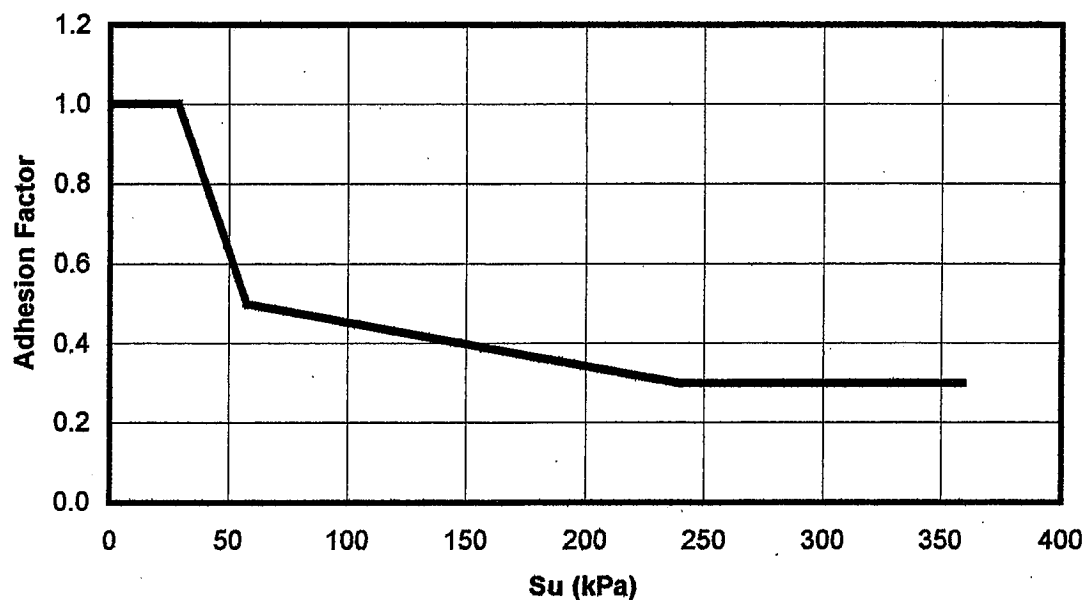


Figure 7.9 Adhesion Factors for Piles in Clay (Dennis and Olson 1983a)

7.3.4 Additional Recommendations

7.3.4.1 Oversized Toe Plates

In all cases, from Caltrans' archives, where the toe plate diameter of a closed-toed steel pipe pile is reported, the toe plate diameter is 12.7 mm larger than the outside diameter of the pile. According to Dennis (1982), the use of such oversized toe plates will reduce the side resistance of the pile relative to a closed-toed pile with a toe plate having a diameter equal to the outside diameter of the pile. Given that the improved method was developed using closed-toed piles with oversized toe plates, the method should be expected to under-predict resistance when applied to piles with a toe plate which is not oversized.

7.4 CONCLUSION

In this chapter, an improved side resistance method, modeled after Décourt's 1982 method, was developed using regression to fit the model parameter against 97 uplift tests. The improved method was also expanded to accommodate vibro-driven piles and piles in gravel, cobbles, boulders and rock. For vibro-driven piles, the method includes a side resistance reduction factor of 0.68. In gravel, cobbles, boulders and rock, the method provides average values of unit side resistance for the prediction of side resistance in profiles containing these materials.

8. DEVELOPMENT OF TOE RESISTANCE METHOD

8.1 INTRODUCTION

In the previous chapter, an improved method for the prediction of uplift side resistance was presented. In the present chapter, a companion method for the prediction of toe resistance is developed. Both of these methods are based on the standard penetration test (SPT) and modeled after Decourt's 1982 methods. In this chapter, the improved side resistance method is also adapted for use in predicting compressive side resistance.

8.2 EXISTING METHODS

8.2.1 Description

8.2.1.1 Caltrans/FHWA Methods

Caltrans now uses the methods recommended by the U.S. Department of Transportation, Federal Highway Administration (FHWA) and incorporated in the DOS program SPILE and the Microsoft Windows program DRIVEN. These programs were developed by FHWA for the calculation of ultimate resistance. For toe resistance, FHWA calculates unit toe resistance as 9 times the undrained shear strength (s_u) in cohesive soils and uses Thurman's (1964) method in cohesionless soils.

In Thurman's method, total toe resistance and unit toe resistance are calculated using Equations 8.1 and 8.2, respectively. The bearing capacity factor and depth factor used in Equation 8.2 are obtained from Figure 8.1 and Figure 8.2, respectively. In Figure

8.2, D is the pile embedment and B is the nominal pile width. The soil's internal angle of friction (ϕ) is estimated from the SPT N -value using Equation 5.3 and Figure 5.6. FHWA applies an upper limit to unit toe resistance in accordance with the recommendations of Meyerhof (1976) as shown in Figure 8.4. In the FHWA program DRIVEN, open-toed piles are assumed to be plugged, and toe resistance is calculated using the area of both the pile toe and the soil plug. For the evaluation of this method with steel H-piles, the author assumed that unit toe resistance acts only on the steel area.

$$Q_t = f_t A_t \quad (8.1)$$

$$f_t = \sigma'_{vo} \alpha N_q \leq f_{t,max} \quad (8.2)$$

$$C_N = 0.77 \log \left(\frac{1.92 \text{ MPa}}{\sigma'_{vo}} \right) \quad (8.3)$$

where,

Q_t = calculated toe resistance

f_t = unit toe resistance

A_t = toe area on which unit toe resistance is assumed to act

σ'_{vo} = free-field vertical effective stress

α = dimensionless depth factor

N_q = bearing capacity factor

$f_{t,max}$ = limiting unit toe resistance from Figure 8.4

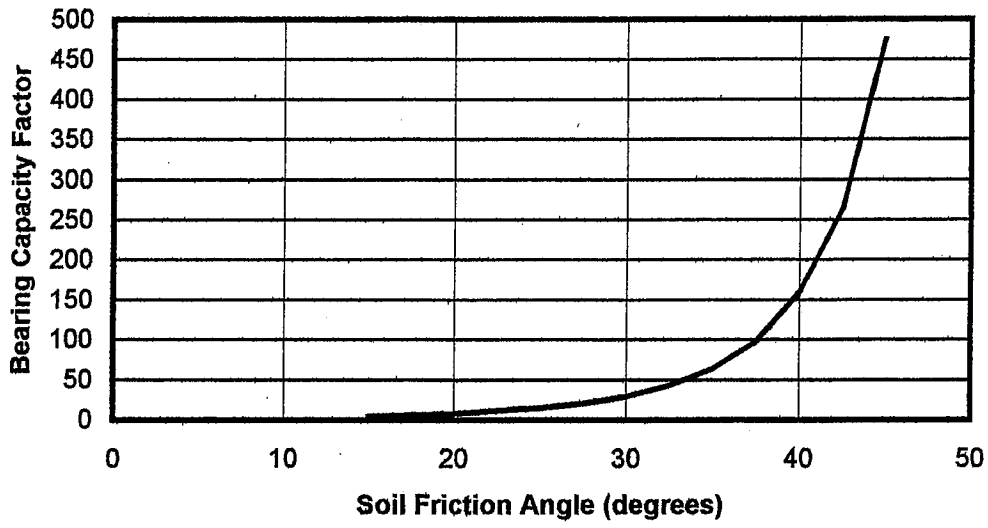


Figure 8.1. Bearing Capacity Factor N_q (Thurman 1964)

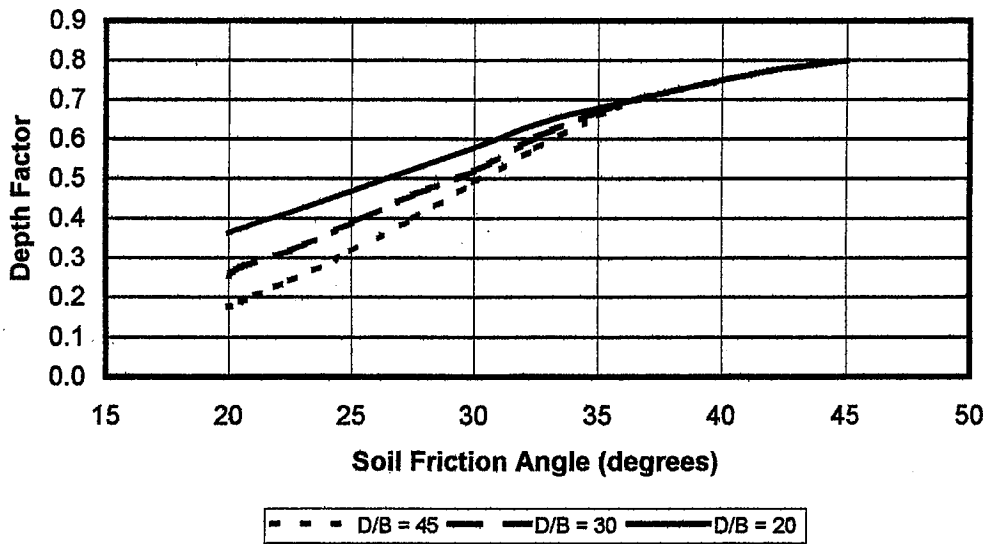


Figure 8.2. Depth Factor α (Thurman 1964)

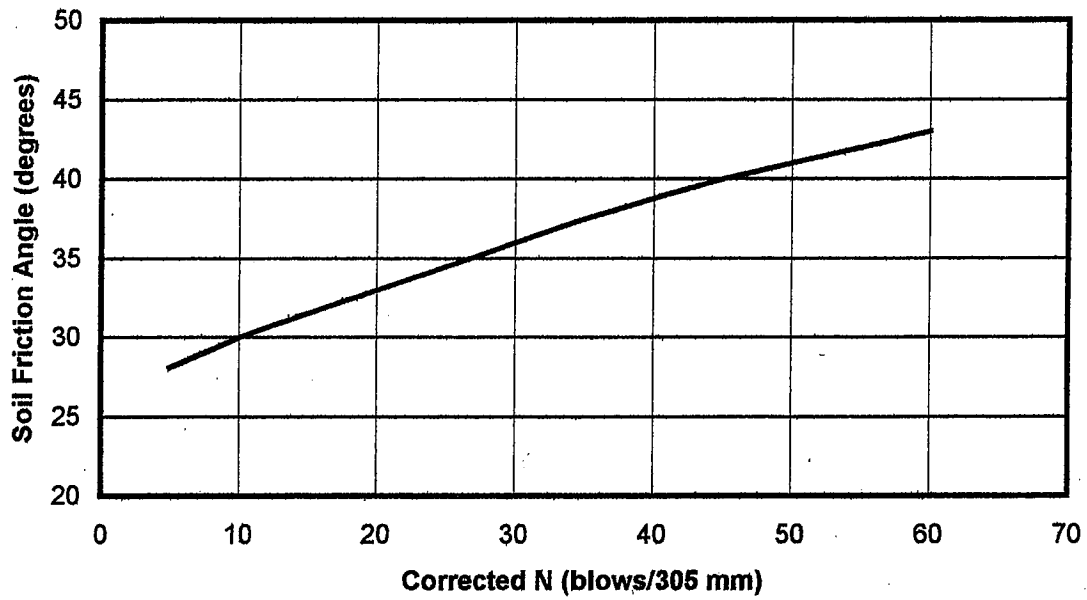


Figure 8.3. Relationship between N_{corr} and ϕ (Peck et al. 1974)

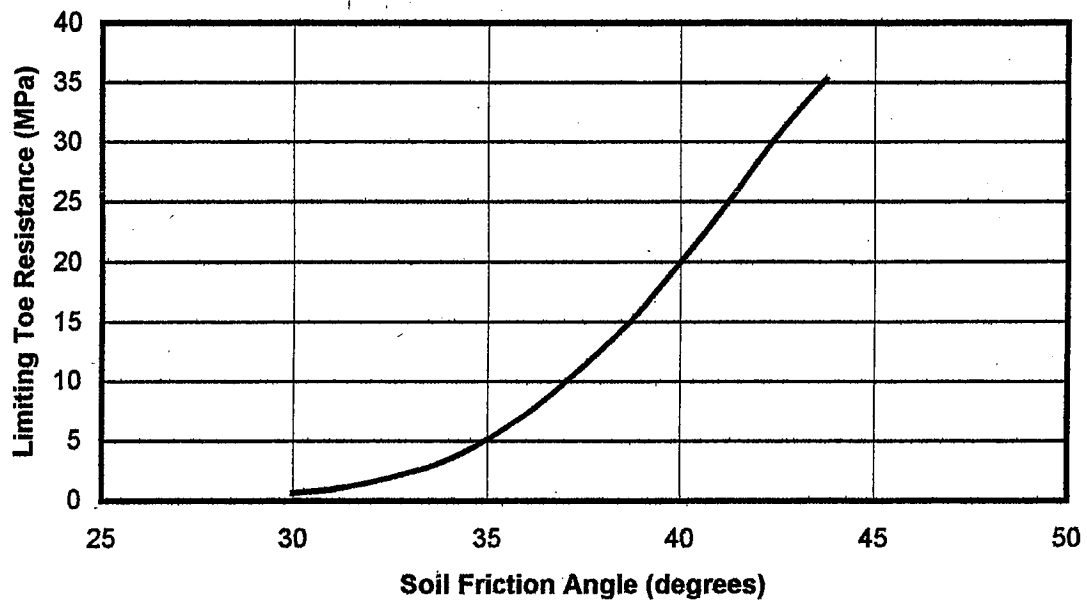


Figure 8.4. Limiting Unit Toe Resistance (Meyerhof 1976)

8.2.1.2 Decourt's Method

Decourt (1982) presented a simple SPT-based method for the prediction of toe resistance in both clay and sand. Unit toe resistance is calculated using Equation 8.4.

$$f_t = K N \quad (8.4)$$

For clay and sand, values of K of 0.12 and 0.40, respectively, are used in this equation. Different values of K are used for residual soils, but these are not relevant to this dissertation because no residual soils are present in the soil profiles in the author's database. The N -value used is that measured immediately below the pile toe, not an average value. Decourt's method was developed based on data collected by Decourt and Quaresma in their respective consulting practices in Brazil. Their original database included a variety of bored and driven piles in both alluvial and residual soils. For the evaluation of this method with open-toed steel pipe piles and steel H-piles, the author assumed that unit toe resistance acts only on the steel area.

8.2.2 Evaluation

For a performance reference, these toe resistance methods were evaluated against 16 compressive test piles. These 16 piles are those satisfying the following criteria:

- The measured ultimate compressive resistances defined by Caltrans' offset-limit (Q_{CT}) and Fleming's extrapolation (Q_m) are known.
- The soil profile (in contact with the side and toe of the pile) is composed of clay and/or sand.
- If the soil profile contains clay, the setup time is at least 7 days.
- There are UU test results in the clay layers and SPT measurements in both the clay and sand layers.
- The pile is either steel pipe or solid precast concrete.

x Did you
eliminate piles
that met all the
criteria except
SPT in clay?

- The pile was installed with an impact hammer.
- The pile was not relief drilled.

The results of this evaluation are provided in Table 8.1. The performance of these methods was evaluated based on the mean (E), standard deviation (σ) and coefficient of variation (COV) of the ratio of the calculated ultimate resistance (Q_c) to the measured ultimate resistance (Q_m).

Table 8.1 Evaluation of Existing Toe Resistance Methods

Methods			Descriptors of Q_c/Q_m		
Side Resistance		Toe Resistance	E	σ	COV
Clay	Sand				
Tomlinson 1971	Nordlund	FHWA	1.24	0.79	0.64
Tomlinson 1979	Nordlund	FHWA	1.19	0.75	0.63
Decourt	Decourt	Decourt	1.01	0.47	0.46

8.3 REGRESSION ANALYSES

8.3.1 Methodology

The regression analyses have two objectives: (1) to develop an improved version of Decourt's toe resistance method as a companion to the improved side resistance method and (2) to establish a side resistance ratio between uplift side resistance and compressive side resistance to increase the utility of the improved side resistance method. The methodology used in these regression analyses follows that described in the previous chapter.

In these regression analyses, 44 test piles were used. These are the database piles with both a compressive test and an uplift test. The regression models for ultimate compressive resistance (Q_c) unit toe resistance (f_t), and effective toe area (A_t) are defined using Equations 8.5 through 8.9, respectively.

$$Q_c = \frac{Q_{mu}}{F_s} + f_t A_t \quad (8.5)$$

$$f_t = F_v (A + B N_{60}) \quad (8.6)$$

$$A_t = A_{pile} \quad \text{for closed-toed piles} \quad (8.7)$$

$$A_t = A_{pile} + F_{pt} A_{plug} \quad \text{for open-toed piles} \quad (8.8)$$

$$A_t = A_{pile} + F_{ph} A_{plug} \quad \text{for steel H-piles} \quad (8.9)$$

where,

Q_c = calculated compressive resistance

Q_{mu} = measured uplift resistance

F_s = side resistance ratio

f_t = calculated unit toe resistance in kPa

A_t = effective toe area

N_{60} = SPT resistance in blows/305 mm normalized to 60% of theoretical energy

F_v = reduction factor for vibro-driven piles

A, B = dimensionless parameters

F_{pt} = plug mobilization factor for open-toed piles

F_{ph} = plug mobilization factor for H-piles

A_{pile} = toe area of pile material (steel or concrete)

A_{plug} = toe area of soil plug

Since these 44 test piles are generally in mixed profiles, a single value of F_s was used for all materials (clay, sand, gravel and rock). To simplify the analyses, A was

assumed to be zero in clay and sand. Likewise, B was assumed to be zero in gravel and rock. This second assumption was based on the conclusion, expressed in the previous chapter, that the SPT N -value is not a good indicator of either the state of stress or the relative density of materials composed of particles having a larger diameter than the SPT sampler.

8.3.2 Test Piles

Forty-four test piles were used in the regression analyses for the development of the toe resistance method. These are the database piles satisfying the following criteria:

- Q_{CT} and Q_m in both uplift and compression are known.
- If the soil profile contains clay, the setup time is at least 7 days.
- The pile is less than 180 cm in width.

A total of 51 piles satisfy the first criterion, but 6 of these piles, which were considered to have insufficient setup times, were eliminated by the second criterion. Also, by limiting the pile width to 180 cm, one 183-cm diameter open-toed steel pipe pile was excluded. For this pile, the measured ultimate resistances in uplift and compression were both 6.74 MN, indicating that virtually no toe resistance was mobilized in the compressive test. This could indicate that as pile diameter increases the plug mobilization factor (F_{pt}) should decrease with increasing pile diameter until F_{pt} is roughly equal to zero at a diameter of 183 cm. However, the remaining 44 piles, with widths ranging from 30 to 107 cm, do not reflect such a trend. A breakdown of the final 44 piles is given in Table 7.1. Recommendations for larger diameter piles will be provided later in this dissertation.

Table 8.2 Test Piles in Regression Analyses for Toe Resistance Method

Pile Type	Hammer	Material immediately below Pile Toe						
		Clay	Sand	Gravel	Rock	All Materials		
Open-Toed Steel Pipe	Impact	6	11	2	4	23	31	
	Vibratory	2	6	0	0	8		
Closed-Toed Steel Pipe	Impact	2	7	0	0	9	10	
	Vibratory	0	1	0	0	1		
Steel H-Pile	Impact	0	0	2	0	2	2	
	Vibratory	0	0	0	0	0		
Solid Precast Concrete	Impact	0	1	0	0	1	1	
All Piles	Impact	8	19	4	4	35	44	
	Vibratory	2	7	0	0	9		
	Total	10	26	4	4	44	44	

8.3.3 Stage 1

In Stage 1, regression analyses were performed on 27 impact-driven test piles tipped in either clay or sand. In these analyses, values of B , F_s and F_{pt} were determined. The results of Stage 1 are provided in Table 7.2. A comparison of Sets 1 and 2 indicates that there is no reduction in COV when separate values of B are used for clay and sand.

The reasons for this are that only 8 of the piles are tipped in clay and that for these 8 piles, relative to the piles tipped in sand, a smaller percentage of the compressive resistance is toe resistance. This means that the performance of the model in Stage 1 is controlled primarily by the value of B in sand and the value of F_s .

Table 8.3 Stage 1 Results

Set	Material	B	F_s	F_{pt}	E	σ	COV
0	Clay	0.12	1.00	0.00	1.08	0.49	0.45
	Sand	0.40	1.00	0.00			
1	Clay/Sand	0.16	0.95	0.51	0.99	0.21	0.21
2	Clay	0.14	0.95	0.51	0.99	0.21	0.21
	Sand	0.16					

8.3.4 Stage 2

In Stage 2, the parameters B , F_s , F_{pt} and F_v were fitted to 36 test piles, consisting of the 27 piles from Stage 1 plus 9 vibro-driven piles tipped in either clay or sand. The results of Stage 2 are given in Table 8.4.

Table 8.4 Stage 2 Results

Set	Material	B	F_s	F_{pt}	F_v	E	σ	COV
0	Clay	0.12	1.00	0.00	1.00	1.07	0.46	0.43
	Sand	0.40						
1	Clay/Sand	0.16	0.95	0.51	1.00	1.07	0.31	0.29
3	Clay/Sand	0.17	0.94	0.42	0.56	0.99	0.23	0.23

As in the improved side resistance method, the introduction of F_v improves the toe resistance model substantially. For Set 3 the optimal values of F_{pt} and F_v are 0.42 and 0.56, respectively. This value of F_v supports the results from the compressive tests in the Bayshore Freeway Viaduct PITP and the I-880 IPTP. This should be expected, since all of the vibro-driven test piles in Stage 2 are from these sites. For a 610-mm diameter open-toed steel pipe pile with a wall thickness of 19.1 mm, which is typical of this dataset, a F_{pt} -value of 0.42 indicates that the toe resistance of an open-toed pile will be approximately 50% of the toe resistance of a closed-toed pile of the same diameter. This value of F_{pt} corresponds to a greater reduction in toe resistance for open-toed piles than, indicated by the model tests of O'Neill and Raines (1991) and De Nicola and Randolph (1999). As discussed in Chapter 4, these model tests indicated that the toe resistance of an open-toed pile is approximately 67% of the toe resistance of a closed-toed pile. However, the value of F_{pt} agrees well with the findings of Jardine and Chow (1996), who in their predictive methods recommend that in both clay and sand the toe resistance of "fully plugged" open-toed piles be calculated as 50% of the toe resistance of a closed-toed pile of the same diameter.

For Set 3 in Stage 2, a scatter diagram of Q_c versus Q_m and a cumulative probability plot are also provided in Figure 8.5 and Figure 8.6, respectively. The cumulative probability plot is described in the previous chapter.

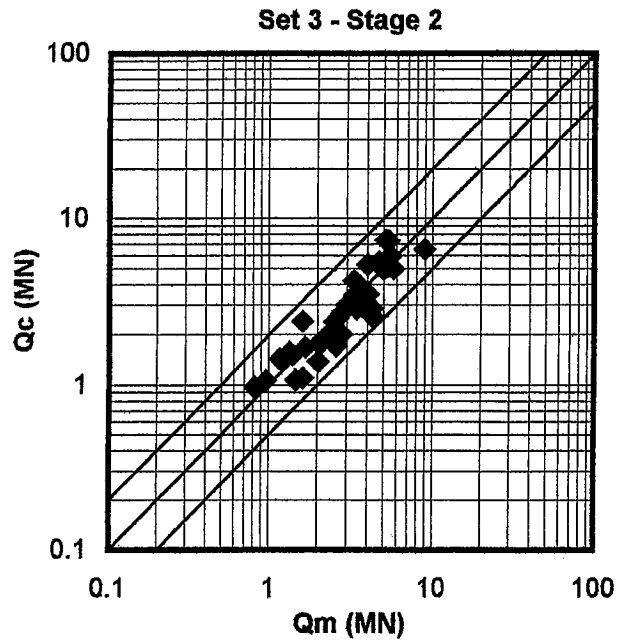


Figure 8.5 Scatter Diagram for Set 3 in Stage 2

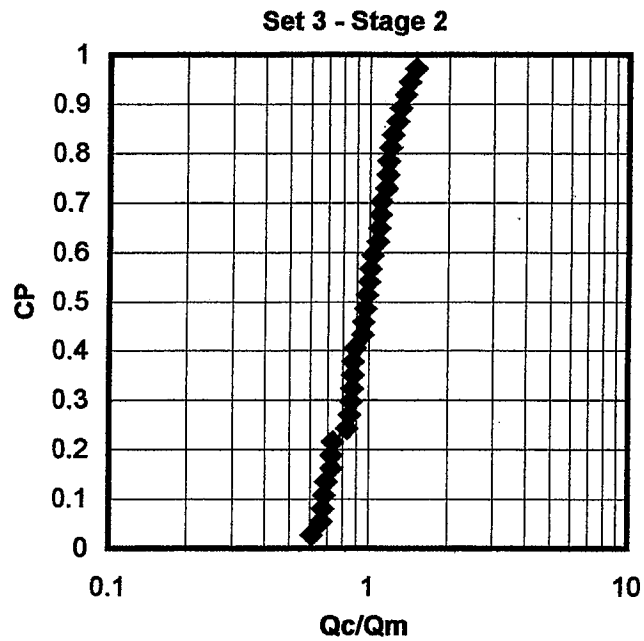


Figure 8.6 Cumulative Probability Plot for Set 3 in Stage 2

8.3.5 Stage 3

Since only 8 of the 44 test piles are tipped in either gravel or rock (4 in each), these two materials were considered together. In Stage 3, a single value of A was determined for these materials. As these 8 piles include two steel H-piles, the parameter F_{ph} was also included in Stage 3. For the other model parameters, the Set 3 values from Stage 2 were assumed to be applicable in Stage 3 and were not changed.

Table 8.5 Stage 3 Results

Set	Material	A	B	F_{ph}	F_s	F_{pt}	F_v	E	σ	COV
0	Gravel/Rock	0	0.40	0.00	1.00	0.00	1.00	0.57	0.23	0.40
3	Gravel/Rock	19	0.00	0.67	0.94	0.42	0.56	1.00	0.21	0.21

For Set 3 in Stage 3, a scatter diagram and a cumulative probability plot are provided in Figure 8.7 and Figure 8.8, respectively. The performance of Set 3 by subset is given in Table 8.6. The one square precast concrete pile is included in the subset with closed-toed steel pipe piles. In Table 8.6, the performance of Set 3 appears to be relatively consistent across the various subsets, with $E(Q_c/Q_m)$ remaining close to 1.0 and $COV(Q_c/Q_m)$ remaining under 0.30.

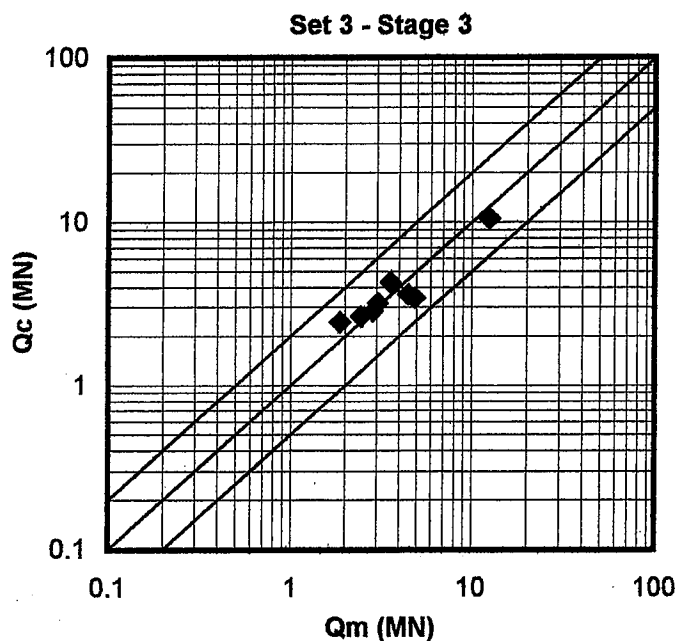


Figure 8.7 Scatter Diagram for Set 3 in Stage 3

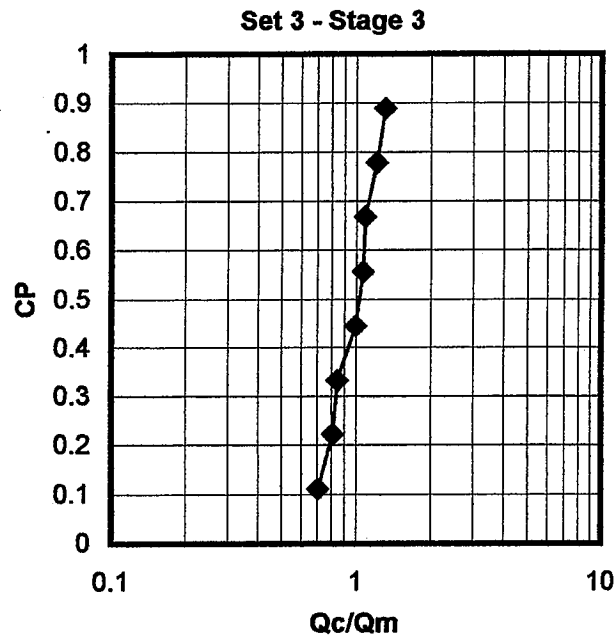


Figure 8.8 Cumulative Probability Plot for Set 3 in Stage 3

Table 8.6 Performance of Set 3 by Subset

Subset		No. Piles	<i>E</i>	σ	<i>COV</i>
All		44	0.99	0.23	0.23
Material	Clay	10	1.08	0.12	0.11
	Sand	26	0.96	0.26	0.27
	Gravel	4	0.99	0.13	0.13
	Rock	4	1.02	0.29	0.28
Pile Type	Open-Toed	31	0.99	0.24	0.24
	Closed-Toed	11	1.00	0.21	0.21
	H-Pile	2	1.04	0.06	0.06
Hammer	Impact	35	1.00	0.21	0.21
	Vibratory	9	0.98	0.30	0.30

8.4 IMPROVED SPT-METHOD

8.4.1 Description

In actual practice, the measured uplift resistance (Q_{mu}) in Equation 8.5 would be replaced by the calculated uplift resistance (Q_{cu}). This revised equation is provided as Equation 8.10. When the Set 3 parameters are incorporated into the regression model, the equations for the improved toe resistance method become Equations 8.10 through 8.12.

$$Q_{cc} = \frac{Q_{cu}}{0.94} + f_t F_v (A_{pile} + F_p A_{plug}) \quad (8.10)$$

$$f_t = 0.17 N_{60} \quad \text{in MPa for clay and sand} \quad (8.11)$$

$$f_t = 19 \text{ MPa} \quad \text{for gravel and rock} \quad (8.12)$$

where,

Q_{cc} = calculated compressive resistance

Q_{cu} = calculated uplift resistance using improved side resistance method

N_{60} = SPT resistance in blows/305 mm normalized to 60% of theoretical energy

F_p = plug mobilization factor from Table 8.7

F_v = 0.56 for vibro-driven piles; 1.00 for impact-driven piles

A_{pile} = toe area of pile material

A_{plug} = toe area of soil plug

Table 8.7 Plug Mobilization Factor F_p

Pile Type	F_p
Open-Toed Steel Pipe	0.42
Steel H-Pile	0.67

8.4.2 Additional Recommendations

8.4.2.1 Large Diameter Piles

Given that the improved toe resistance method was developed using piles with diameters ranging from 30 to 107 cm, caution should be exercised when applying the method to piles larger than 107 cm. For piles with diameters greater than 107 cm, the author recommends that compressive tests be performed to evaluate the mobilization of toe resistance on a case-by-case basis. To mobilize significant toe resistance, these large diameter piles, especially open-toed piles, appear to require a relatively large toe displacement, greater than that typically developed under working loads.

8.4.2.2 Jetted Piles

The two jetted piles in the author's database were not included in the development of the improved methods. Based on the improved methods, the calculated compressive resistances of these two 137-cm diameter hollow precast concrete piles are 125% greater than the measured compressive resistances. Based on this, the author recommends that the ultimate resistance of jetted piles be taken as 45% of that calculated using the improved methods. This only applies to piles re-struck with an impact hammer prior to loading. Jetted piles which are not re-struck with an impact hammer prior to loading, should be assumed to have no toe resistance.

8.4.3 Evaluation

Using Equation 8.10 and removing the criterion that Q_{CT} and Q_m in uplift be known, the improved toe resistance method can be evaluated against a larger set of 71 compressive test piles. The results of this evaluation against various subsets of the 71 test piles are given in Table 8.8. The 10 solid precast concrete piles are included in the subset of closed-toed piles. For this evaluation, a scatter diagram and cumulative probability plot are provided in Figure 8.9 and Figure 8.10.

Table 8.8 Performance of Improved Toe Resistance Method by Subset

Subset		No. Piles	E	σ	COV
All		71	1.00	0.38	0.38
Material	Clay	15	1.03	0.34	0.33
	Sand	46	1.00	0.41	0.41
	Gravel	6	1.04	0.28	0.27
	Rock	4	0.97	0.50	0.51
Pile Type	Open-Toed	38	0.95	0.33	0.35
	Closed-Toed	30	1.06	0.45	0.42
	H-Pile	3	1.11	0.29	0.26
Hammer	Impact	61	1.00	0.39	0.39
	Vibratory	10	1.04	0.38	0.37

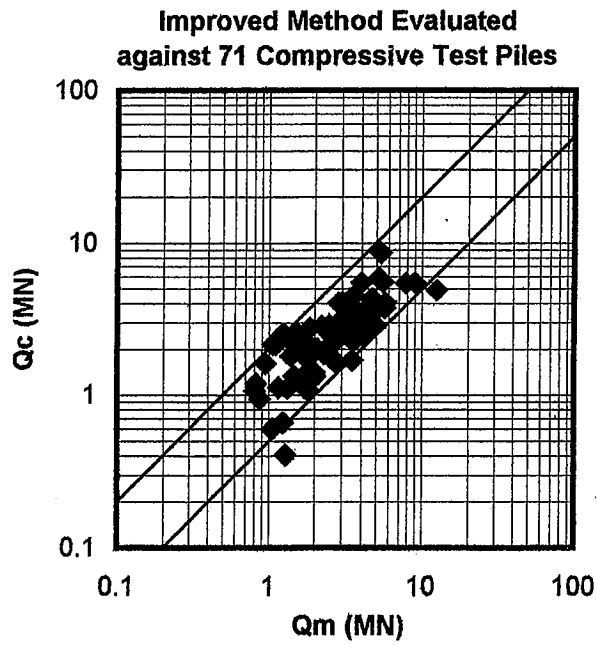


Figure 8.9 Scatter Diagram of Improved Method

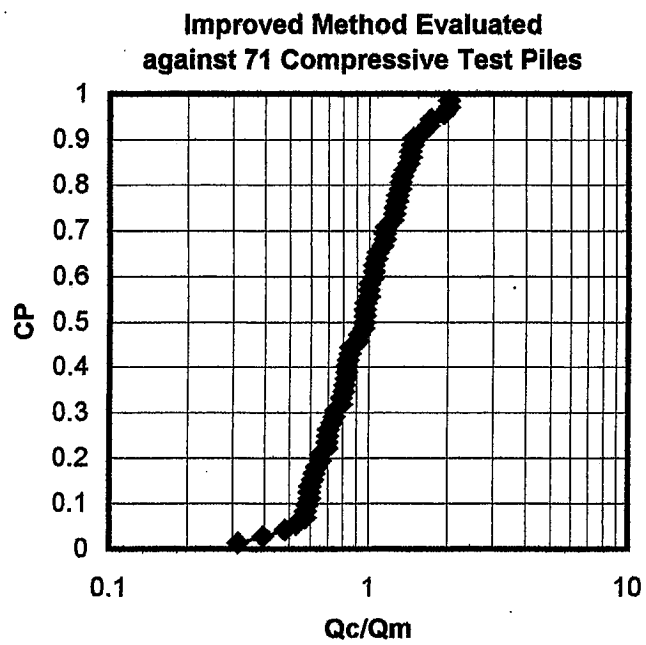


Figure 8.10 Cumulative Probability Plot of Improved Method

8.5 CONCLUSION

In this chapter, regression analyses were performed using 44 tests piles having both compressive and uplift tests. From these analyses, an improved toe resistance method was developed to complement the improved side resistance method presented in Chapter 7. Both of these methods are SPT-based methods derived from Decourt's (1982) methods. The regression analyses also served to establish an empirical side resistance ratio relating uplift side resistance to compressive side resistance. The analyses indicated that uplift side resistance is 94% of compressive side resistance. This is an average for the test piles included in the analyses.

In the next chapter the reliability of the improved method is evaluated to provide recommendations for appropriate factors of safety. This evaluation of reliability is made using the reliability of Caltrans' current methods as a reference.

9. RELIABILITY

9.1 INTRODUCTION

In this chapter, the reliability of the improved method is evaluated using the reliability of Caltrans' current methods as a reference. The primary objective of this chapter is to determine an appropriate factor of safety for the improved method in light of Caltrans' current practice

9.2 METHODOLOGY

To determine the allowable resistance of a single pile during the design phase of a project, the engineer first calculates an ultimate resistance (Q_c) then divides Q_c by a factor of safety (FS) to obtain an allowable resistance (Q_a) for design. The general relationship between Q_c and Q_a is indicated in Equation 9.1.

$$Q_a = \frac{Q_c}{FS} \quad (9.1)$$

In this chapter, the reliability of a method is evaluated based on the probability (P) that Q_a/Q_m will not exceed some maximum allowable value. This maximum allowable value should be selected based on the pile-head displacement which can be tolerated by the structure supported by the pile foundation. For example, the pile-head displacement for a given value of Q_a/Q_m could be determined from charts like Figure 9.1 and Figure 9.2, which respectively contain average normalized load-displacement curves for the 97 uplift tests and 71 compressive tests used in the development of the improved method. The pile-head load (Q) and displacement (S) have been normalized by dividing

them by Q_m and the pile width (B), respectively. In these two figures, the error bars extend one standard deviation of S/B above and below the average curve. For reference, the average value of B for both the uplift and compressive test piles is 53 cm.

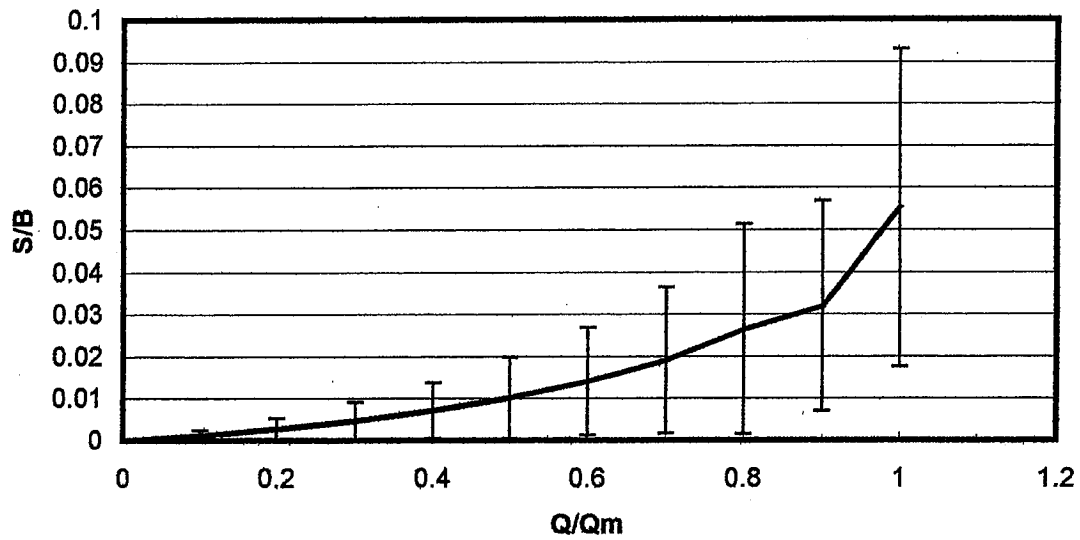


Figure 9.1 Average Normalized Load-Displacement Curve in Uplift

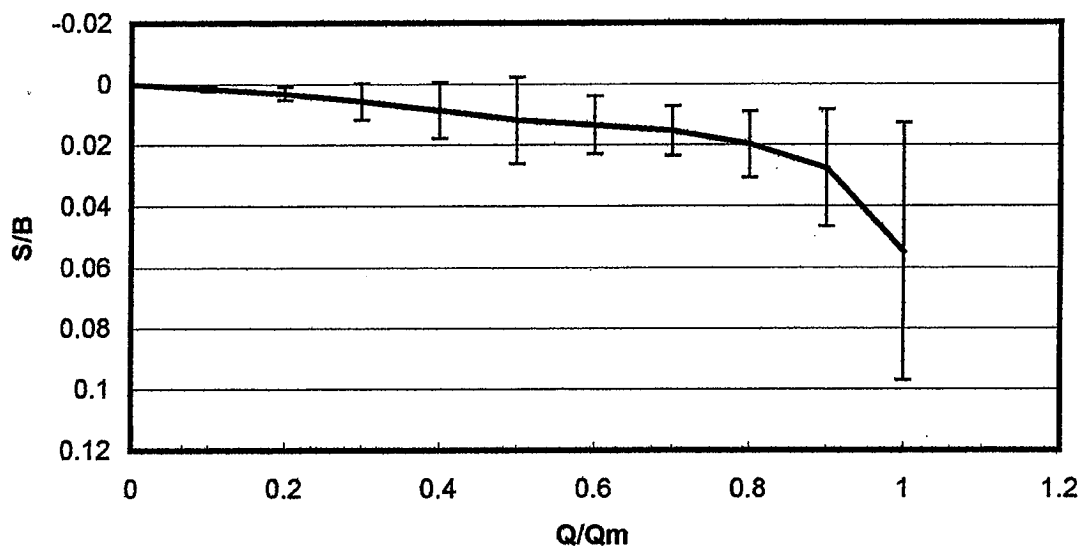


Figure 9.2 Average Normalized Load-Displacement Curve in Compression

One objective of this chapter was to determine the factor of safety (FS) for the improved method which would provide a value of P equal to the value of P for Caltrans' current methods. To determine the appropriate factor of safety for the improved method, a relationship between FS and P was first established

To establish a relationship between FS and P , the author first assumed that Q_c/Q_m is log-normally distributed. This assumption is supported by Figure 9.3 and Figure 9.4, in which Q_c/Q_m for the improved method is plotted on log-normal probability paper. Figure 9.3 is a plot of Q_c/Q_m for the improved method applied to 97 uplift tests, and Figure 9.4 is a plot of Q_c/Q_m for the improved method applied to 71 compressive tests. The linearity of the plots indicates that a log-normal distribution is a reasonable approximation for the actual distribution of Q_c/Q_m (Ang and Tang 1975).

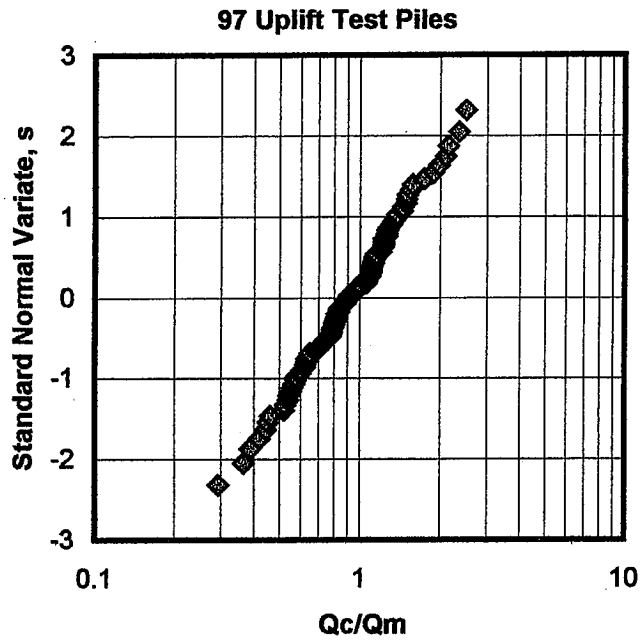


Figure 9.3 Plot of Q_c/Q_m for 97 Uplift Test Piles on Log-Normal Paper

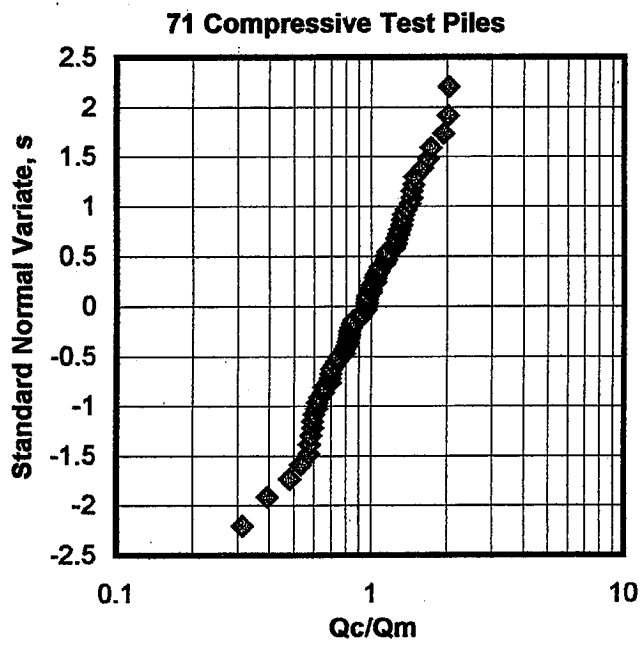


Figure 9.4 Plot of Q_c/Q_m for 71 Compressive Test Piles on Log-Normal Paper

For Q_c/Q_m log-normally distributed, P is defined in Equation 9.2, which can be rewritten as Equation 9.3 (Ang and Tang 1975).

$$P = \Phi \left[\frac{\ln(Q_c/Q_m) - \lambda}{\zeta} \right] \quad (9.2)$$

$$\frac{Q_c}{Q_m} = e^{\zeta \Phi^{-1}(P) + \lambda} \quad (9.3)$$

According to Equation 9.1, Q_c can be replaced by $FS Q_a$. With this substitution,

$$\frac{FS Q_a}{Q_m} = e^{\zeta \Phi^{-1}(P) + \lambda} \quad (9.4)$$

which can be simplified to,

$$FS = \frac{e^{\zeta \Phi^{-1}(P) + \lambda}}{Q_a/Q_m} \quad (9.5)$$

and rewritten as,

$$P = \Phi \left[\frac{\ln \left(FS \frac{Q_a}{Q_m} \right) - \lambda}{\zeta} \right] \quad (9.6)$$

These last two equations provide the needed relationship between FS and P .

In Equation 9.5, the terms λ and ζ are the mean and standard deviation of $\ln(Q_c/Q_m)$. These terms are related to the sample mean (E) and sample variance (Var) of Q_c/Q_m using Equations 9.7 through 9.9 (Ang and Tang 1975).

$$\delta = COV = \frac{\sigma}{E} = \frac{\sqrt{Var}}{E} \quad (9.7)$$

$$\zeta = \sqrt{\ln(1 + \delta^2)} \quad \text{what is } \delta \quad (9.8)$$

$$\lambda = \ln(E) - \frac{\zeta^2}{2} \quad (9.9)$$

In using this approach, the author assumed that $E(Q_c/Q_m)$ and $Var(Q_c/Q_m)$ are equal to the mean and variance of Q_c/Q_m for the population represented by the sample. Actually, $E(Q_c/Q_m)$ and $Var(Q_c/Q_m)$ are estimates of the population mean and variance. The accuracy of these estimates is dependent on the relative sizes of the sample and the population it represents. Nevertheless, the author proceeded with this assumption, as it allowed for a quick and simple evaluation of reliability for both Caltrans' current methods and the improved method.

9.3 CALTRANS' CURRENT PRACTICE

Currently, Caltrans effectively uses two different factors of safety depending on whether or not an axial load test used to determine ultimate resistance. Both of these approaches are discussed below.

9.3.1 Without an Axial Load Test

Since Caltrans current predictive methods are only standardized for piles in clay and sand, not gravel and rock, the evaluation of Caltrans' methods had to be based solely on the test piles in profiles of clay and sand. To evaluate Caltrans' methods against the largest possible dataset, it was necessary to include piles in profiles for which the undrained shear strength (s_u) had to be estimated either from pocket penetrometer readings in SPT samples or directly from the energy-corrected SPT resistance (N_{60}). To estimate s_u from N_{60} , the correlation of Terzaghi and Peck (1967) was used. This

correlation, which was actually developed using N rather than N_{60} , is shown in Figure 9.5. The accuracy of this correlation is unknown.

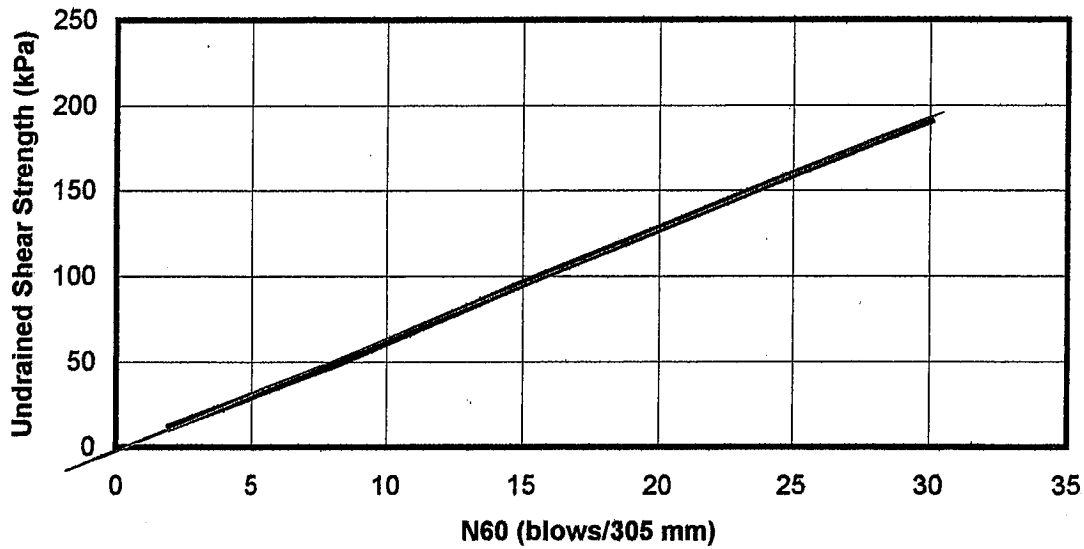


Figure 9.5 Correlation between N_{60} and s_u

Outside of the those piles in profiles containing gravel or rock, the only piles excluded from this dataset were those greater than 180 cm in diameter. The expanded dataset consisted of 45 uplift tests and 46 compressive tests. The results of the evaluation of Caltrans' methods against this dataset are provided in Table 9.1 and Table 9.2, respectively.

Table 9.1 Evaluation of Caltrans' Methods against 45 Uplift Tests

Methods		Descriptors of Q_a/Q_m		
Side Resistance		E	σ	COV
Clay	Sand			
Tomlinson 1971	Nordlund	0.96	0.62	0.65
Tomlinson 1979	Nordlund	0.91	0.62	0.68

Table 9.2 Evaluation of Caltrans' Methods against 46 Compressive Tests

Methods			Descriptors of Q_c/Q_m		
Side Resistance		Toe Resistance	E	σ	COV
Clay	Sand				
Tomlinson 1971	Nordlund	FHWA	1.45	1.17	0.81
Tomlinson 1979	Nordlund	FHWA	1.44	1.13	0.78

For these methods, Caltrans' uses a factor of safety of 2.0. With a factor of safety of 2.0 and the values of E and COV in Table 9.1 and Table 9.2, these methods have the values of P given in Table 9.3. The values of P in this table were calculated using Equation 9.6 with Q_a/Q_m equal to 1.0, since the concern here was that Q_a not exceed Q_m . In uplift and compression, the average values of P for Caltrans' current methods are roughly 94 and 79%, respectively. Although this analysis indicates that Caltrans' current methods result in the use of allowable resistances which exceed the measured ultimate resistance 21% of the time, the author is not aware that Caltrans has experienced any foundation failures. The implications of this situation are discussed later in this chapter.

Table 9.3 Reliability of Caltrans' Methods for $Q_a/Q_m = 1$

Methods			Mode	No. Piles	P (%)
Side Resistance		Toe Resistance			
Clay	Sand				
Tomlinson 1971	Nordlund	-	Uplift	45	93.7
Tomlinson 1979	Nordlund	-	Uplift	45	94.4
Tomlinson 1971	Nordlund	FHWA	Comp.	46	79.0
Tomlinson 1979	Nordlund	FHWA	Comp.	46	79.4

9.3.2 With an Axial Load Test

In an axial load test, Caltrans defines the measured ultimate resistance as the pile-head load at 12.7 mm of pile-head displacement. In this dissertation, this load is referred to as Q_{CT} . When a load test is available, Caltrans calculates Q_a as 50% of Q_{CT} .

For the 97 uplift test piles and 71 compressive test piles used in the development of the improved methods, on average Q_{CT} is, respectively, 82 and 83% of Q_m , which is the measured ultimate resistance defined by Fleming's extrapolation. Given this relationship, when Q_a is determined from a load test, the average value of Q_a/Q_m is 0.41. The inverse of 0.41 is 2.44, which is effectively the average factor of safety Caltrans applies to Q_m when determining Q_a from a load test.

9.4 IMPROVED METHOD

Having established reference values for P of 94% in uplift and 79% in compression and for Q_a/Q_m of 0.41, the next step was to determine the factors of safety needed for the improved method to meet these performance requirements. For the reference values of P , the corresponding factors of safety for the improved method are given in Table 9.4.

Table 9.4 Factors of Safety for Reference Values of P

Mode	No. Piles	E	COV	P (%)	FS
Uplift	97	1.00	0.44	94	1.76
Comp.	71	1.00	0.38	79	1.26

Given the relatively low P -values associated with these factors of safety, the author cannot recommend their use with the improved method. For a comparison at higher P -value, the relationships between FS and P for both the improved method and

Caltrans' current methods are provided in Figure 9.6. To provide a more useful plot, the x-axis is "1 - P" rather P itself.

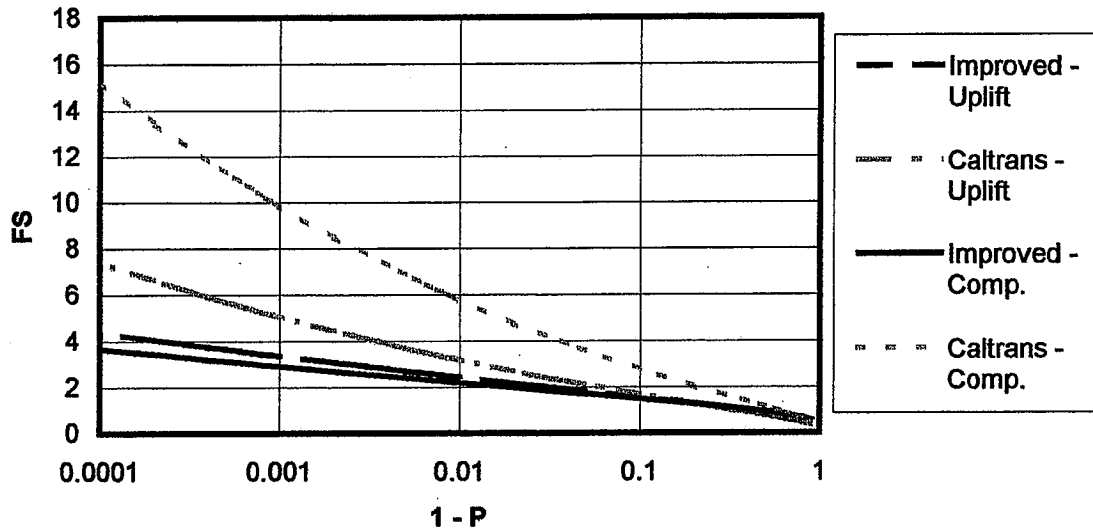


Figure 9.6 Relationship between *FS* and *P*

For values of *P* greater than 70%, the factors of safety required for the improved method are lower than those required for Caltrans' current methods. The adoption of the improved method, which has considerably less variability than Caltrans' current methods, would allow Caltrans to reduce the number of piles used in future projects. The possible reduction in piling is calculated using Equation 9.10. Since *FS* is dependent on *P*, the reduction in piling is also dependent on *P*. The relationship between the resulting reduction in piling and *P* is given in Figure 9.7. At the reference *P*-values, Caltrans could realize a reduction of 17% for uplift and 9% for compression.

$$\text{Reduction} = \frac{FS/E \text{ (Caltrans)} - FS/E \text{ (Improved)}}{FS/E \text{ (Caltrans)}} \quad (9.10)$$

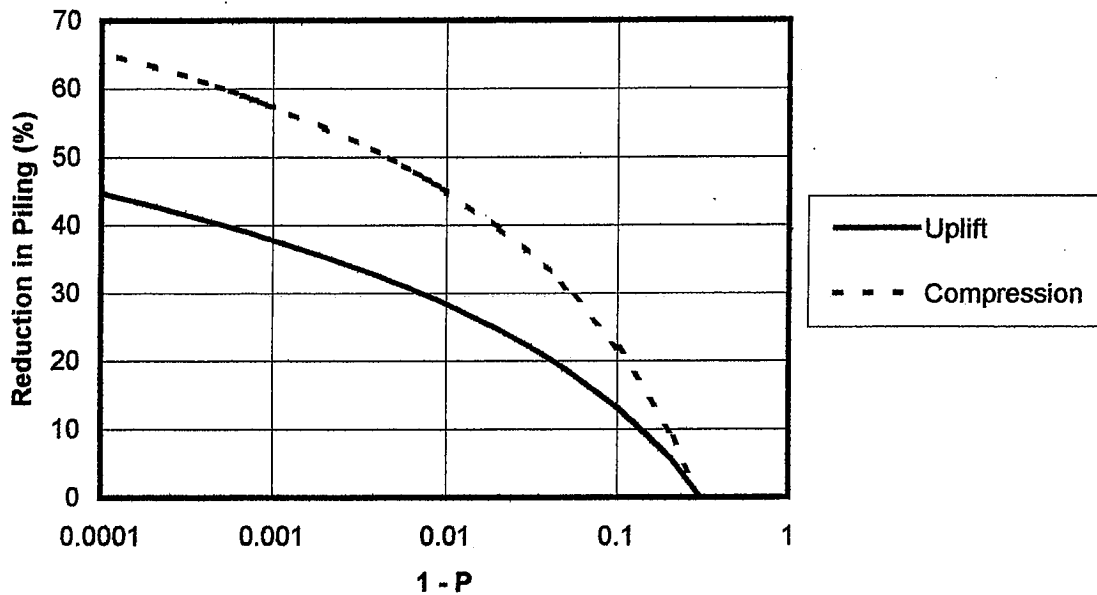


Figure 9.7 Caltrans' Reduction in Piling with Improved Method

For the factors of safety in Table 9.4, the mean values of Q_d/Q_m for the improved method would be 0.57 in uplift and 0.79 in compression. Both of these values are higher than 0.41, the mean value of Q_d/Q_m when Caltrans determines Q_d from a load test. If the factors of safety in Table 9.4 were used, the mean pile-head displacement of piles designed by the improved method would be higher than the mean displacement of piles designed from the results of a load test. The author recommends using the higher factor of safety of 2.44.

9.5 CONCLUSION

Ultimately, the selection of a factor of safety is the responsibility of the engineer who chooses to use the improved method in practice. As illustrated in this chapter, prior to selecting a factor of safety, the engineer must first determine the value of P which provides the desired level of reliability and the limiting value of Q_a/Q_m which corresponds to the desired pile-head displacement.

In Caltrans' case, if they were willing to continue to operate at the level of reliability provided by their current methods, then they could use the factors of safety in Table 9.4. By adopting the improved method with these factors of safety, Caltrans could reduce the number of piles used in future projects and realize at least a 10% savings in the cost of pile foundations. However, if Caltrans is more concerned with limiting pile-head displacements, as they currently do when determining Q_a from a load test, then they would want to use a factor of safety of 2.44 for the improved method. With a factor of safety of 2.44, the improved method would have P -values of 99.0 and 99.6% for uplift and compression, respectively. These P -values are much higher than the values associated with Caltrans' current methods. This is a decision that Caltrans must make before putting the improved method into practice. The author recommends using the factor of safety of 2.44.

If Caltrans is actually operating at P -values of 94% in uplift and 79% in compression without foundation failures, then the overall reliability of Caltrans' foundations must not be very sensitive to single-pile reliability. This situation could exist, to some degree, because the behavior of Caltrans' pile groups is controlled by factors other than the ultimate resistance of the single piles comprising the groups. If this

is true, then group behavior rather than single-pile behavior should be the focus of Caltrans' future research.

The insensitivity to single-pile reliability could also be explained by the use of rather conservative design loads, which is typical in civil engineering practice. Since the author is unfamiliar with Caltrans' structural design practices, he cannot confirm this. However, if this is true, then the only way in which Caltrans' could substantially increase the economic efficiency of their foundations would be to re-evaluate their entire design practice, in terms of reliability, from both structural and geotechnical perspectives.

10. CONCLUSION

10.1 SUMMARY

In this dissertation, sixteen existing methods of predicting the ultimate side resistance of single driven piles were evaluated against the uplift test pile database compiled from Caltrans' archives. These methods included methods based on standard penetration tests (SPT), laboratory tests, electric cone penetration tests (CPT), and piezocone penetration tests (CPTU). From this evaluation, the overall variability in the predictions made by these methods was found to be due primarily to variability in the predictions of the methods in sand. For this particular dataset, of the methods for piles in sand, the method with the lowest variability was Decourt's (1982) SPT-based method. Decourt's method, which is applicable to piles in both sand and clay, was also found to perform reasonably well in clay.

Based on this evaluation, Decourt's method was selected as the basis for the development of an improved side resistance method for Caltrans' use. The improved side resistance method, modeled after Decourt's method, was developed using regression analyses to fit the model parameters to a dataset of 97 uplift tests.

To develop a companion toe resistance method and to establish an empirical relationship between uplift side resistance and compressive side resistance, regression analyses were also performed to fit these additional model parameters to a dataset of 44 tests piles having both uplift and compressive tests.

Once the improved method for the prediction of the axial resistance of single piles was developed, an analysis of the reliability of the method was conducted to provide

recommendations for appropriate factors of safety. In this analysis, the reliability of Caltrans' current methods was used as a benchmark.

10.2 IMPROVED METHOD

10.2.1 Uplift Resistance

10.2.1.1 Ultimate Resistance

In the improved method, ultimate uplift resistance (Q_{cu}) is calculated using Equation 10.1 on a layer-by-layer basis. The weight of the pile is ignored.

$$Q_{cu} = PF_{vs} \sum_{i=1}^n f_{si} H_i \quad (10.1)$$

where,

Q_{cu} = ultimate uplift resistance

P = exterior perimeter of pile

f_{si} = unit side resistance (f_s) in layer i

H_i = height of layer i

F_{vs} = 0.68 for vibro-driven piles; 1.00 for impact-driven piles

10.2.1.2 Unit Side Resistance

The equations used to calculate f_s in various materials are provided below. In clay, silt and sand,

$$f_s = 25 + 1.8 N_{60} \text{ in kPa} \quad (10.2)$$

with the constraint that,

$$3 \leq N_{60} \leq 50 \quad \text{with } N_{60} \text{ in blows/305 mm.} \quad (10.3)$$

In gravel, cobbles and boulders,

$$f_s = 40 \text{ kPa.} \quad (10.4)$$

In intact rock, both weathered and unweathered,

$$f_s = 130 \text{ kPa.} \quad (10.5)$$

10.2.1.3 Modified α -Method

Following the development the of improved side resistance method, it was found that use of Dennis and Olson's (1983a) α -method in cohesive soils reduced the variability of the improved method without significantly altering calculated mean value of predicted uplift resistance. A modified α -method based on Dennis and Olson's method is provided as alternative in clay and clayey silt.

In the modified α -method, f_s is calculated using Equation 10.6. The adhesion factors α are determined from Figure 10.1. The value of s_u should be measured in an unconsolidated-undrained triaxial compression (UU) test.

$$f_s = \alpha s_u \quad (10.6)$$

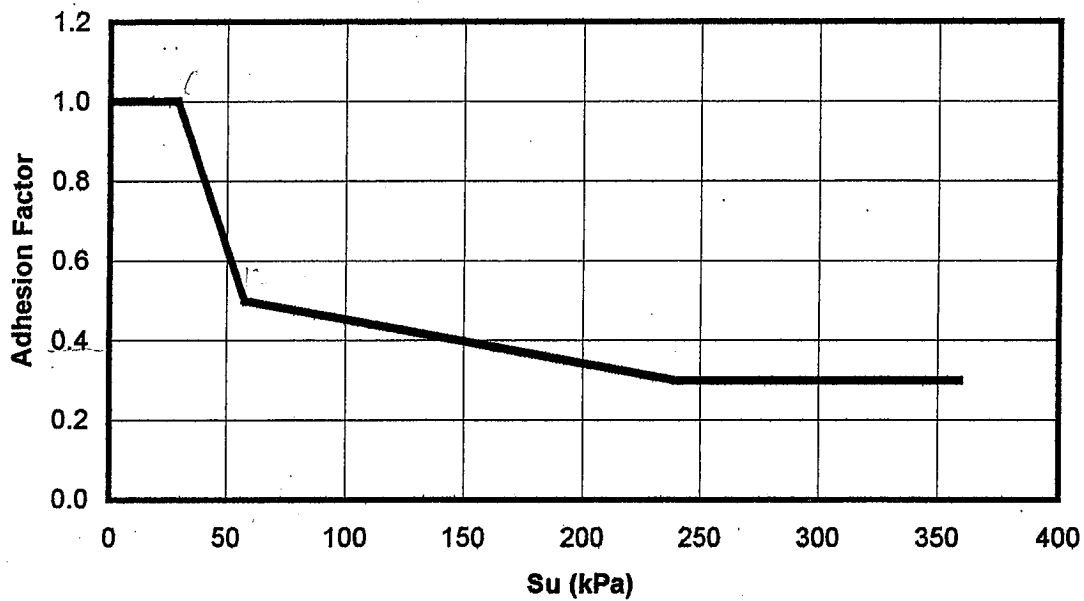


Figure 10.1 Adhesion Factors for Piles in Clay (Dennis and Olson 1983a)

10.2.2 Compressive Resistance

In the improved method, ultimate compressive resistance (Q_{cc}) is calculated using Equation 10.7. Unit toe resistance (f_t) is calculated using Equation 10.8 in clay, silt and sand and Equation 10.9 in gravel, cobbles, boulders and intact rock, both weathered and unweathered.

$$Q_{cc} = \frac{Q_{cu}}{0.94} + f_t F_{vt} (A_{pile} + F_p A_{plug}) \quad (10.7)$$

$$f_t = 0.17 N_{60} \quad \text{in MPa for clay and sand} \quad (10.8)$$

$$f_t = 19 \text{ MPa} \quad \text{for gravel and rock} \quad (10.9)$$

where,

Q_{cc} = ultimate compressive resistance

N_{60} = SPT resistance in blows/305 mm normalized to 60% of theoretical energy

F_p = plug mobilization factor from Table 10.1

F_{vt} = 0.56 for vibro-driven piles; 1.00 for impact-driven piles

A_{pile} = toe area of pile material

A_{plug} = toe area of soil plug

Table 10.1 Plug Mobilization Factor F_p

Pile Type	F_p
Open-Toed Steel Pipe	0.42
Steel H-Pile	0.67

10.2.3 Additional Recommendations

10.2.3.1 Pile Weight

In the improved method, pile weight is ignored. For the 155 piles used in this dissertation, the pile weight is negligible when compared to the measured ultimate resistance. However, for larger piles, especially precast concrete piles or concrete-filled steel pipe piles, it could be unconservative in compression or uneconomical in uplift to ignore the weight of the pile. In cases where the pile weight is equal to a significant percentage of the calculated axial resistance, the pile weight should be added to the calculated uplift resistance and subtracted from the calculated compressive resistance before establishing the allowable resistances in uplift and compression.

10.2.3.2 Oversized Toe Plates

In all cases, from Caltrans' archives, where the toe plate diameter of a closed-toed steel pipe pile is reported, the toe plate diameter is 12.7 mm larger than the outside diameter of the pile. According to Dennis (1982), the use of such oversized toe plates

will reduce the side resistance of the pile relative to a closed-toed pile with a toe plate having a diameter equal to the outside diameter of the pile. Given that the improved method was developed using closed-toed piles with oversized toe plates, the method should be expected to under-predict resistance when applied to piles with a toe plate which is not oversized.

10.2.3.3 Large Diameter Piles

Given that the improved toe resistance method was developed using piles with diameters ranging from 30 to 107 cm, caution should be exercised when applying the method to piles larger than 107 cm. For piles with diameters greater than 107 cm, the author recommends that toe resistance be assumed equal to zero when estimating ultimate compressive resistance. To mobilize significant toe resistance, these large diameter piles, especially open-toed piles, appear to require a relatively large toe displacement, greater than that typically developed under working loads.

10.2.3.4 Jetted Piles

The two jetted piles in the author's database were not included in the development of the improved method. Based on the improved method, the calculated compressive resistances of these two 137-cm diameter hollow precast concrete piles are 125% greater than the measured compressive resistances. Based on this, the author recommends that the ultimate resistance of jetted piles be taken as 45% of that calculated using the improved method. This only applies to piles re-struck with an impact hammer prior to loading. Jetted piles which are not re-struck with an impact hammer prior to loading, should be assumed to have no toe resistance.

10.3 FACTORS OF SAFETY

To determine the allowable resistance of a single pile during the design phase of a project, the engineer first calculates an ultimate resistance (Q_c) then divides Q_c by a factor of safety (FS) to obtain an allowable resistance (Q_a) for design. The general relationship between Q_c and Q_a is indicated in Equation 10.10.

$$Q_a = \frac{Q_c}{FS} \quad (10.10)$$

In the reliability analysis of Caltrans' current methods, it was determined that the probability (P) that the calculated ultimate resistance will not exceed the measured ultimate resistance is 94% in uplift and 79% in compression. These P -values correspond to the factor of safety of 2.0 applied to Caltrans' current methods. An analysis of the improved method, found that to obtain these same P -values (94% in uplift and 79% in compression), factors of safety 1.76 in uplift and 1.26 in compression would have to be applied to the improved method.

In Caltrans' case, if they were willing to continue to operate at the level of reliability provided by their current methods, then they could use the factors of safety in Table 9.4. By adopting the improved method with these factors of safety, Caltrans could reduce the number of piles used in future projects and realize at least a 10% savings in the cost of pile foundations. However, if Caltrans is more concerned with limiting pile-head displacements, as they currently do when determining Q_a from a load test, then they would want to use a factor of safety of 2.44 for the improved method. With a factor of safety of 2.44, the improved method would have P -values of 99.0 and 99.6% for uplift and compression, respectively. These P -values are much higher than the values associated with Caltrans' current methods. This is a decision that Caltrans must make before putting the improved method into practice. The author recommends using the factor of safety of 2.44.

If Caltrans is actually operating at P -values of 94% in uplift and 79% in compression without foundation failures, then the overall reliability of Caltrans' foundations must not be very sensitive to single-pile reliability. This situation could exist, to some degree, because the behavior of Caltrans' pile groups is controlled by factors other than the ultimate resistance of the single piles comprising the groups. If this is true, then group behavior rather than single-pile behavior should be the focus of Caltrans' future research.

The insensitivity to single-pile reliability could also be explained by the use of rather conservative design loads, which is typical in civil engineering practice. Since the author is unfamiliar with Caltrans' structural design practices, he cannot confirm this. However, if this is true, then the only way in which Caltrans' could substantially increase the economic efficiency of their foundations would be to re-evaluate their entire design practice, in terms of reliability, from both structural and geotechnical perspectives.

10.4 RECOMMENDATIONS FOR FUTURE RESEARCH

Caltrans' purpose in funding this research was to develop improved methods of predicting the ultimate axial resistance of single driven piles with the aim of using the methods to provide more cost effective pile foundations for new bridges and seismic retrofits of existing bridges. In pursuit of this aim, the author recommends three topics for future research:

- Site characterization for piles in gravel, cobbles, boulders and rock,
- Pile acceptance criteria, and
- Pile group behavior.

10.4.1 Site Characterization for Piles in Gravel and Rock

In his analyses, the author found that CPT/CPTU and even SPT are inadequate for the characterization of gravel, cobbles, boulders and intact rock. Without better methods for characterizing these materials, predictions of pile performance in these materials during the design phase of a project will continue to be a challenge.

During the field exploration phase of the author's project, the author recommended that Caltrans use spectral analysis of surface waves (SASW) to estimate the shear wave velocity (V_s) profile and then develop correlations between V_s and both unit side resistance and unit toe resistance. This recommendation was accepted by Caltrans', but the project did not have sufficient resources to conduct the necessary SASW testing.

For piles in gravel, cobbles, boulders and rock, the author recommends that Caltrans initially develop V_s -based methods using the axial load test database created for this dissertation. This would first require that V_s -profiles be determined for a large number of test pile in the database. If the methods developed appear promising, the author would recommend that full-scale instrumented axial load tests be conducted in these materials to further refine both the developed V_s -based methods and the SPT-based improved method presented in this dissertation.

10.4.2 Pile Acceptance Criteria

The author also recommends that Caltrans evaluate pile acceptance criteria, including indicator piles, dynamic testing, and static load testing. Using the driving records in the load test reports furnished to the author, Caltrans could easily develop improved dynamic pile formulae. Beyond this, the author recommends that Caltrans' use the data in their archives, supplemented by more recent data which they have collected, to

examine the performance of the Pile Driving Analyzer (PDA) and the Case Pile Wave Analysis Program (CAPWAP) which Caltrans currently uses for dynamic testing of piles and the estimation of static resistance from these dynamic tests, respectively. Ideally, Caltrans should investigate the development of statistical models which could be used in decision analyses to determine the most economical manner in which to use indicator piles, dynamic testing, and static load testing in combination with the adopted predictive methods.

10.4.3 Group Behavior

The foundations of Caltrans' bridges are typically composed of large groups of piles. An analysis of the reliability of Caltrans' current methods, leads the author to believe that the overall reliability of Caltrans' foundations is not very sensitive to errors in the prediction of single-pile resistance. To be able to predict better the performance of these foundations, Caltrans should pursue research into pile group behavior rather than single-pile behavior.

The problem in investigating group behavior is that load-displacement measurements of pile groups, even model pile groups, are scarce. To obtain the necessary data to analyze group behavior, the author recommends that Caltrans instrument newly constructed pile groups and monitor the load-displacement behavior of the piles during both construction and subsequent service. Laboratory model testing of driven pile groups would also be a relatively cost-effective source of additional data on pile group behavior. Using the collected data, Caltrans could then develop a method, perhaps an elastic-continuum analysis, to predict the load-displacement behavior of pile groups under working loads.

11. REFERENCES

- Abe, S.K. and Teferra, W. (1998), "SPT Energy Measurements, Sonoma Valley CSD, Reclamation Ponds R1 and R2, Sonoma County, California," *Report No. 988031*, Goble Rauchshe Likins and Associates, Inc.
- American Petroleum Institute (1993), "Recommended Practice for Planning, Designing and Constructing Fixed Offshore Platforms – Working Stress Design: API Recommended Practice 2A-WSD (RP 2A-WSD)," Washington, DC.
- Ang, A.H-S. and Tang, W.H. (1975), *Probability Concepts in Engineering Planning and Design: Vol. 1, Basic Principles*, John Wiley and Sons, New York.
- Bond, A.J. and Jardine, R.J. (1995), "Shaft Capacity of Displacement Piles in a High OCR Clay," *Geotechnique*, Vol. 45, No. 1, 3-23.
- Briaud, J-L. and Miran, J. (1992), "The Cone Penetrometer Test," *Report FHWA-SA-91-043*, U.S. Federal Highway Administration
- Briaud, J-L., Tucker L., and Olsen, R. (1985), "Cone Penetrometer and Foundation Design," short course notes, Texas A&M University.
- Brown, R.E. (1977), "Drill Rod Influence on Standard Penetration Test," *Journal of the Geotechnical Engineering Division, ASCE*, Vol. 103, No. 11, 1332-1336.

- Bustamante, M. and Gianceselli, L. (1982), "Pile Bearing Capacity Predictions by Means of Static Penetrometer CPT," *Proceedings*, 2nd European Symposium on Penetration Testing, ESOPT-II, Amsterdam, Vol. 2, 493-500.
- Chin, F.K. (1970), "Evaluation of the Ultimate Load of Piles from Tests Not Carried to Failure," *Proceedings*, 2nd Southeast Asian Conference on Soil Engineering, Singapore, 81-90.
- Davissou, M.T. (1972), "High Capacity Piles," *Proceedings*, Lecture Series on Innovations in Foundation Construction, Illinois Section, ASCE, Chicago, 81-112.
- Decourt, L. (1982), "Prediction of the Bearing Capacity of Piles Based Exclusively on N Values of the SPT," *Proceedings*, 2nd European Symposium on Penetration Testing, ESOPT-II, Amsterdam, Vol. 1, 29-34.
- De Nicola, A. and Randolph, M.F. (1999), "Centrifuge Modeling of Pipe Piles in Sand under Axial Loads," *Geotechnique*, Vol. 49, No. 3, 295-318.
- De Ruiter, J. and Beringen, F.L. (1970), "Design of Large North Sea Structures," *Marine Geotechnique*, Vol. 1, No. 1, 1-10.
- Dennis, N.D. (1982), "Development of an ENGINE MODEL for the Prediction of Axial Pile Capacity," PhD dissertation, Texas A&M University, Austin, Texas.
- Dennis, N.D. and Olson, R.E. (1983a), "Axial Capacity of Steel Pipe Piles in Clay," *Proceedings*, Geotechnical Practice in Offshore Engineering, ASCE, Austin, Texas, 370-388.
- Dennis, N.D. and Olson, R.E. (1983b), "Axial Capacity of Steel Pipe Piles in Sand," *Proceedings*, Geotechnical Practice in Offshore Engineering, ASCE, Austin, Texas, 389-402.

- Douglas, B.J. and Olsen, R.S. (1981), "Soil Classification Using Electric Cone Penetrometer," *Cone Penetration Testing and Experience*, proceedings, ASCE National Convention, St. Louis, 209-227.
- Eslami, A. and Fellenius, B.H. (1997), "Pile Capacity by Direct CPT and CPTu Methods Applied to 102 Case Histories." *Canadian Geotechnical Journal*, Vol. 34, 886-904.
- Fellenius, B.H. (1996), *Basics of Foundation Design*, BiTech, Richmond, BC, Canada.
- Fleming, W.G.K. (1992), "A New Method for Single Pile Settlement Prediction and Analysis," *Geotechnique*, Vol. 42, No. 3, 411-425.
- Frost, J.D. (1992), "Evaluation of Repeatability and Efficiency of Energy Delivered with a Diedrich Automatic SPT Hammer System," report prepared for Diedrich Drill, Inc.
- Hannigan, P.J., Goble, G.G., Thendean, G., Likins, G.E. and Rausche, F. (1997), "Design and Construction of Driven Pile Foundations," Vol. 1, *Report FHWA-HI-97-013*, U.S. Federal Highway Administration
- X Jardine, R.J. and Chow, F.C. (1996), "New Design Methods for Offshore Piles," *Report No. 96-103*, Marine Technology Directorate, Ltd., London.
- Jeffries, M.G. and Davies, M.P. (1991), "Soil Classification by the Cone Penetration Test", discussion, *Canadian Geotechnical Journal*, Vol. 28, No. 1, 173-176.
- Jeffries, M.G. and Davies, M.P. (1993). "Use of CPT to Estimate Equivalent SPT N_{60} ", *ASTM Geotechnical Testing Journal*, Vol. 16, No. 4, 458-468.

- Karlsrud, K. (1999), "Lesson Learned from Instrumented Axial Pile Load Tests in Clay," distributed as separate, OTRC Conference on Analysis, Design, Construction and Testing of Deep Foundations, Austin, Texas.
- Konder, R.L. (1963), "Hyperbolic Stress-Strain Response: Cohesive Soils". *Journal of the Soil Mechanics and Foundations Division*, ASCE, Vol. 89, No. 4, 241-242.
- Kraft, L.M., Focht, J.A., Amerasinghe, S.F. (1981), "Friction Capacity of Piles Driven into Clay," *Journal of the Geotechnical Engineering Division*, ASCE, Vol. 107, No. 11, 1521-1541.
- Ladd, C.C., Foott, R., Ishihara, K., Schlosser, F. and Poulos, H.G. (1977), "Stress Deformation and Strength Characteristics," *Proceedings*, 9th International Conference on Soil Mechanics and Foundation Engineering, Tokyo, Vol. 2, 421-494.
- Lake, L.M. (1974), "Discussion on Granular Materials," *Proceedings*, Conference on Settlement of Structures, Cambridge, 663.
- Lehane, B.M. and Jardine, R.J. (1994), "Displacement-Pile Behavior in a Soft Marine Clay," *Canadian Geotechnical Journal*, Vol. 31, No. 2, 181-191.
- Lehane, B.M., Jardine, R.J., Bond, A.J. and Frank, R. (1993), "Mechanisms of Shaft Friction in Sand from Instrumented Pile Tests," *Journal of the Geotechnical Engineering Division*, ASCE, Vol. 119, No. 1, 19-35.
- Lunne, T., Robertson, P.K. and Powell, J.J.M. (1997), *Cone Penetration Testing in Geotechnical Practice*, Blackie, New York.

- Matsumoto, K. and Matsubara, M. (1982), "Effects of Rod Diameter in the Standard Penetration Test," *Proceedings*, 2nd European Symposium on Penetration Testing, ESOPT-II, Amsterdam, Vol. 1, 107-122.
- Meyerhof, G.G. (1976), "Bearing Capacity and Settlement of Pile Foundations," *Journal of the Geotechnical Engineering Division*, ASCE, Vol. 102, No. 3, 195-228.
- Nordlund, R.L. (1963), "Bearing Capacity of Piles in Cohesionless Soils", *Journal of the Soil Mechanics and Foundations Division*, ASCE, Vol. 89, No. 3, 1-35.
- O'Neill, M.W. and Raines, R.D. (1991), "Load Transfer for Pipe Pile in Highly Pressurized Dense Sand," *Journal of the Geotechnical Engineering Division*, ASCE, Vol. 117, No. 8, 1208-1226.
- O'Neill, M.W., Vipulanandan, C. and Wong, D. (1990), "Laboratory Modeling of Vibro-Driven Piles," *Journal of the Geotechnical Engineering Division*, ASCE, Vol. 116, No. 8, 1190-1209.
- Olson, R.E. (1990), "Axial Load Capacity of Steel Pipe Pile in Sand," *Proceedings*, Offshore Technology Conference, Houston, OTC Paper No. 6419, Vol. 4, 17-24.
- Olson, R.E. and Dennis, N.D. (1982), "Review and Compilation of Pile Test Results, Axial Capacity," *Report GR83-4*, Geotechnical Engineering Center, The University of Texas at Austin.
- Peck, R.B., Hanson, W.E. and Thornburn, T.H. (1974), *Foundation Engineering*, 2nd ed., John Wiley and Sons, New York.

- Pelletier, J.H., Murff, J.D. and Young, A.C. (1993), "Historical Development and Assessment of the Current API Design Methods for Axially Loaded Pipes," *Proceedings*, Offshore Technology Conference, Houston, OTC Paper No. 7517, Vol. 2, 253-282.
- Randolph, M.F. and Murphy, B.S. (1985), "Shaft Capacity of Driven Piles in Clay," *Proceedings*, Offshore Technology Conference, Houston, Vol. 1 371-378.
- Richman, R.L. and Speer, D. (1989), "Comparison of Measured Pile Capacity to Pile Capacity Predictions Made using Electronic Cone Penetration Data." *Report No. FHWA/CA/TL-89/16*, Division of New Technology, Materials and Research, Office of Transportation Materials and Research, California Department of Transportation, Sacramento, California.
- Sanglerat, G. and Sanglerat, T.R.A. (1982), "Pitfalls of the SPT," *Proceedings*, 2nd European Symposium on Penetration Testing, ESOPT-II, Amsterdam, Vol. 1, 143-145.
- Schmertmann, J.H. (1978), "Guidelines for Cone Penetration Test: Performance and Design," *Report FHWA-TS-78-209*, U.S. Federal Highway Administration.
- Schmertmann, J.H. and Palacios, A. (1979), "Energy Dynamics of SPT," *Journal of the Geotechnical Engineering Division*, ASCE, Vol. 105, No. 8, 909-926.
- Seed, H.B. and Reese, L.C. (1957), "The Action of Soft Clay along Friction Piles," *Transactions*, ASCE, Vol. 122, 731-764.
- Skaug, T.M. (1998), "CPT/SPT Site-Specific Correlation and Calibration Program," *Report No. IP2/598/159*, Taber Consultants.

- Skempton, A.W. (1986), "Standard Penetration Test Procedures and the Effects in Sands of Overburden Pressure, Relative Density, Particle Size, Ageing and Overconsolidation," *Geotechnique*, Vol. 36, No. 3, 425-447.
- Takesue, K., Sasao, H. and Matsumoto, T. (1998), "Correlation between Ultimate Pile Skin Friction and CPT Data," *Proceedings*, Conference on Geotechnical Site Characterization, ISC '98, Atlanta.
- Thurman, A.G. (1964). "Computed Load Capacity and Movement of Friction and End-Bearing Piles Embedded in Uniform and Stratified Soil," Ph.D. dissertation, Carnegie Institute of Technology.
- Tomlinson, M.J. (1957), "The Adhesion of Piles in Clay Soils," *Proceedings*, 4th International Conference on Soil Mechanics and Foundation Engineering, Vol. 2, 66-71.
- Tomlinson, M.J. (1971), "Some Effects of Pile Driving on Skin Friction," *Proceedings*, Conference on Behavior of Piles, Institution of Civil Engineers, London, 107-114, 149-152.
- Toolan, F.E., Lings, M.L. and Mirza, U.A. (1990), "An Appraisal of API RP2A Recommendations for Determining Skin Friction of Piles in Sand," *Proceedings*, Offshore Technology Conference, Houston, OTC Paper No. 6422,, Vol. 4, 33-42.
- Tumay, M.T. and Fakhroo, M. (1981), "Pile Capacity in Soft Clays using QCPT Data," *Cone Penetration Testing and Experience*, proceedings, ASCE National Convention, St. Louis, 434-455.
- Vesic, A.S. (1977), "Design of Pile Foundations," *NCHRP Synthesis 42*, Transportation Research Board, National Academy of Sciences, Washington, DC.

Vijayvergiya, V.N. and Focht, J.A. (1972), "A New Way to Predict the Capacity of Piles in Clay," *Proceedings, Offshore Technology Conference, Houston*, Vol. 2, 865-874.